Facies and Stratigraphy of the San Andres Formation (Mid-Permian) Petroleum Province, Northwest Shelf of the Permian Basin, West Texas: A Resurgent Play

Kevin A. Hiss

David B. Williamson

The University of Texas at Dallas

GSA South-Central Section

March 9, 2020

Introduction

- Environments of the San Andres formation on the Northwest Shelf in West Texas

- Complex interaction between sea level, climate, and geomorphology formed “world-class” carbonate reservoirs

- Varying targets for hydrocarbon production

- Quantitative approach to indicate the geologic history of the San Andres and effects of paleoenvironment on reservoir quality

San Andres Formation Age – Middle Permian

Base Wordian 268.8 Ma

Base Roadian 272.3 Ma

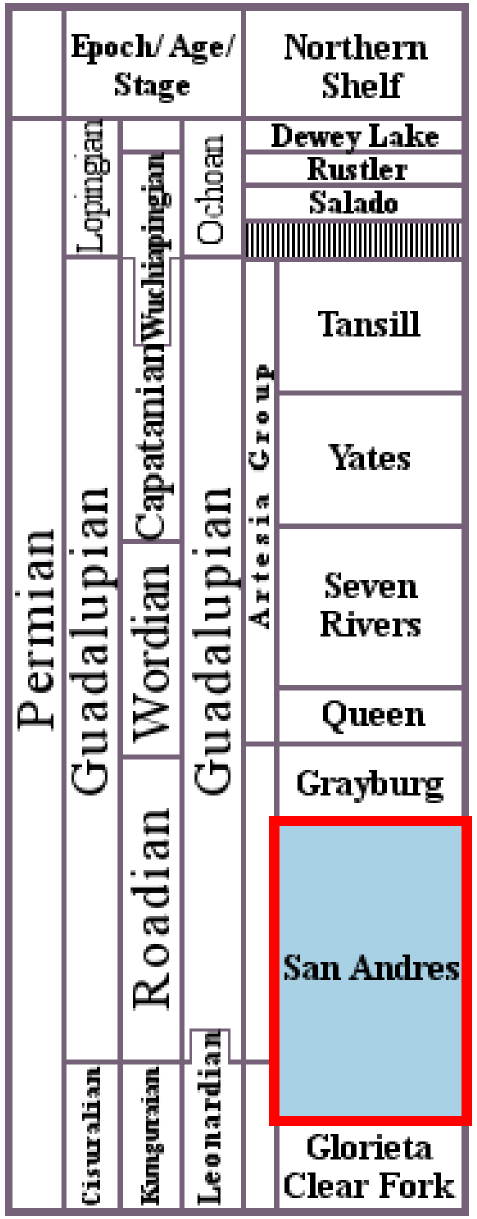

(Ruppel, 2019)

lower Guadalupian

upper Leonardian

San Andres Reservoirs Occur on Carbonate Platforms and Shelves

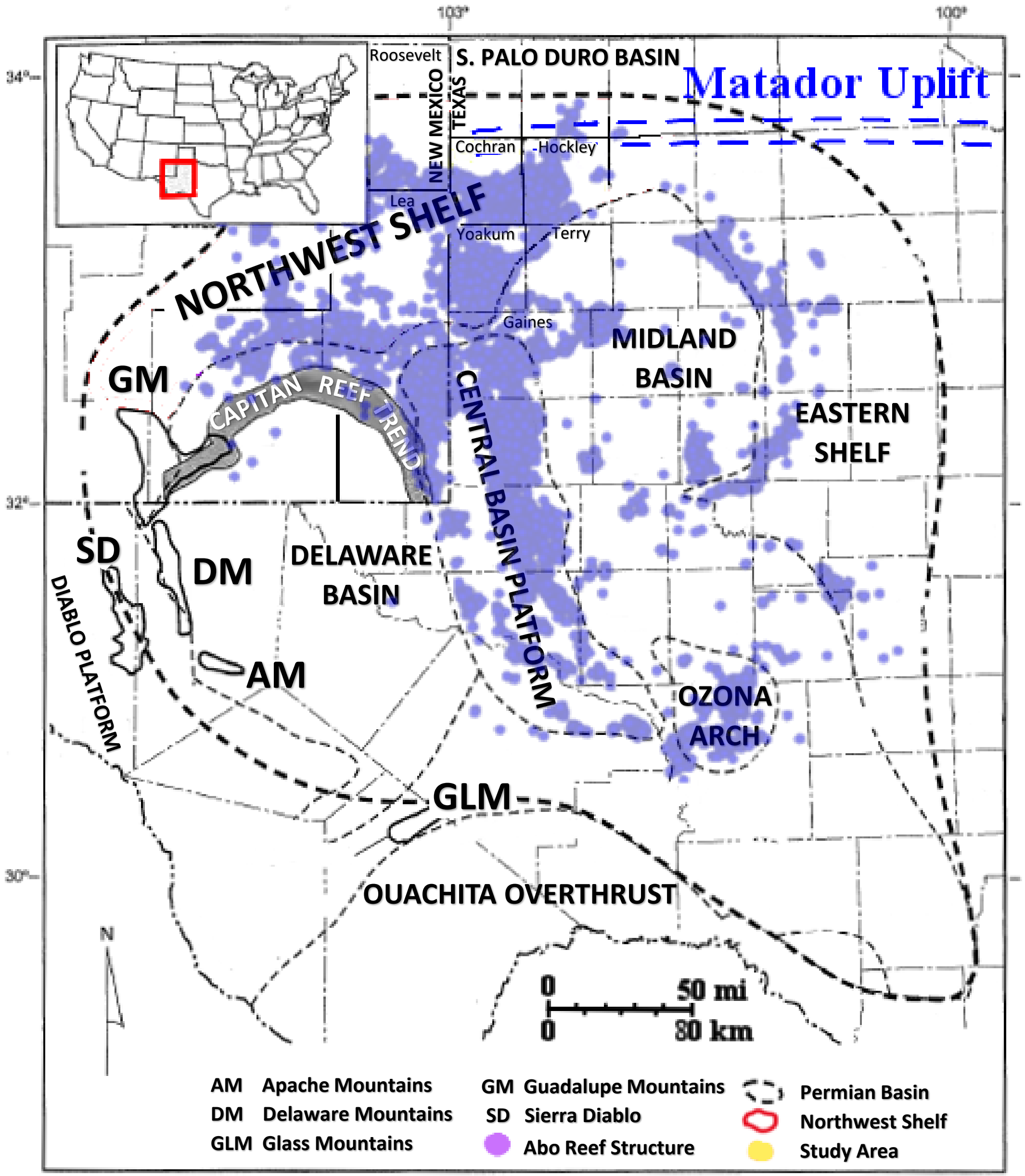

San Andres production – shelf and platform carbonate reservoirs

(Dutton, 2005; Ruppel, 2019)

San Andres Reservoirs – Highest Cumulative Production of Permian Basin

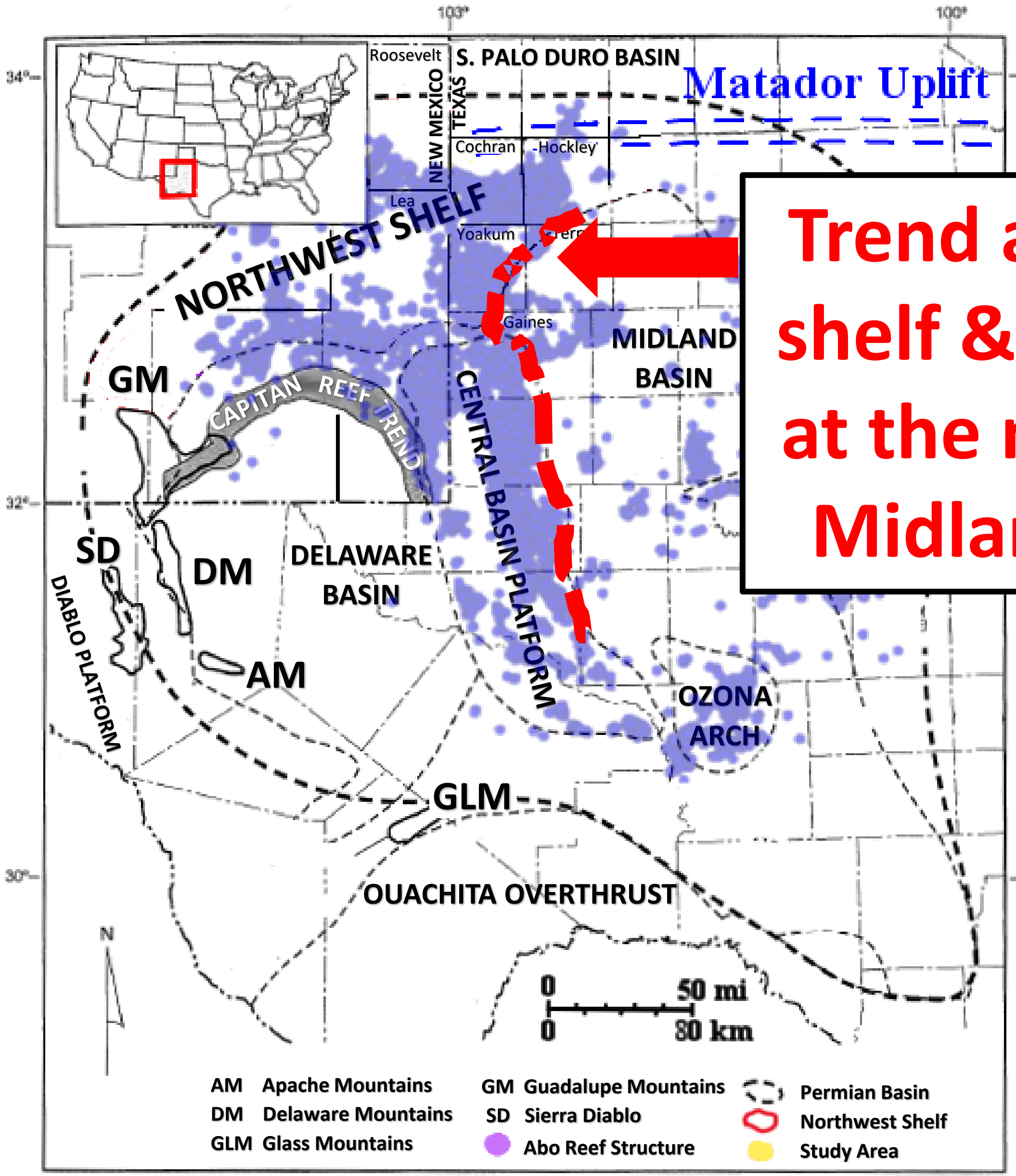

Trend along the shelf & platform at the margin of Midland Basin

San Andres production – shelf and platform carbonate reservoirs

Cumulative Conventional Permian Production

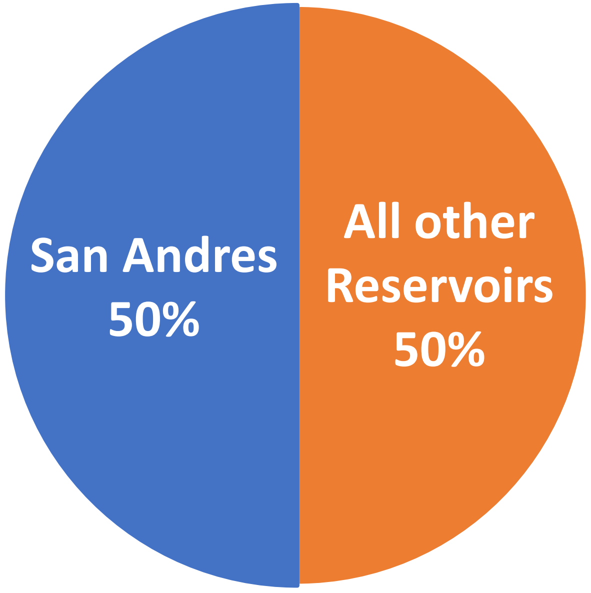

(Dutton, 2005; Ruppel, 2019)

San Andres Northwest Shelf – Rimmed Carbonate Shelf

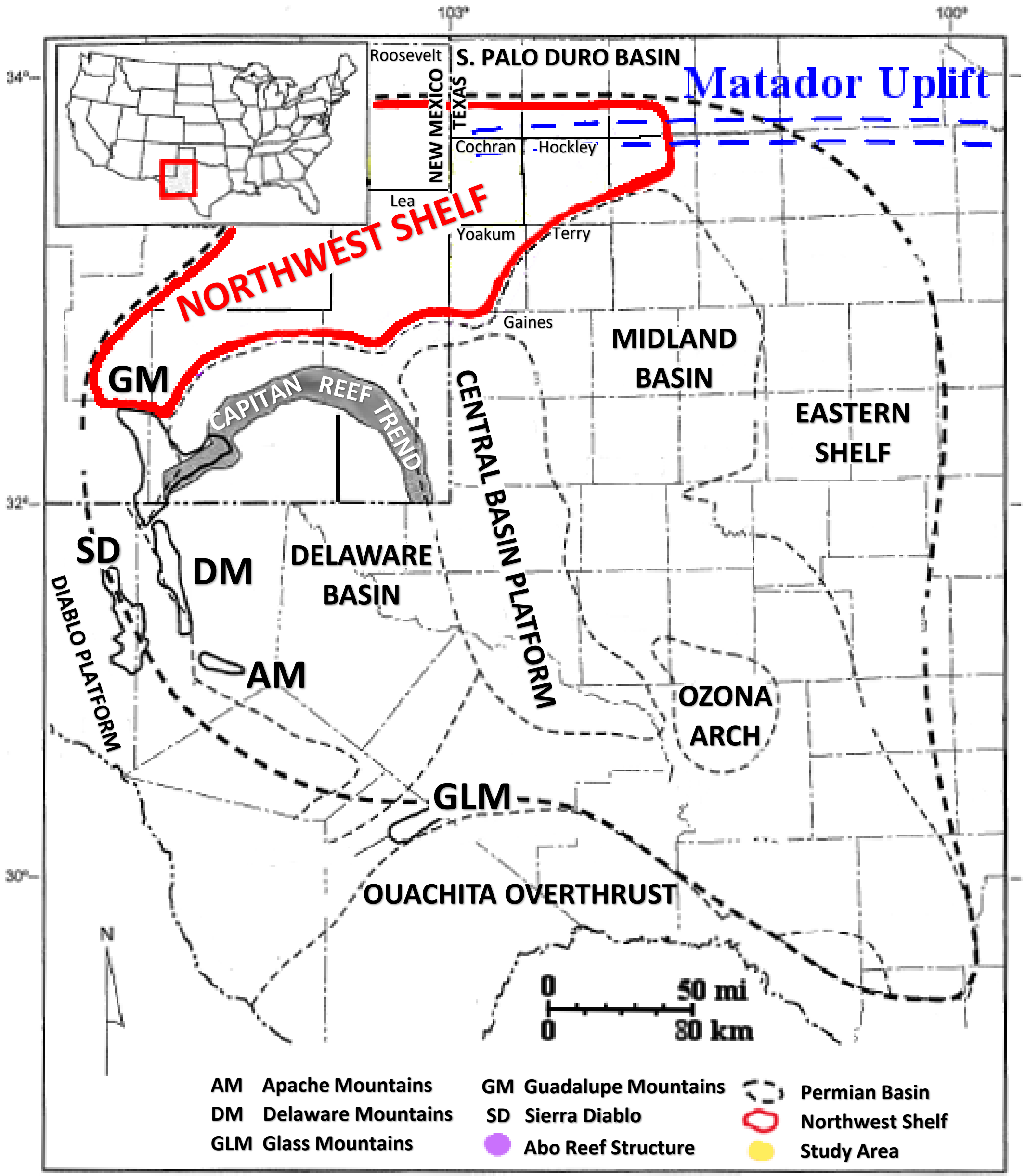

Rimmed Carbonate Shelf

Morphology:	Broad, low relief (~0.6°)
Dominant lithologies:	Dolomitized carbonates & anhydrites
Depositional environment:	Shallow lagoon & sabkha complexes
Sedimentation pattern:	Upward-shoaling prograding-aggrading sequences
Thickness:	1,200 – 1650 ft.

(Dutton, 2005; Ruppel, 2019)

Carbonate Shelf Rim Overlies a Deep-Seated Shelf Margin

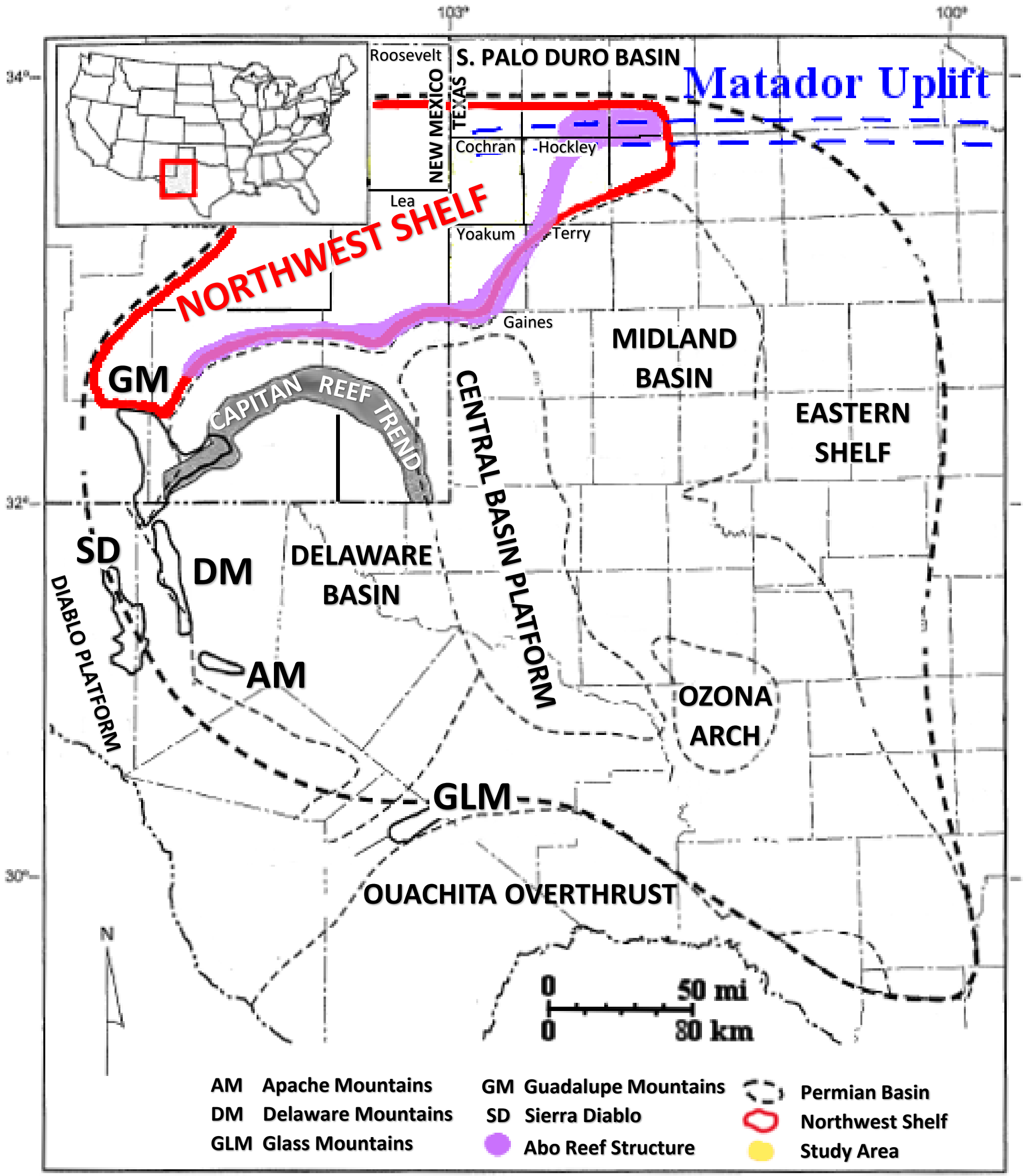

Abo Reef Structure – lower Permian (Leonardian) shelf margin

(Dutton, 2005; Ruppel, 2019)

San Andres Play Fairway – West Texas

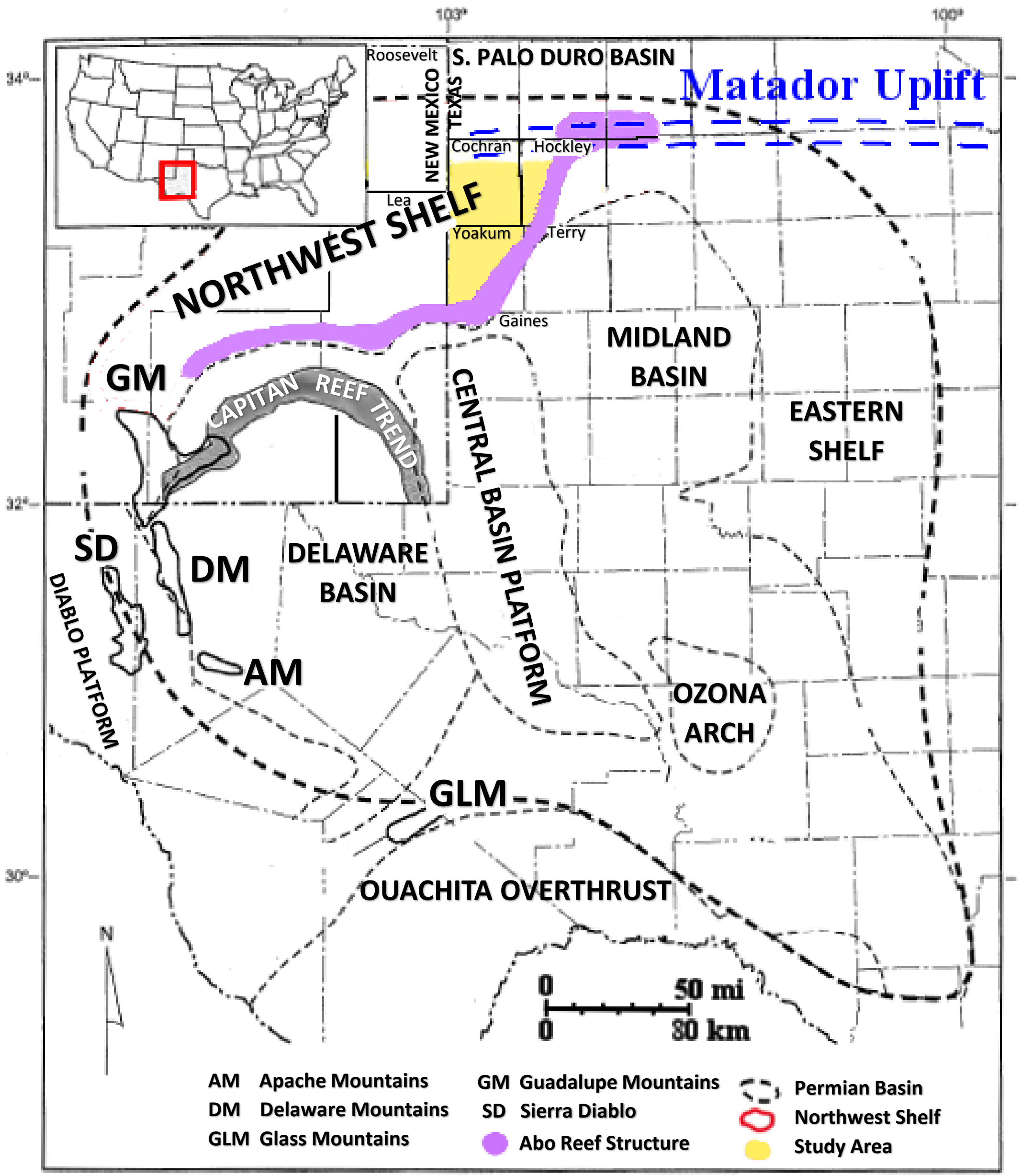

Abo Reef Structure – lower Permian (Leonardian) shelf margin

West Texas San Andres Play Fairway

Cumulative San Andres Production

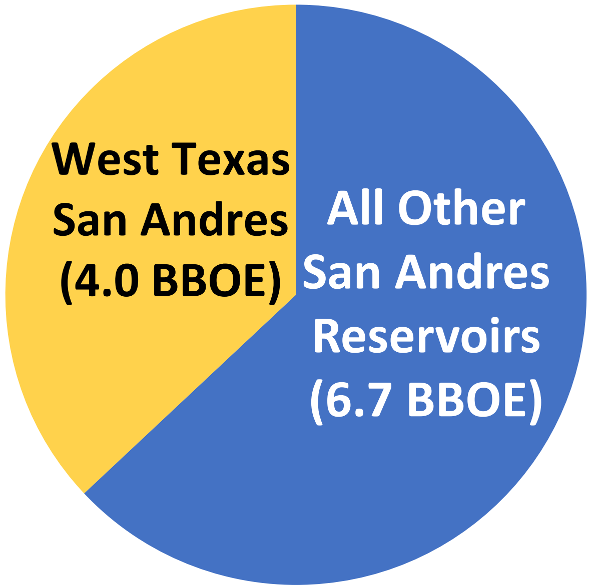

(Dutton, 2005; Ruppel, 2019)

San Andres Play Fairway – West Texas

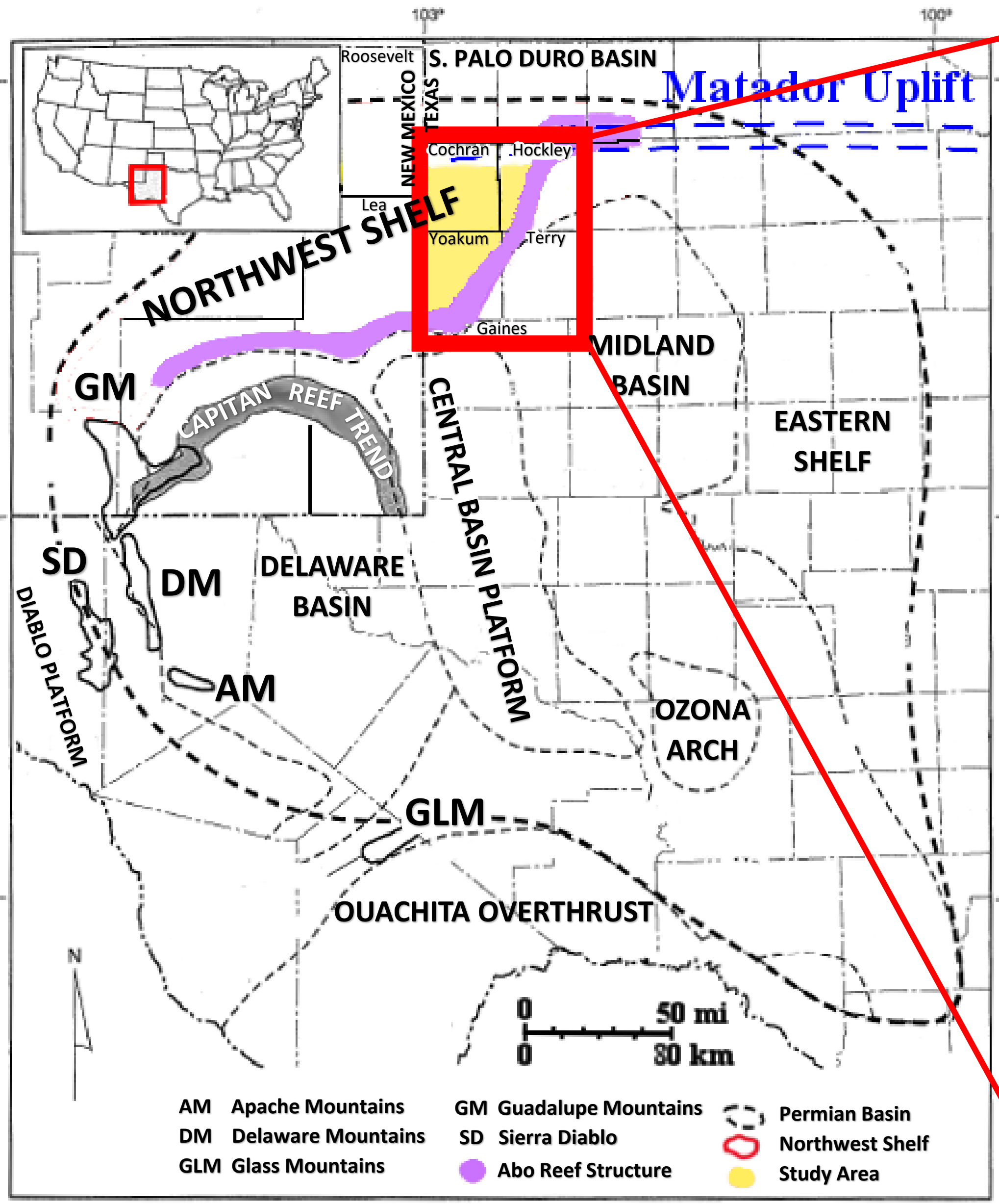

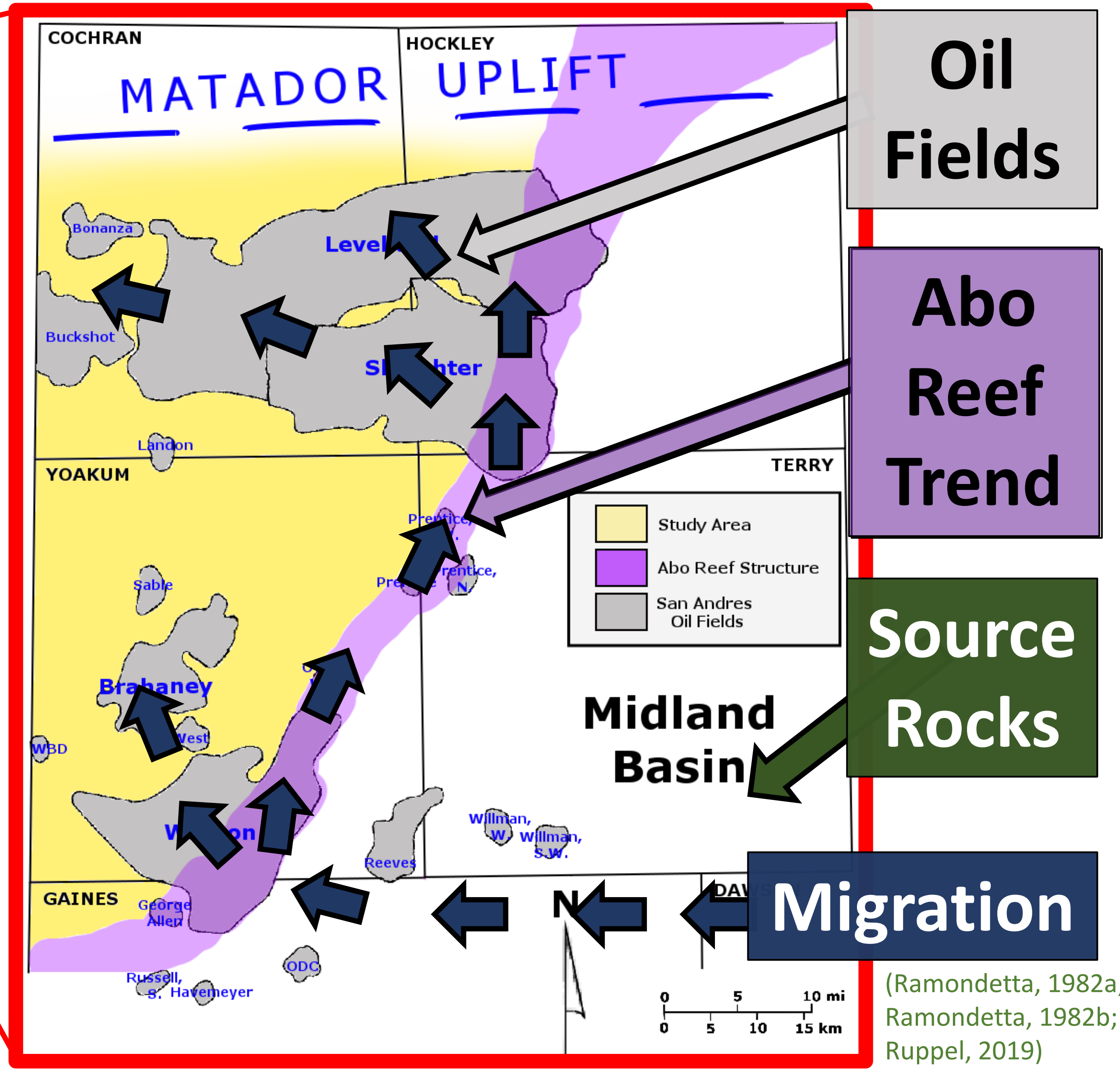

(Ramondetta, 1982a; Ramondetta, 1982b; Ruppel, 2019)

Warming Climate and Near-Equatorial Latitude: Favorable for Sabkha Evaporites

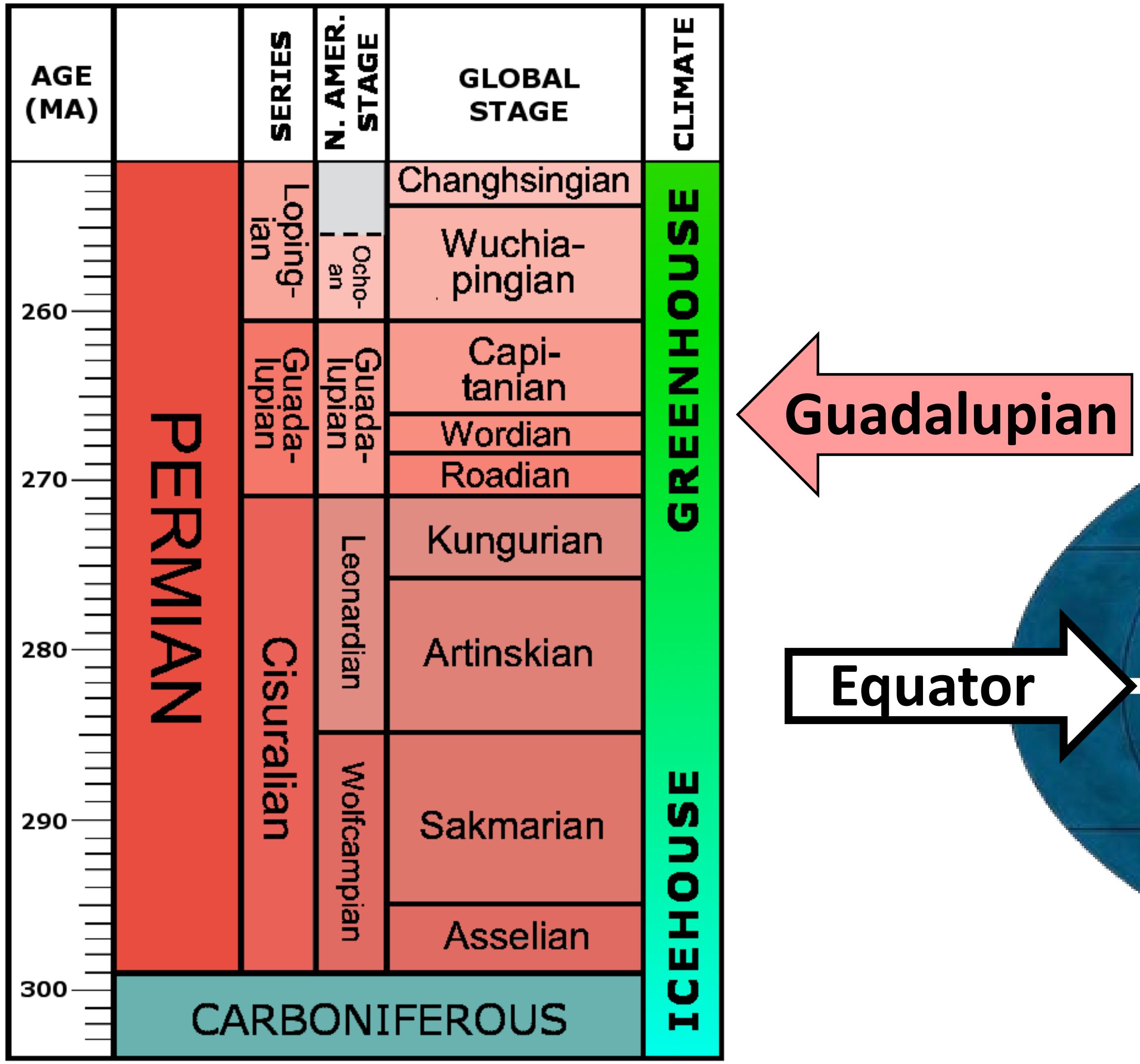

Permian Basin

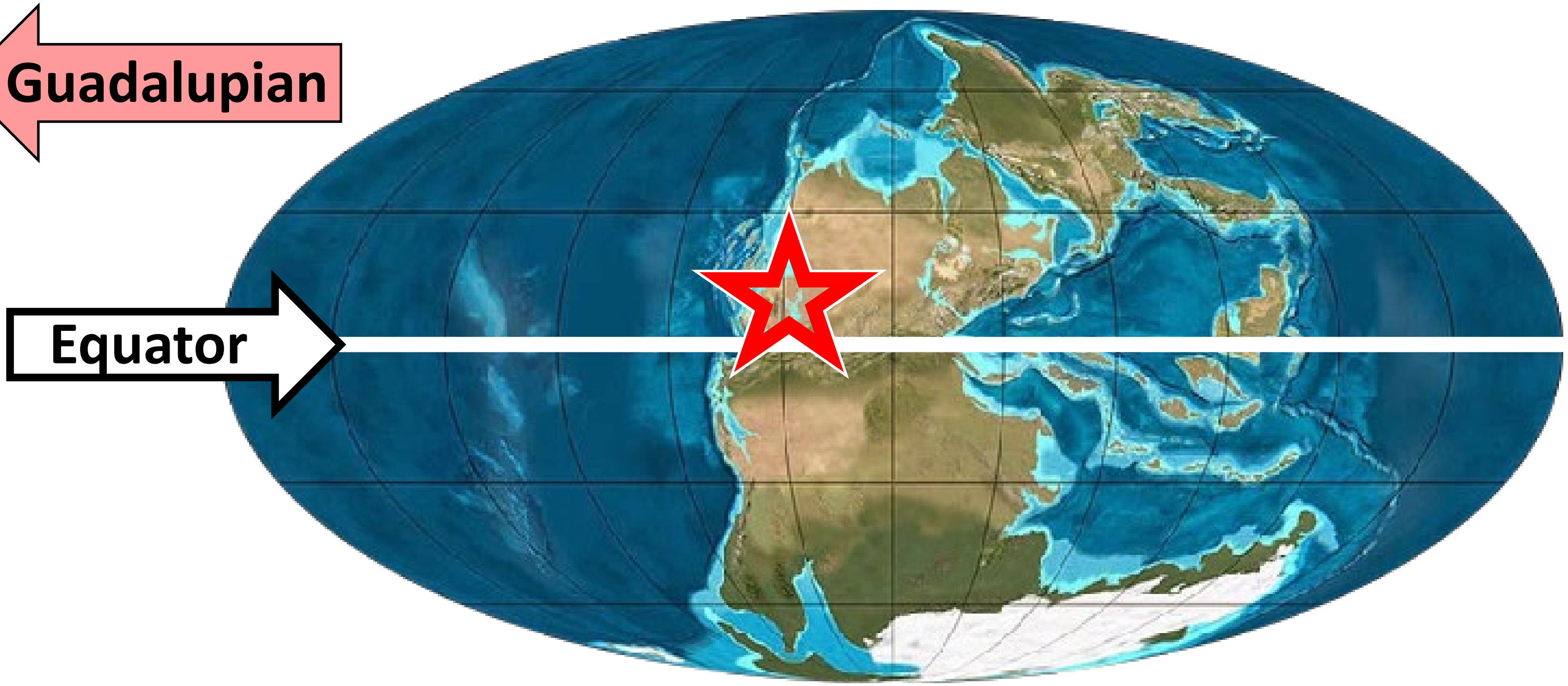

(Blakey, 2019)

Inner-Shelf Environments and Facies Tract

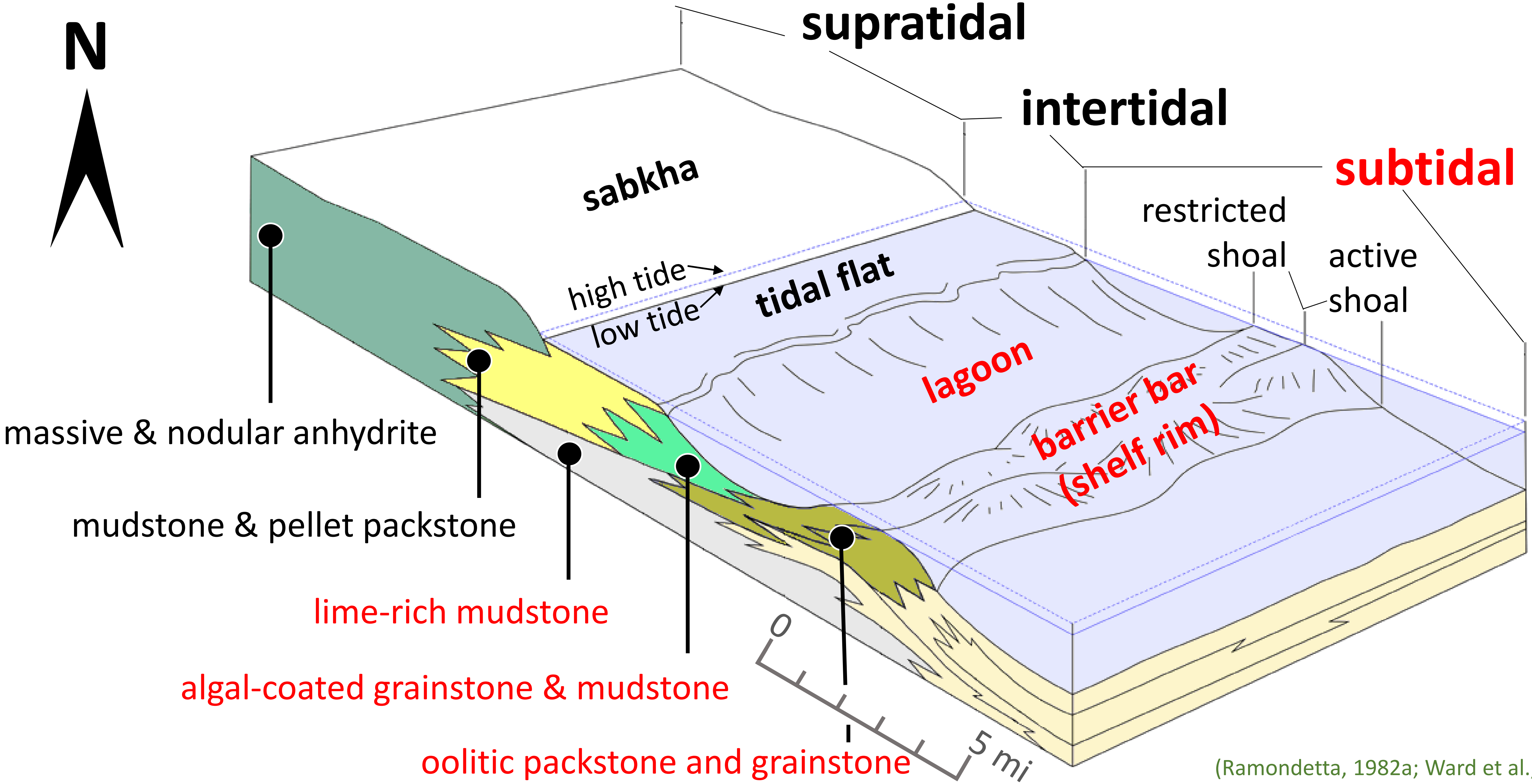

(Ramondetta, 1982a; Ward et al., 1986)

Secondary Porosity Formed by Reflux Dolomitization

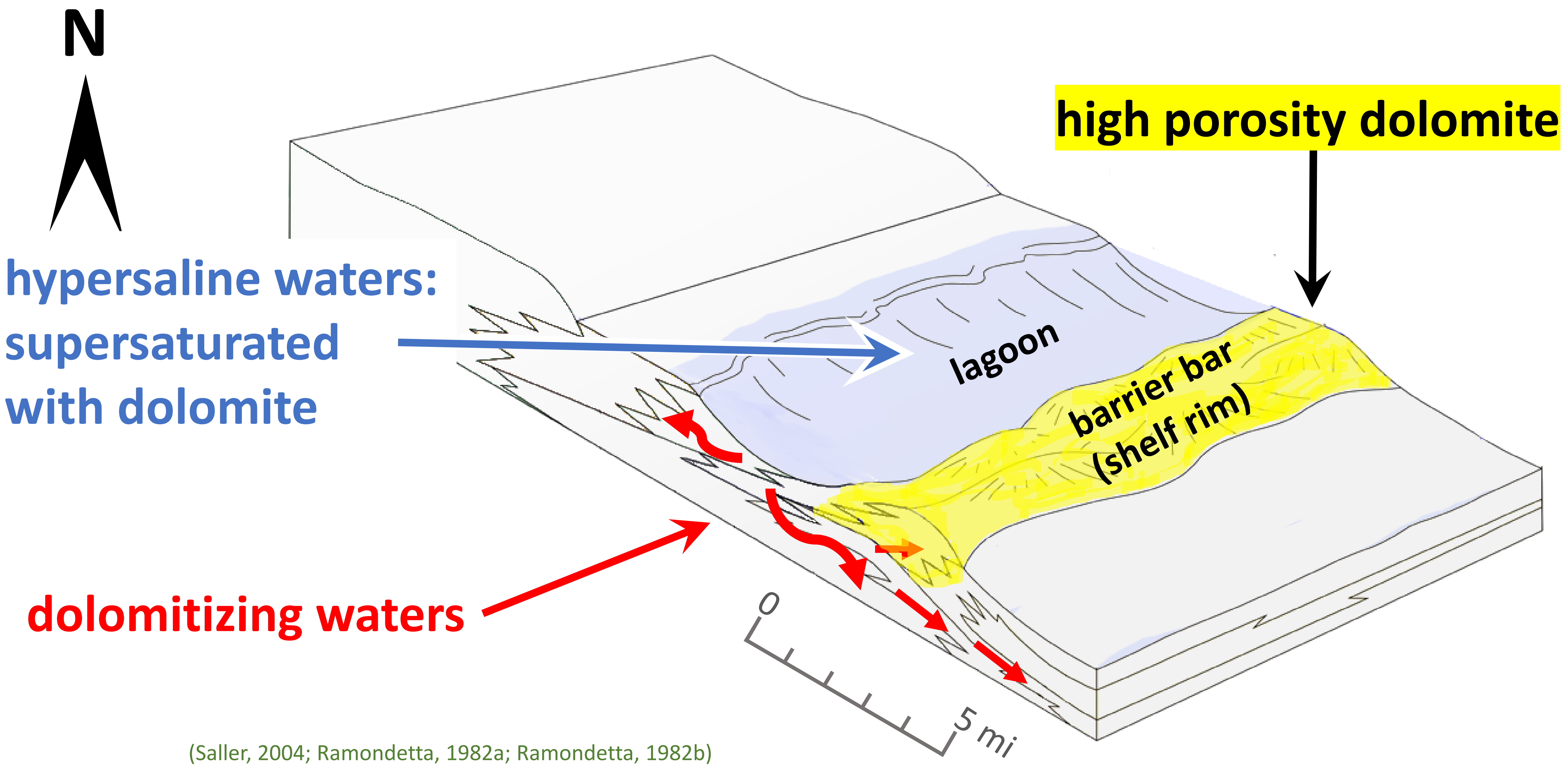

(Saller, 2004; Ramondetta, 1982a; Ramondetta, 1982b)

Porosity Occlusion by Anhydrite Cement

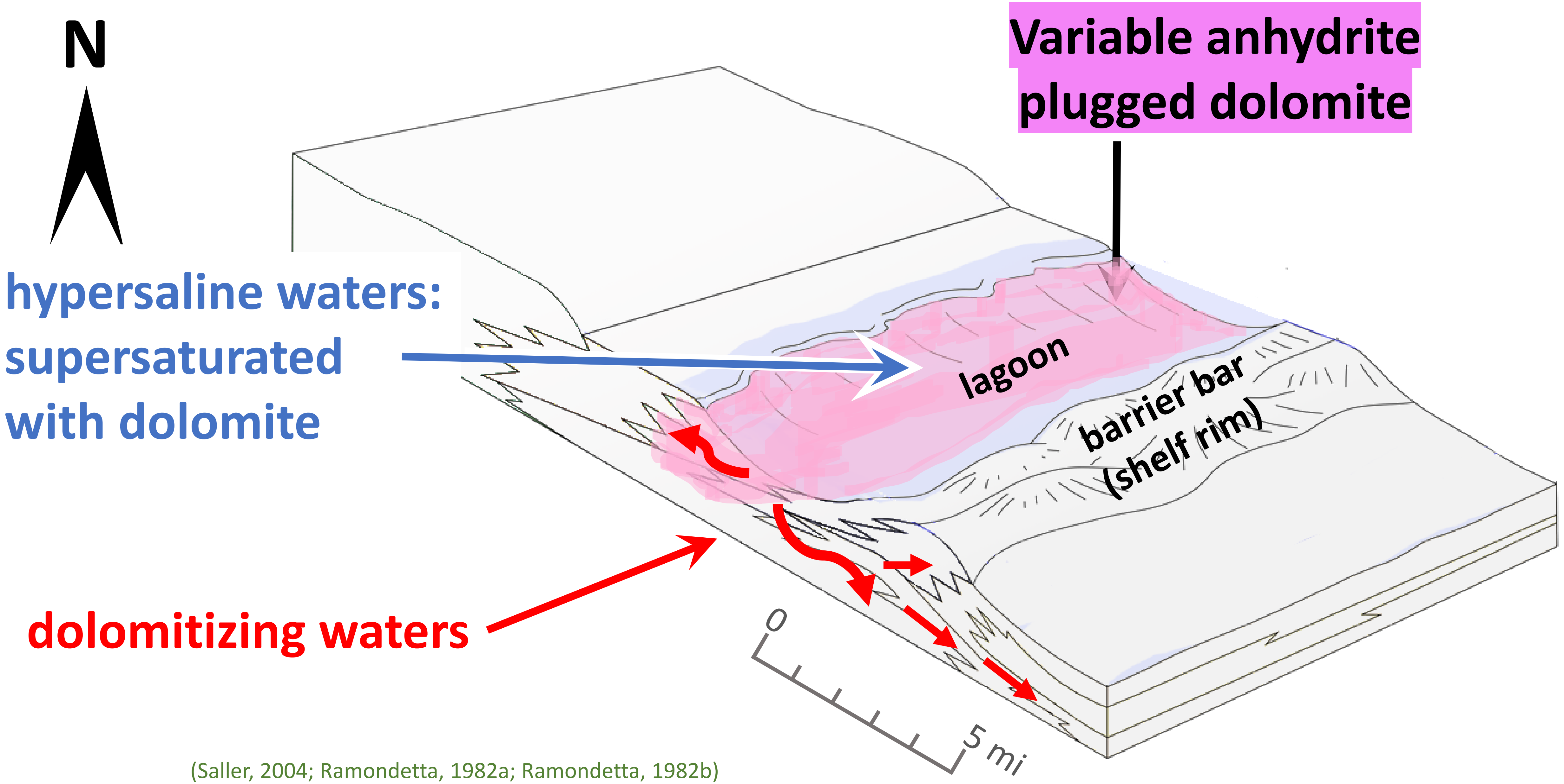

(Saller, 2004; Ramondetta, 1982a; Ramondetta, 1982b)

Hierarchy of Sea Level Fluctuations

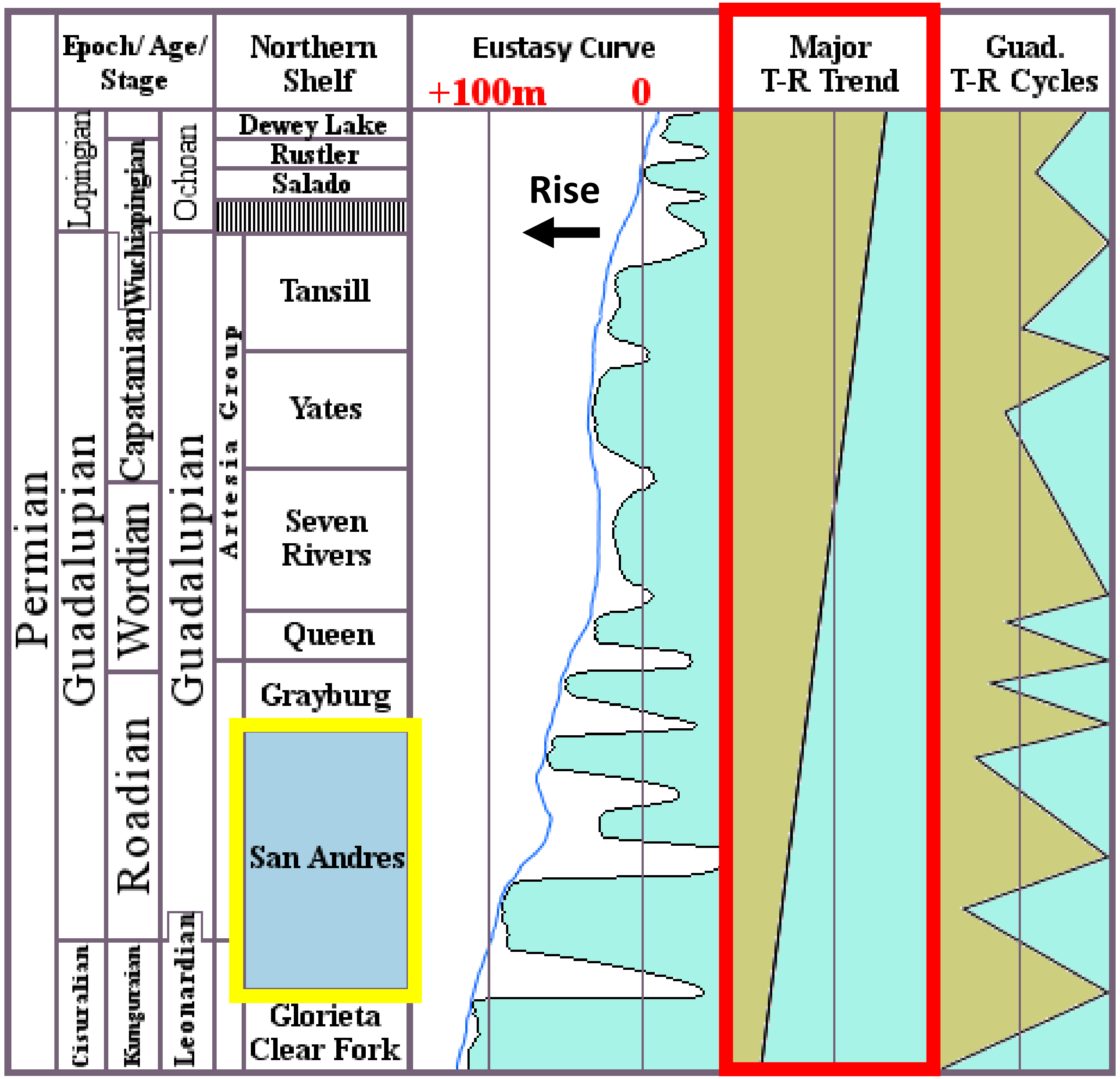

middle-Permian eustatic regression

San Andres eustatic transgressions

(Lopez-Gamundi, 2019; Ross and Ross, 1987; Ruppel, 2019)

π Marker Bed Deposited at Sea Level Lowstand

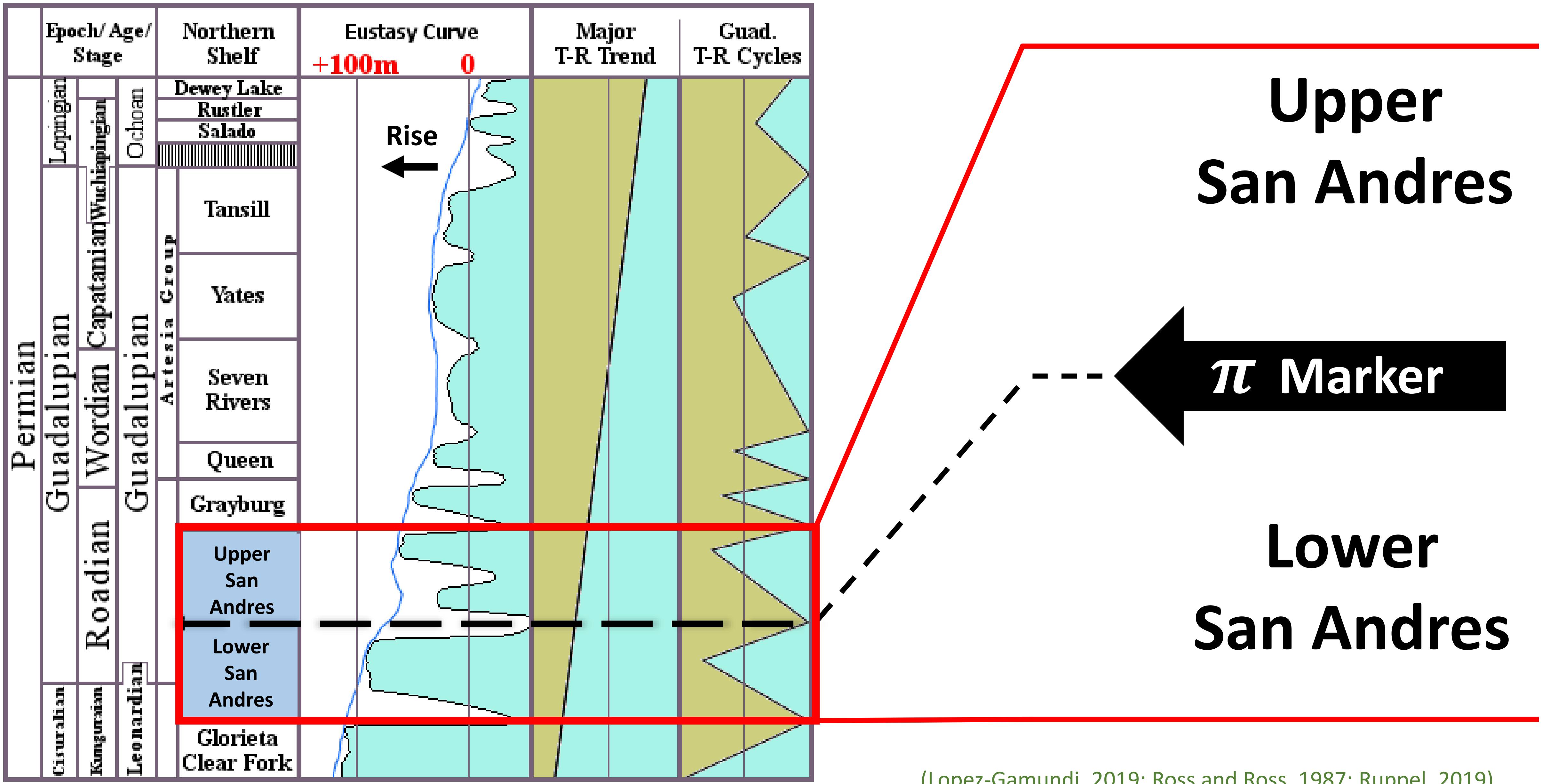

(Lopez-Gamundi, 2019; Ross and Ross, 1987; Ruppel, 2019)

High-Frequency Transgressive-Regressive Cycles

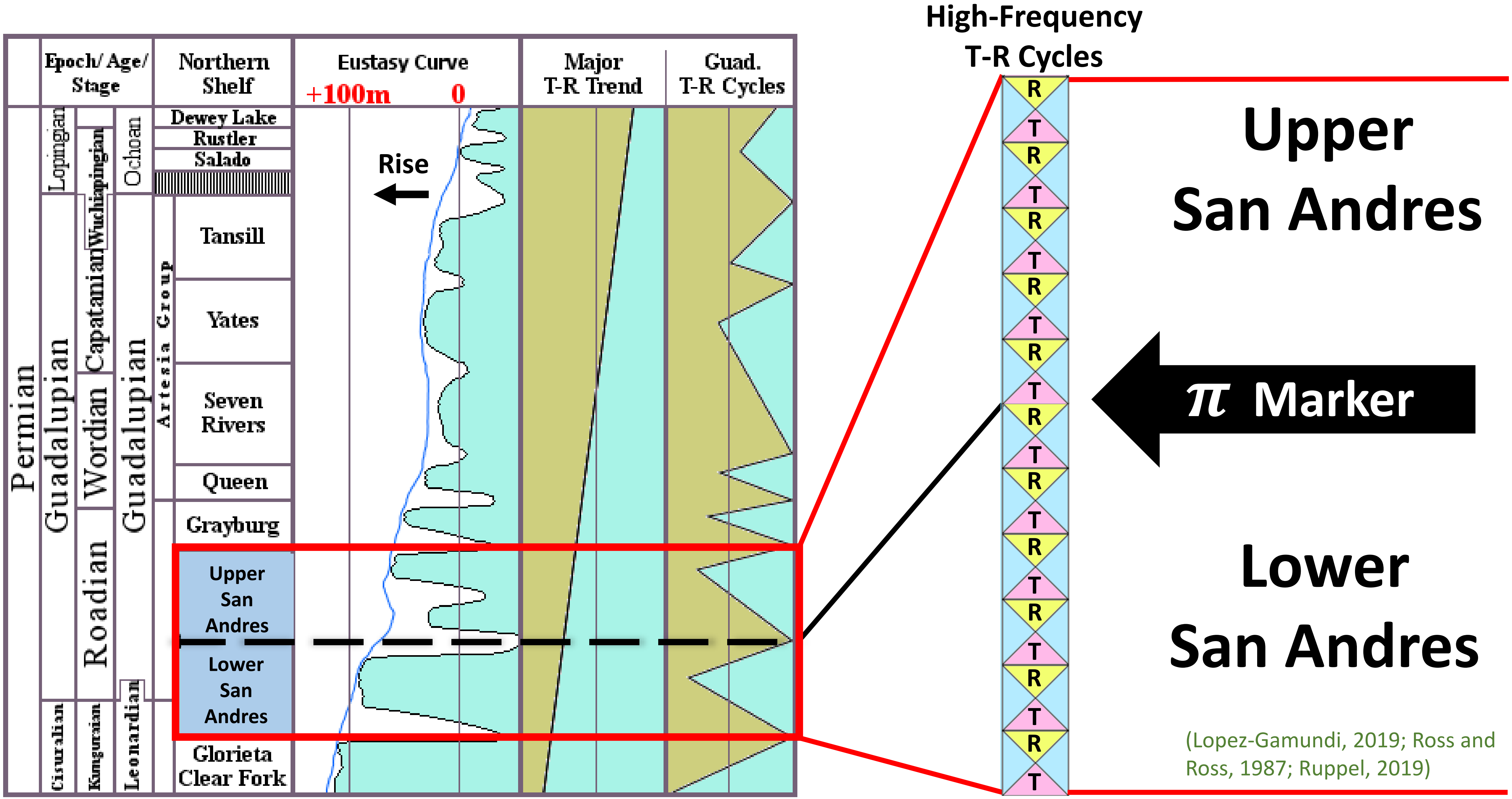

(Lopez-Gamundi, 2019; Ross and Ross, 1987; Ruppel, 2019)

Tight Supratidal Anhydrites & High Porosity Subtidal Dolomites

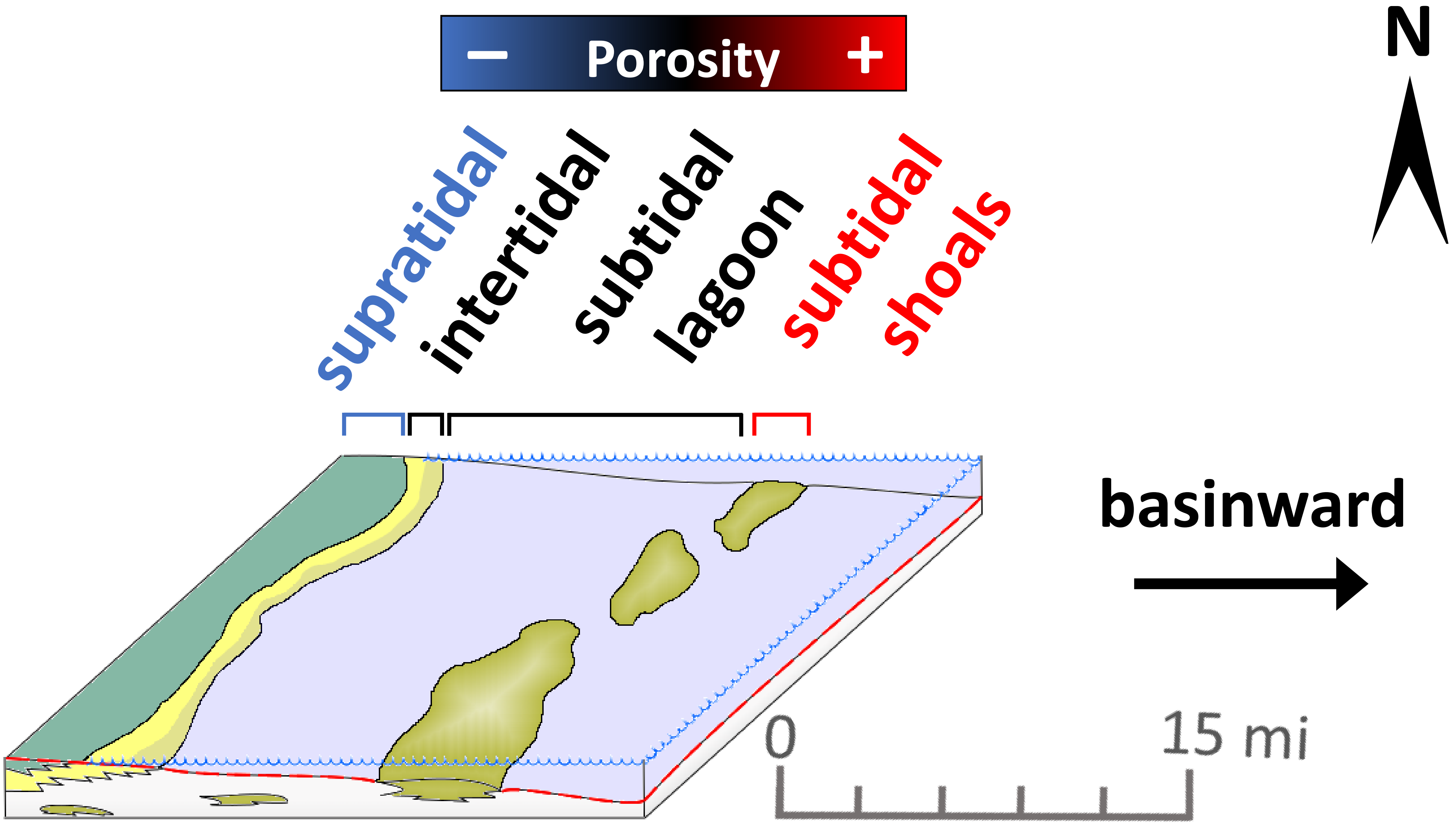

(Saller, 2004; Ramondetta, 1982a; Ramondetta, 1982b)

Cyclical Stacking of Porous & Tight Facies

High-Frequency T-R Cycles

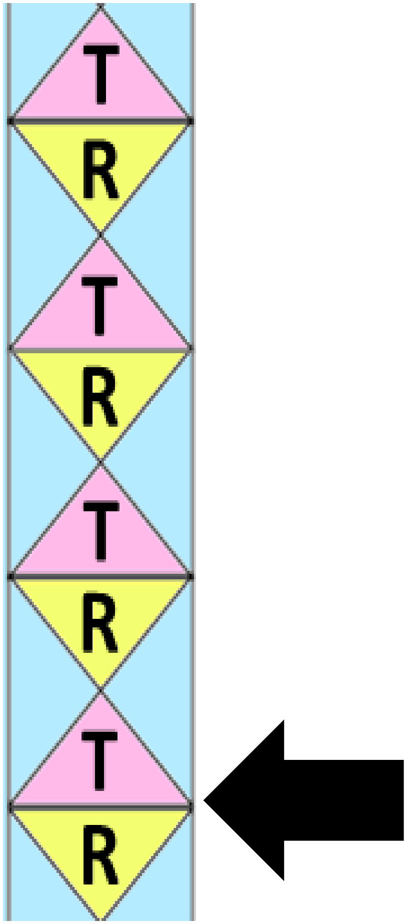

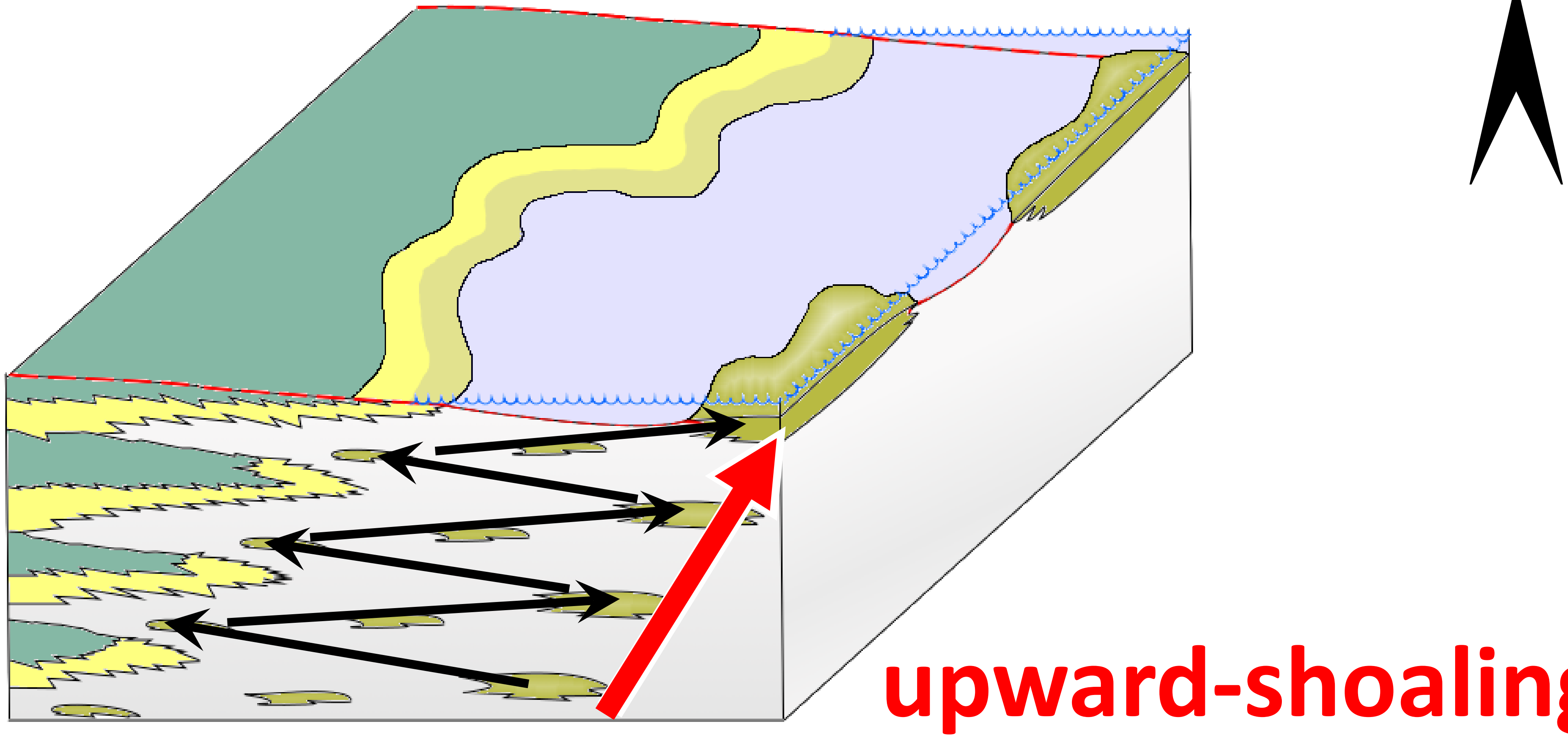

upward-shoaling
progradational-aggradational

(Ramondetta, 1982a; Ramondetta, 1982b; Ward et al., 1986)

Thick Reservoir Facies Grade Northward to Thin Beds

interbedded dolomite & anhydrite

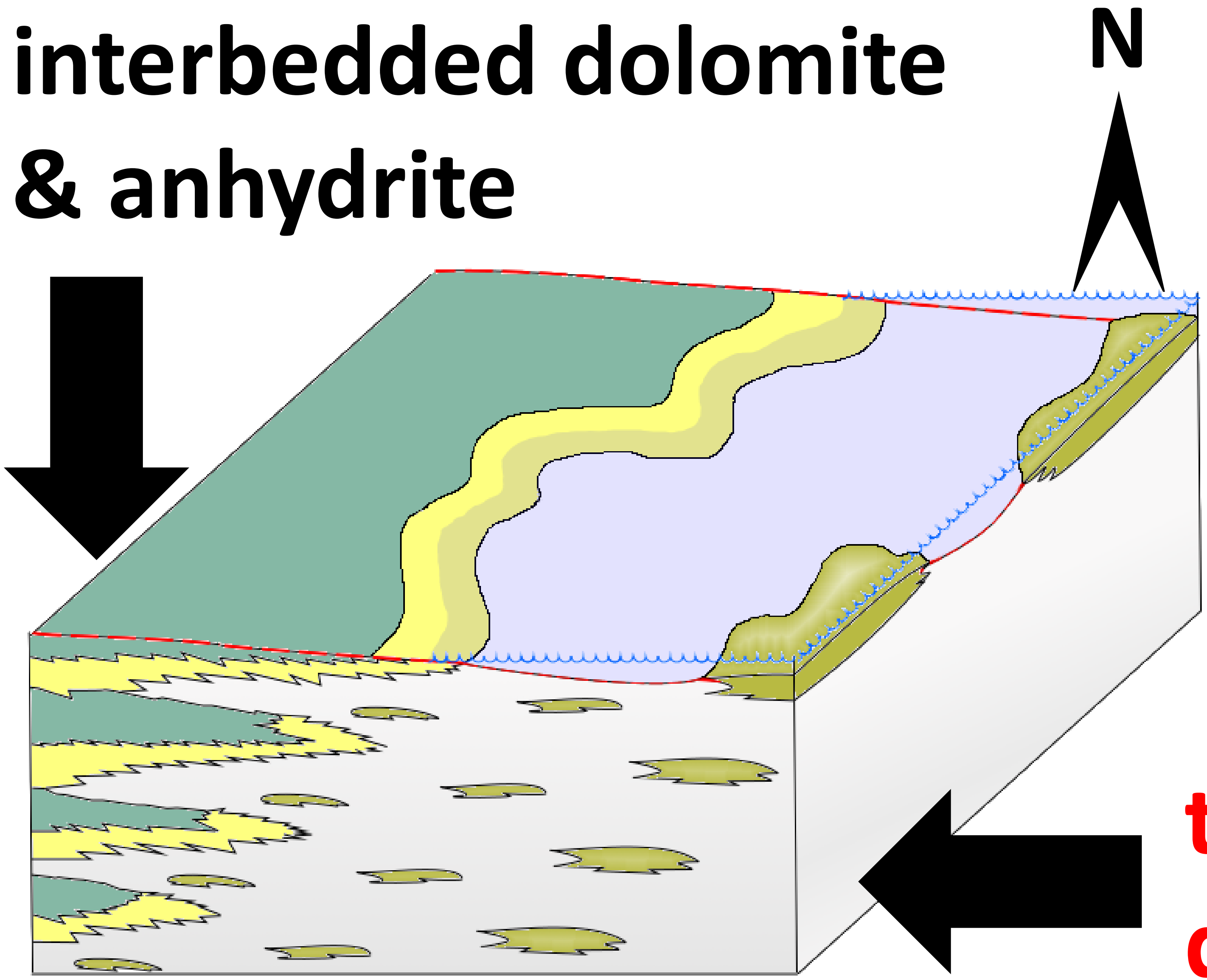

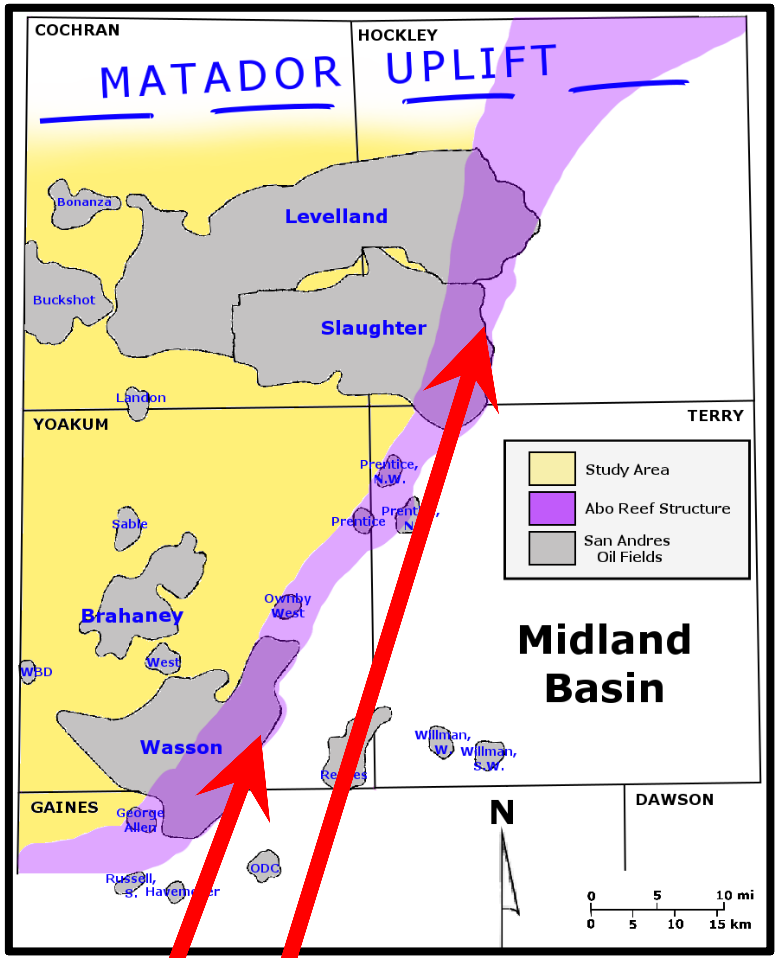

thick porous dolomite

(Ramondetta, 1982a; Ramondetta, 1982b)

Intercrystalline Macroporosity – Vugular Pores Increase With Depth

16186-01C 5000X

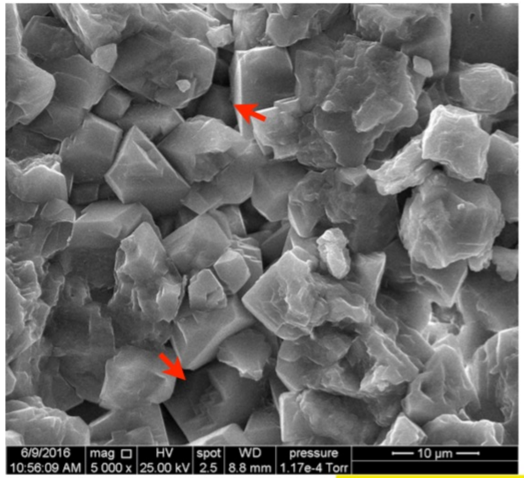

16186-02E 800X

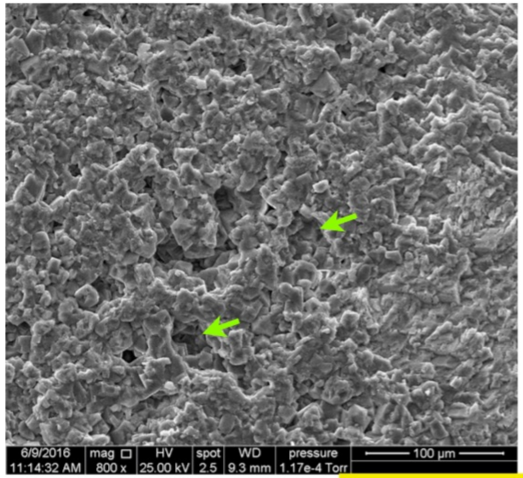

16186-03E 1300X

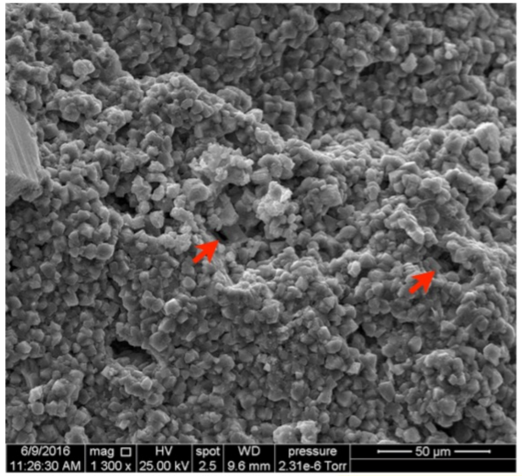

intercrystalline macroporosity

16186-01D 500X

Intercrystalline macroporosity (red arrows) and skel-moldic voids (green arrows).

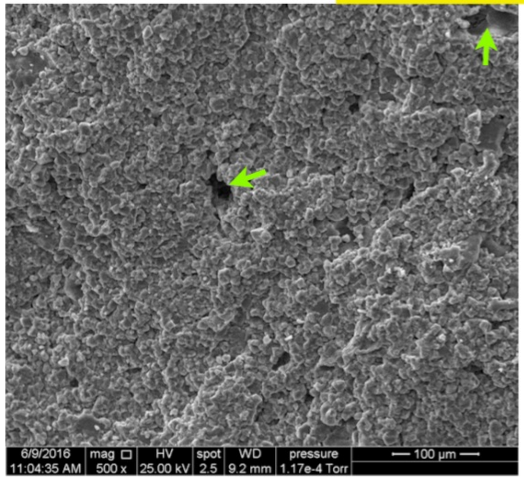

16186-02F 3000X

Over-sized voids (green arrows) suggesting the possible dissolution of precursor allochem grains

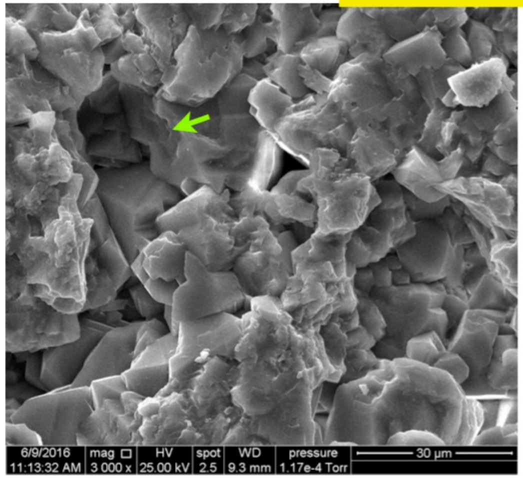

16186-03F 5000X

Over-sized void suggestive of a possible grain-moldic pore (red arrows)

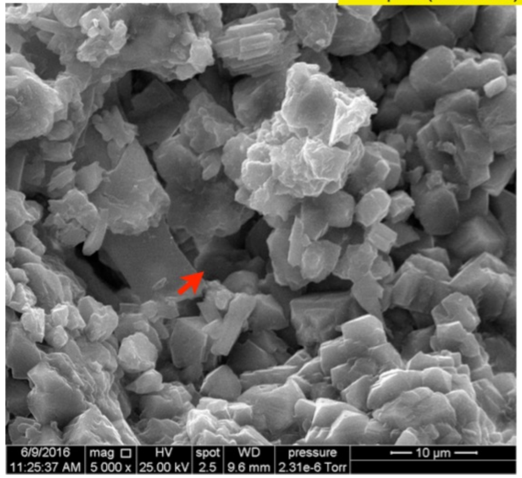

Oversized grain-moldic pores

(SEM images courtesy of Monadnock Resources, LLC)

Intercrystalline Macroporosity – Vugular Pores Increase With Depth

16186-01C 5000X

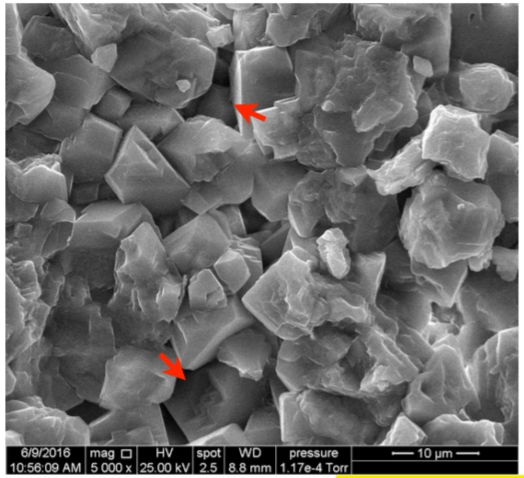

16186-02E 800X

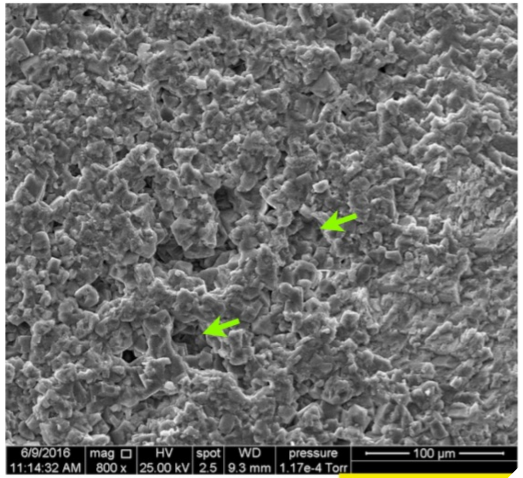

16186-03E 1300X

Intercrystalline macroporosity (re... arrows).

Over-sized void... suggesting the p... of precursor allo...

...oid suggestive ...e grain-moldic ...d arrows)

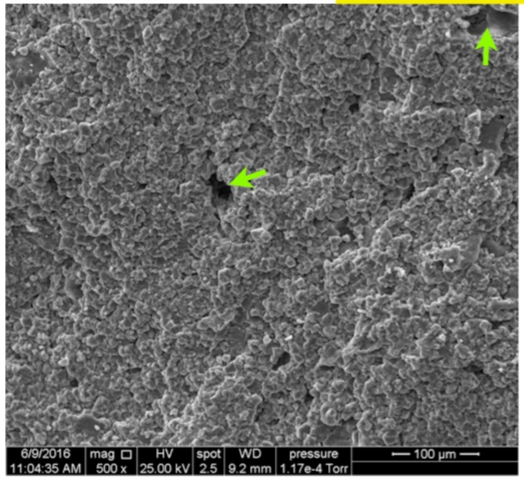

16186-02F 3000X

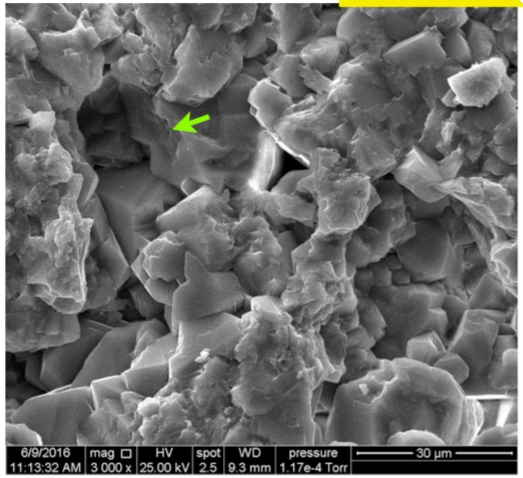

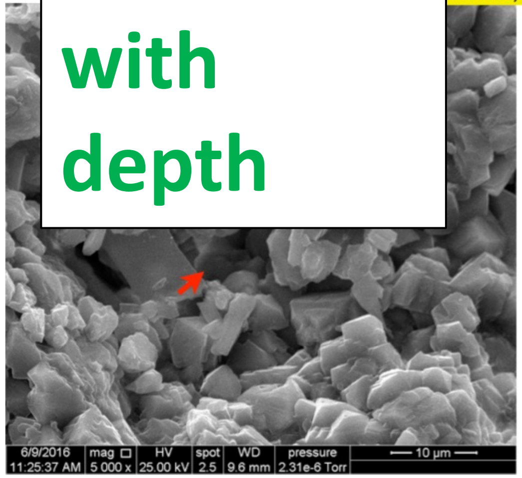

vugular porosity increases with depth

intercrystalline macroporosity

Oversized grain-moldic pores

(SEM images courtesy of Monadnock Resources, LLC)

Thick Reservoir Facies Grade Northward to Discrete Beds

interbedded dolomite & anhydrite

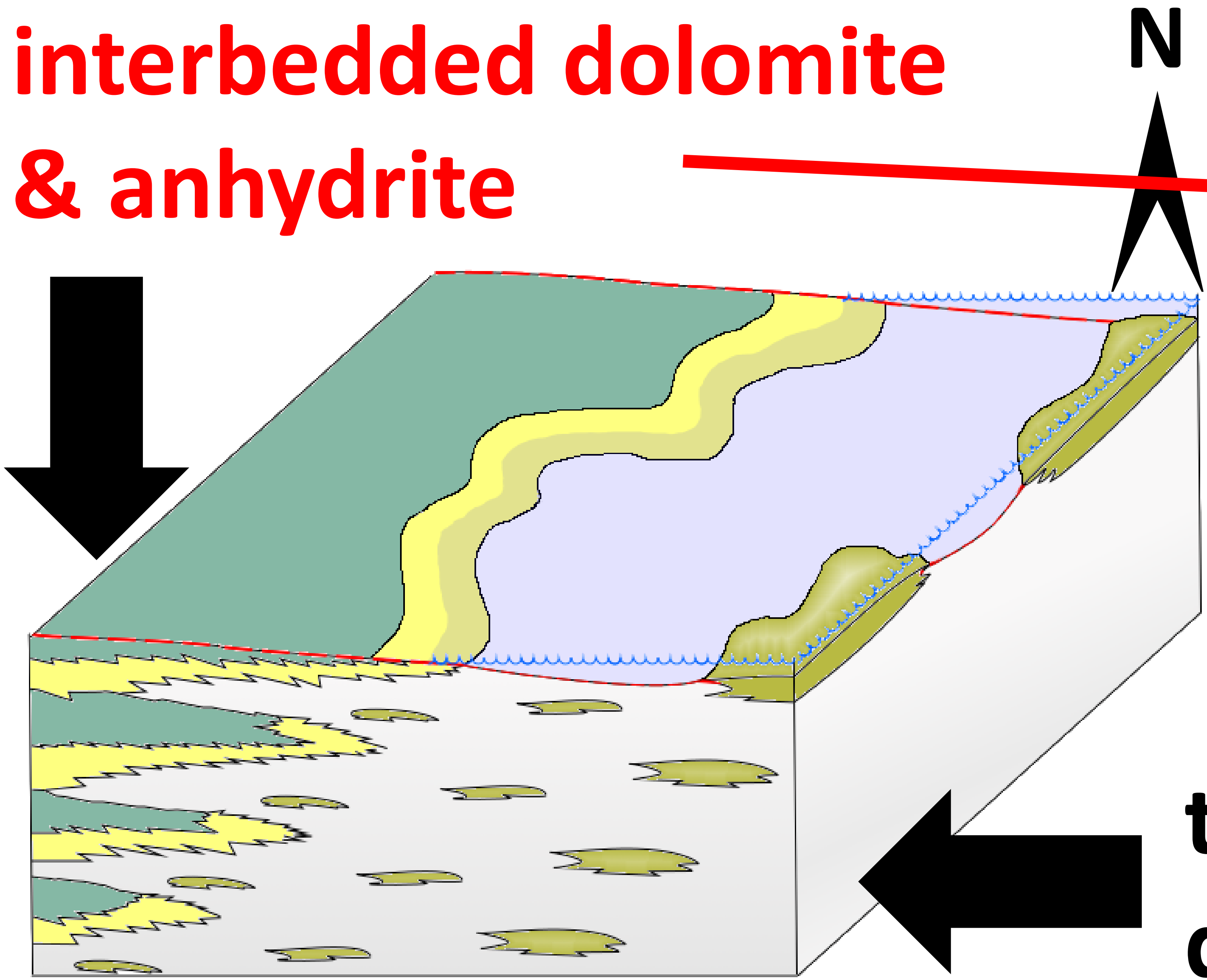

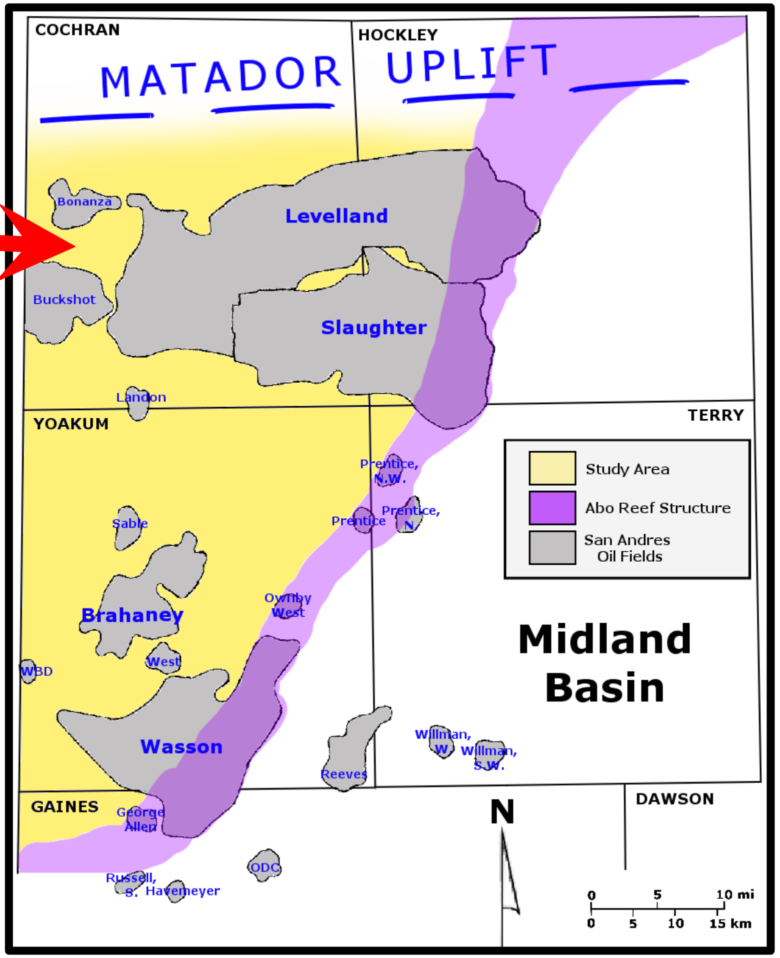

thick porous dolomite

(Ramondetta, 1982a; Ramondetta, 1982b)

Compaction Drape and Fracturing Atop Low-Relief Structures

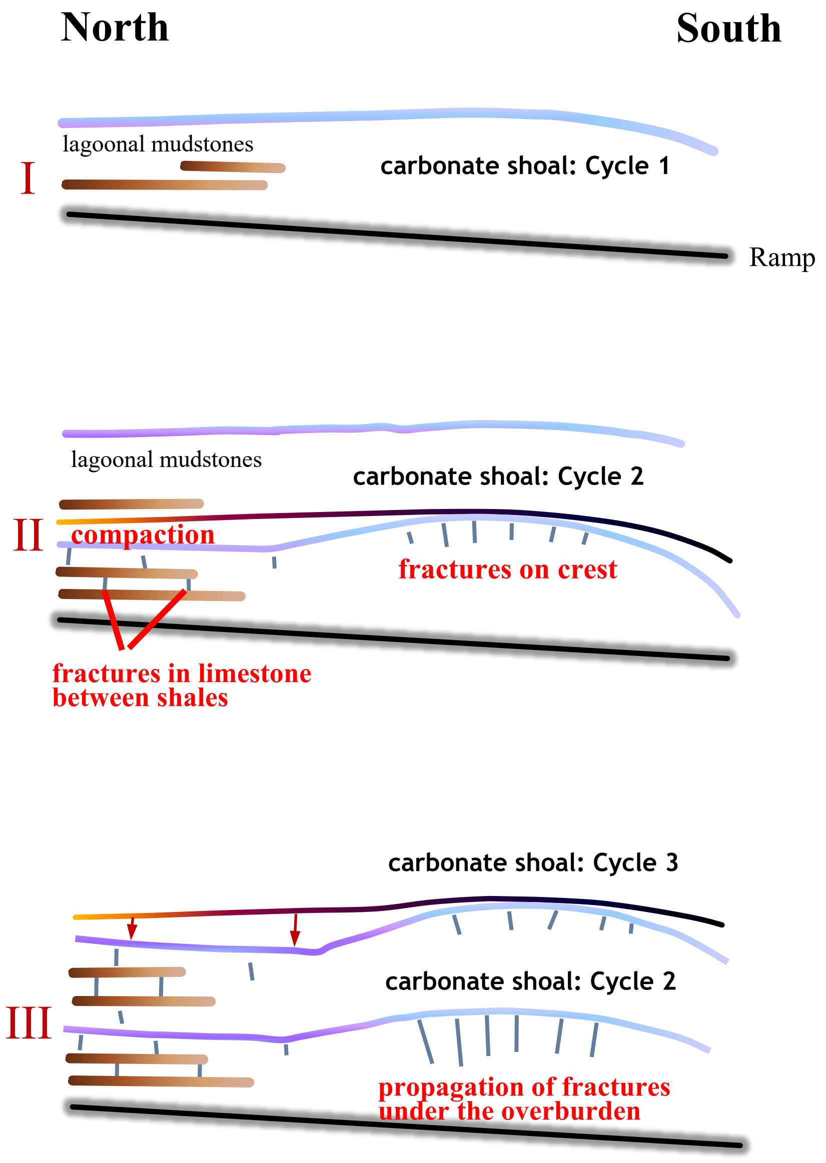

Deposition of Carbonates

Shallow Burial and Compaction of Mudstones

Further Burial and Compaction

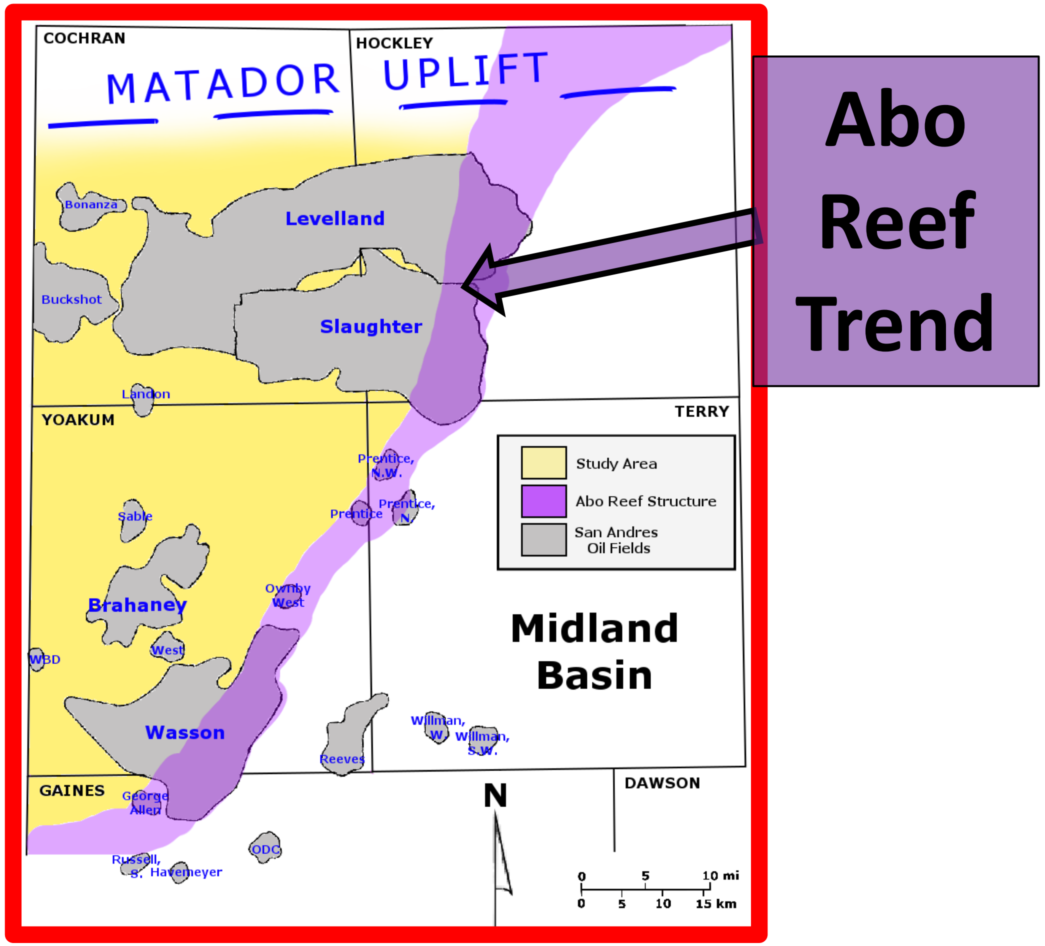

Outcrops in Guadalupe Mts. - ~150 mi. From W. Texas Reservoirs

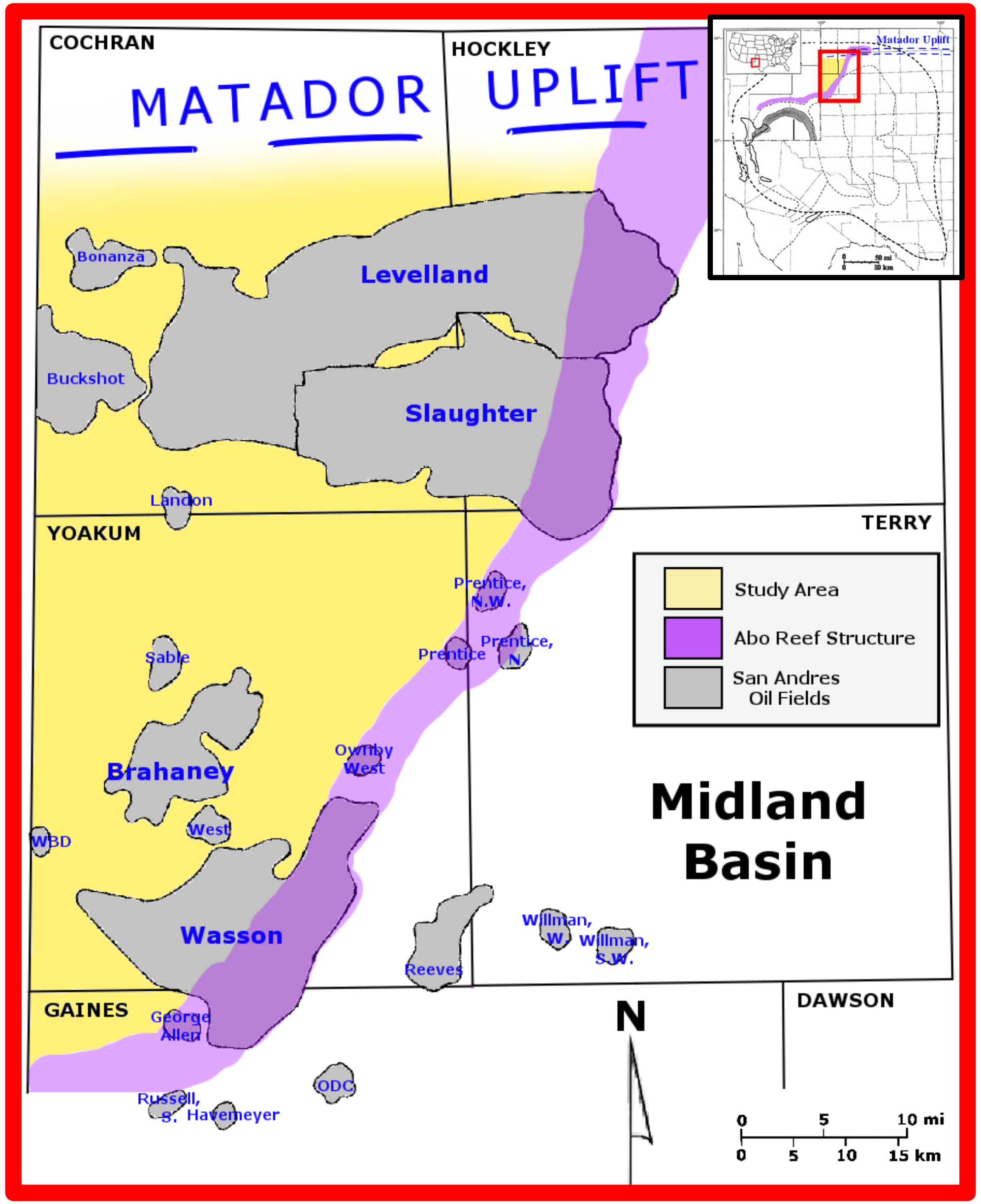

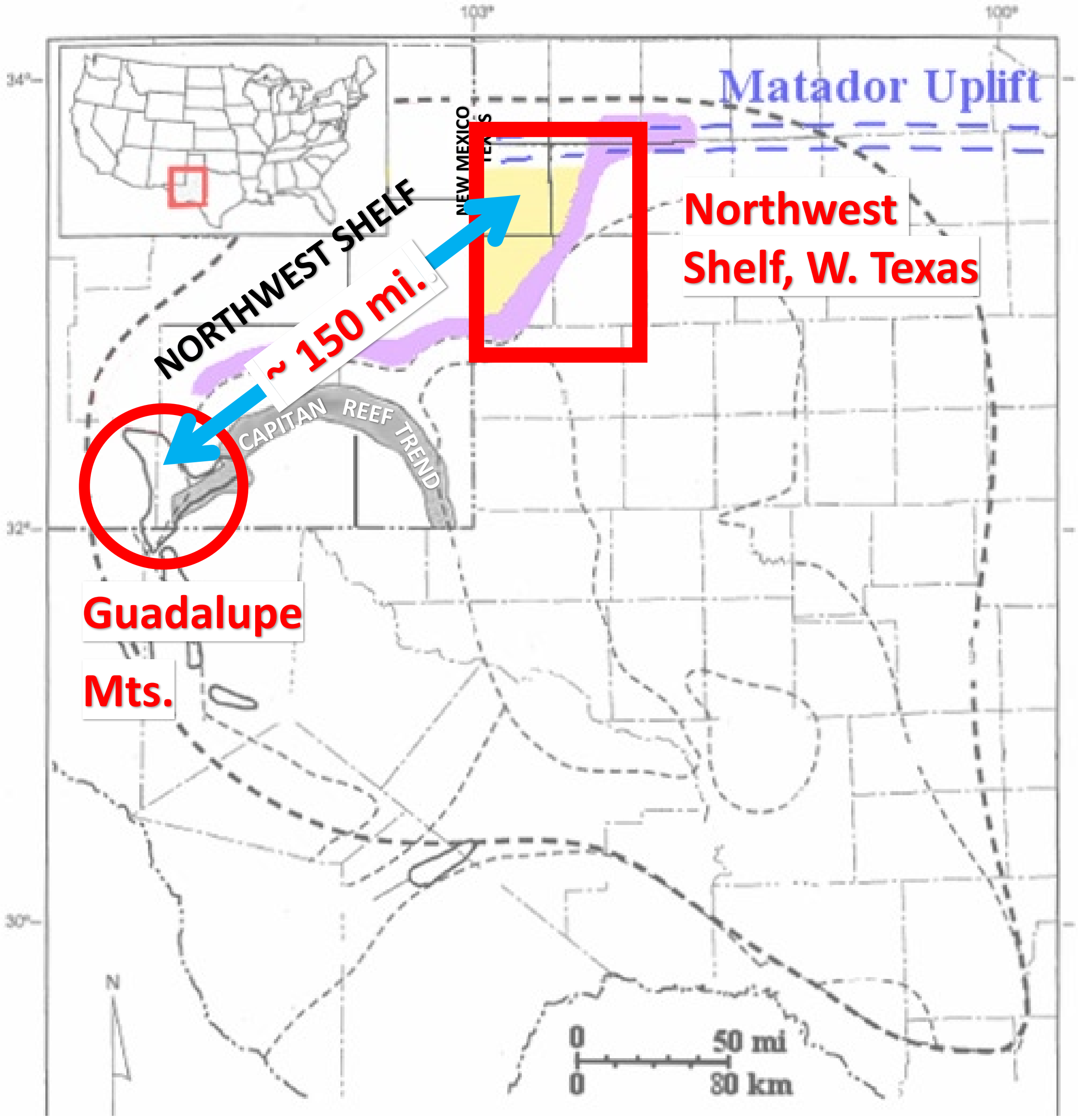

(Kerans, 2014; Ruppel, 2019)

Progradational-Aggradational San Andres Shelf Migration

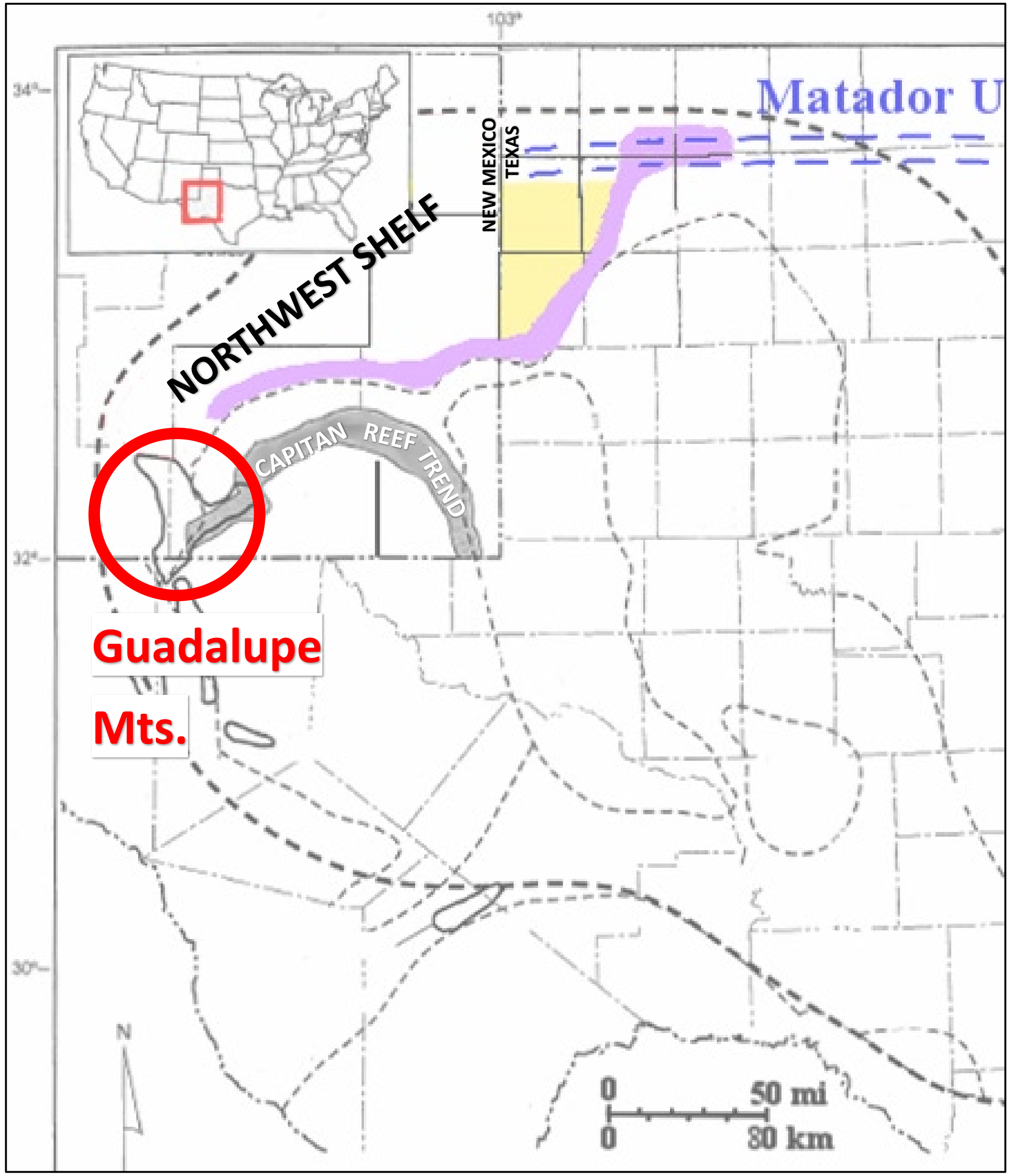

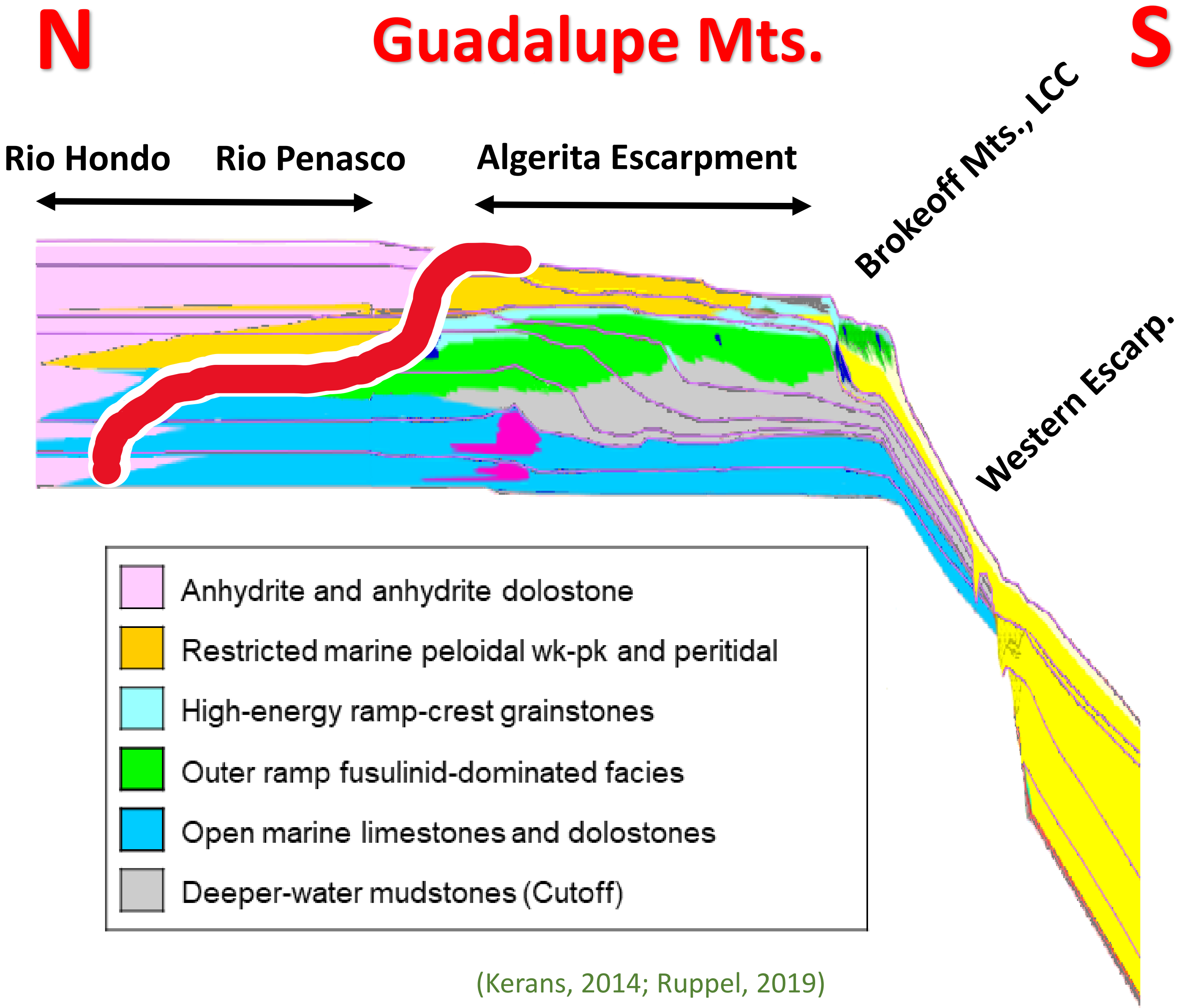

(Kerans, 2014; Ruppel, 2019)

Oil Fields Occur in Increasingly Younger Strata – Offsetting Basinward

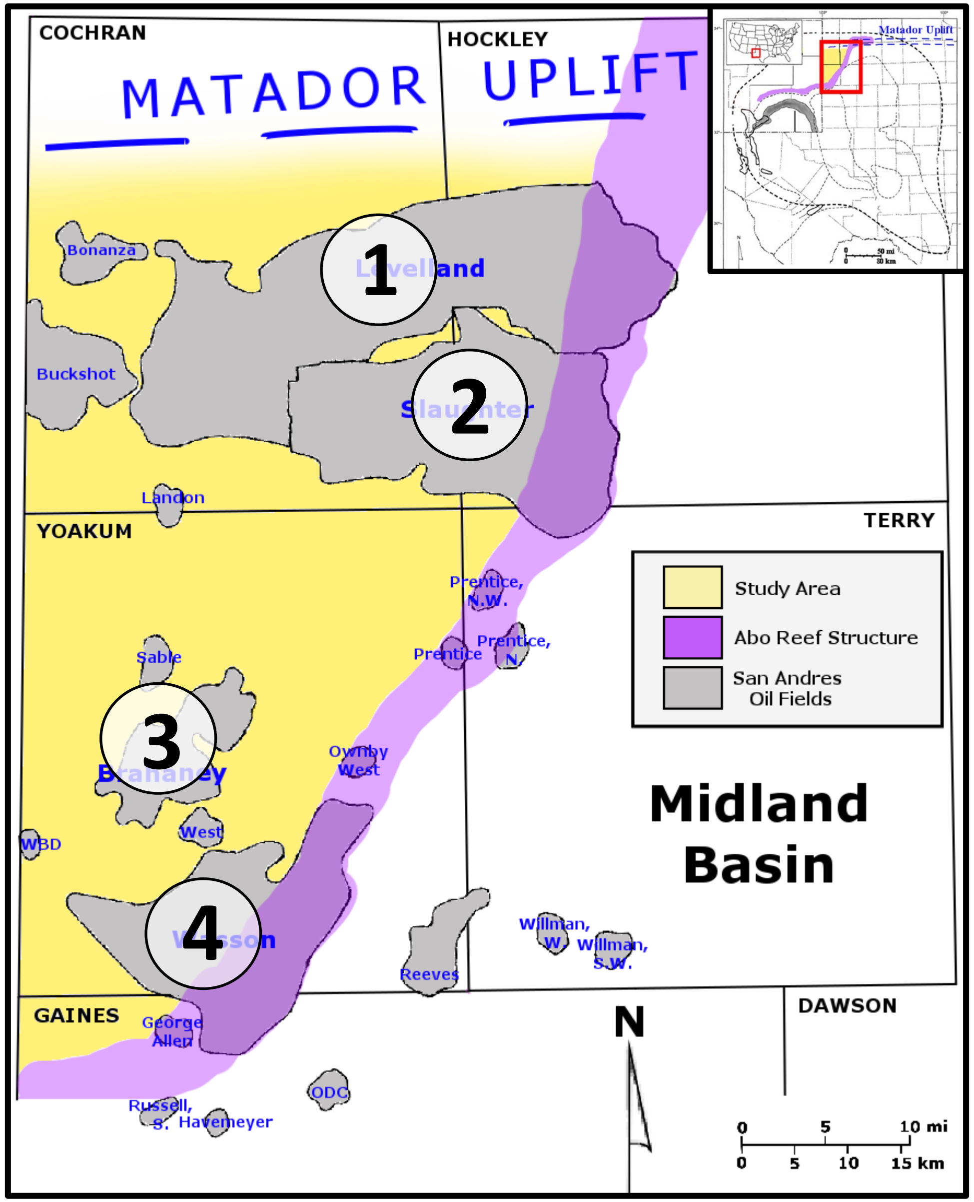

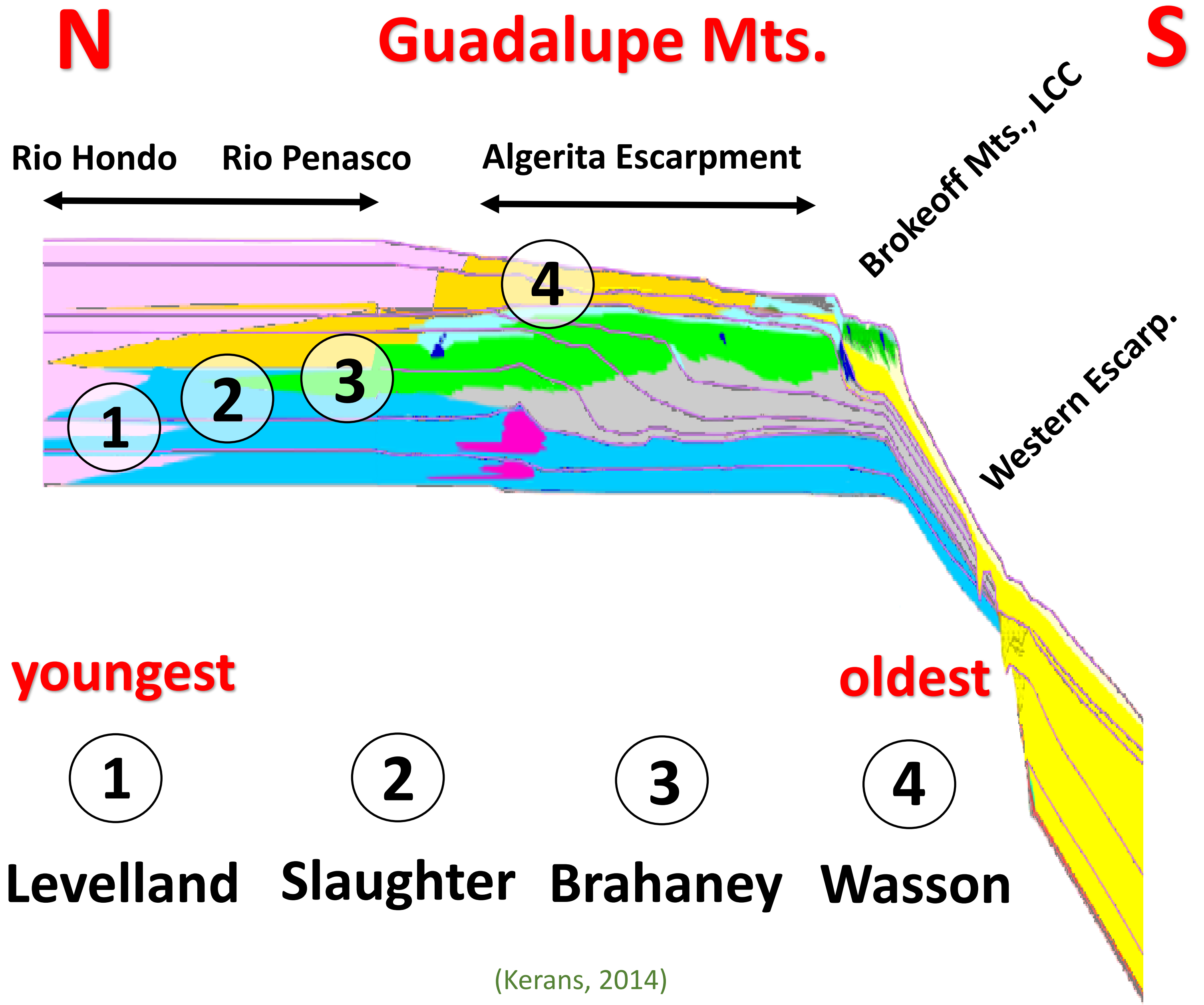

(Kerans, 2014)

Sabkha Evaporites Extend Southward During Mid-Permian Regression

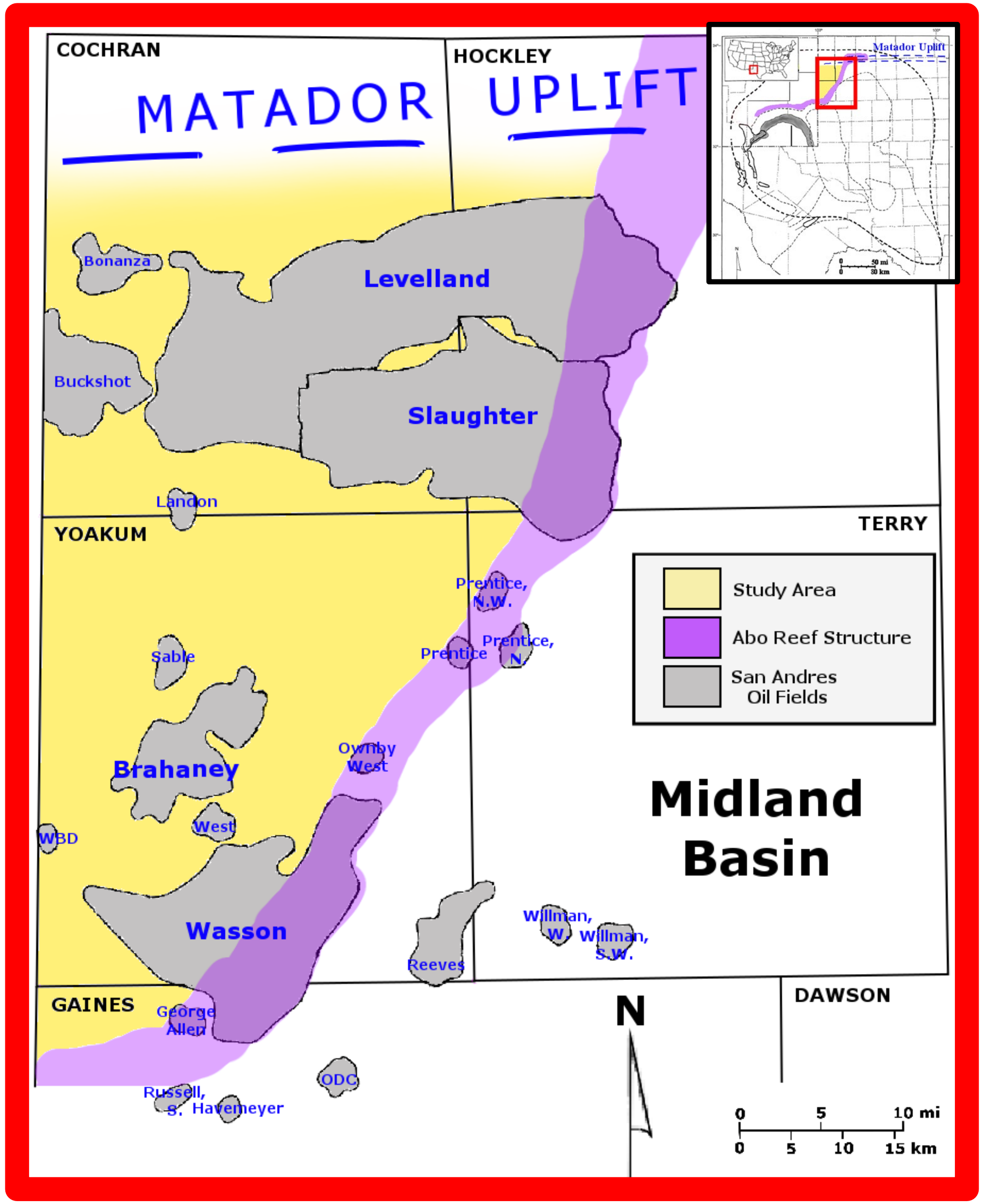

Early Guadalupian (268 Ma)

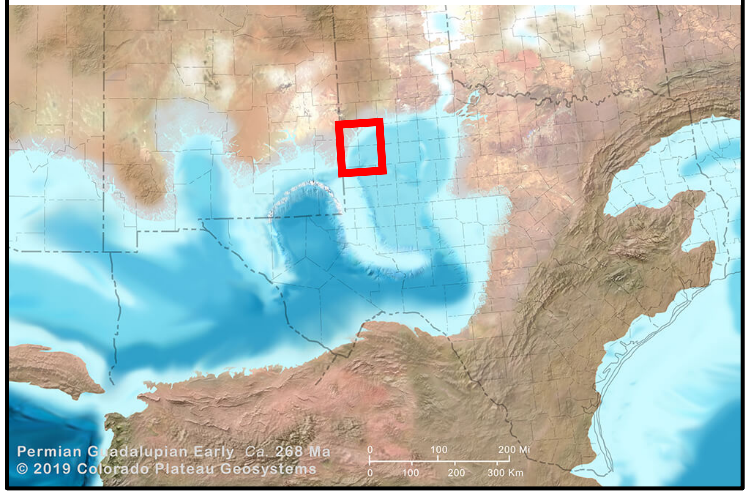

Late Guadalupian (263 Ma)

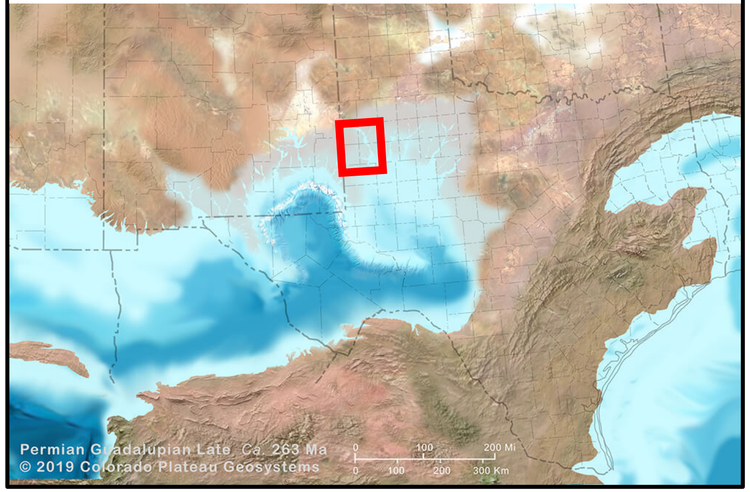

(Blakey, 2019)

San Andres at margin of Midland Basin open marine waters

Continued sea level fall: supratidal sabkhas extend over the Midland Basin

Structure Map of the π Marker – The Base of the Reservoir Seal

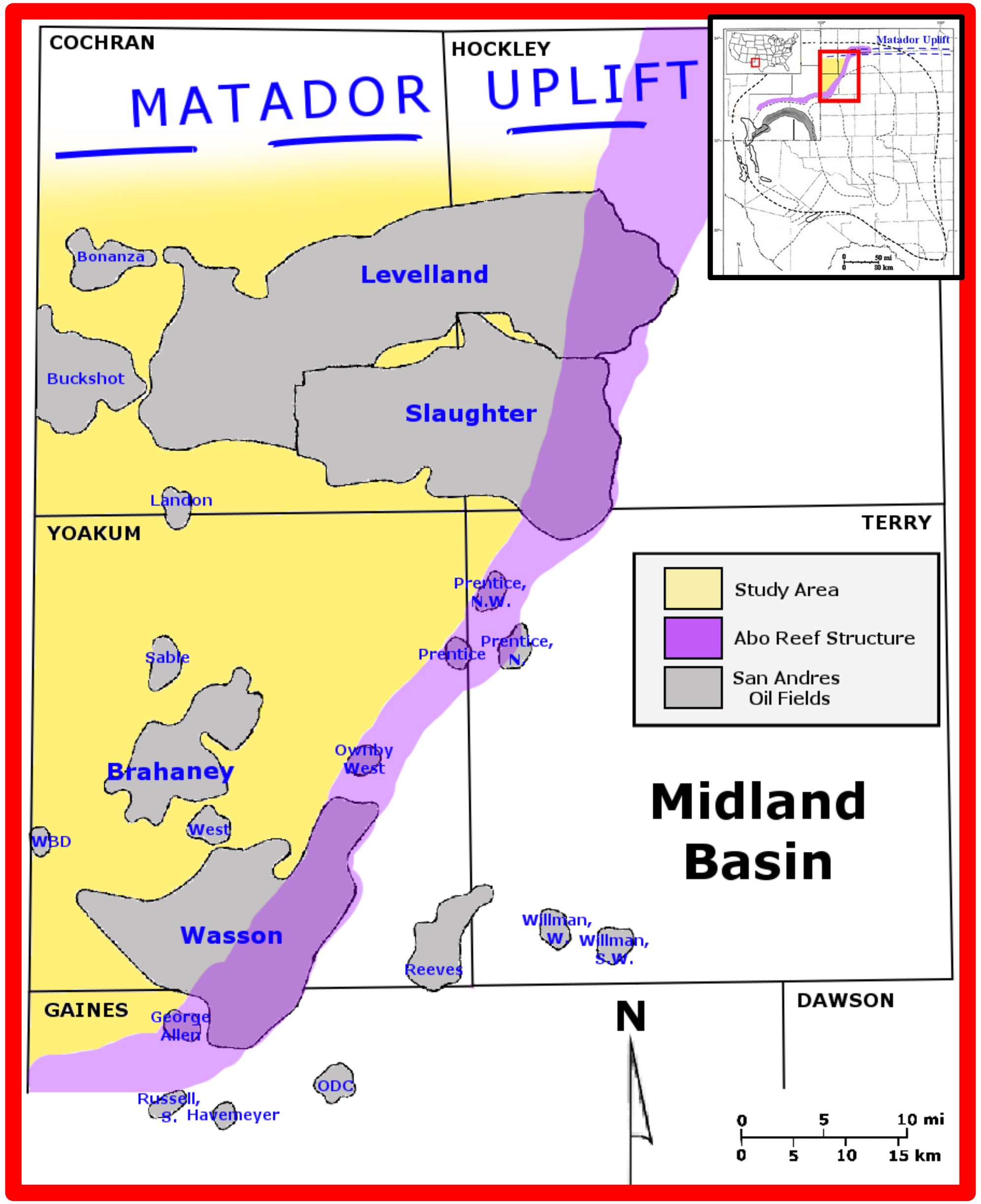

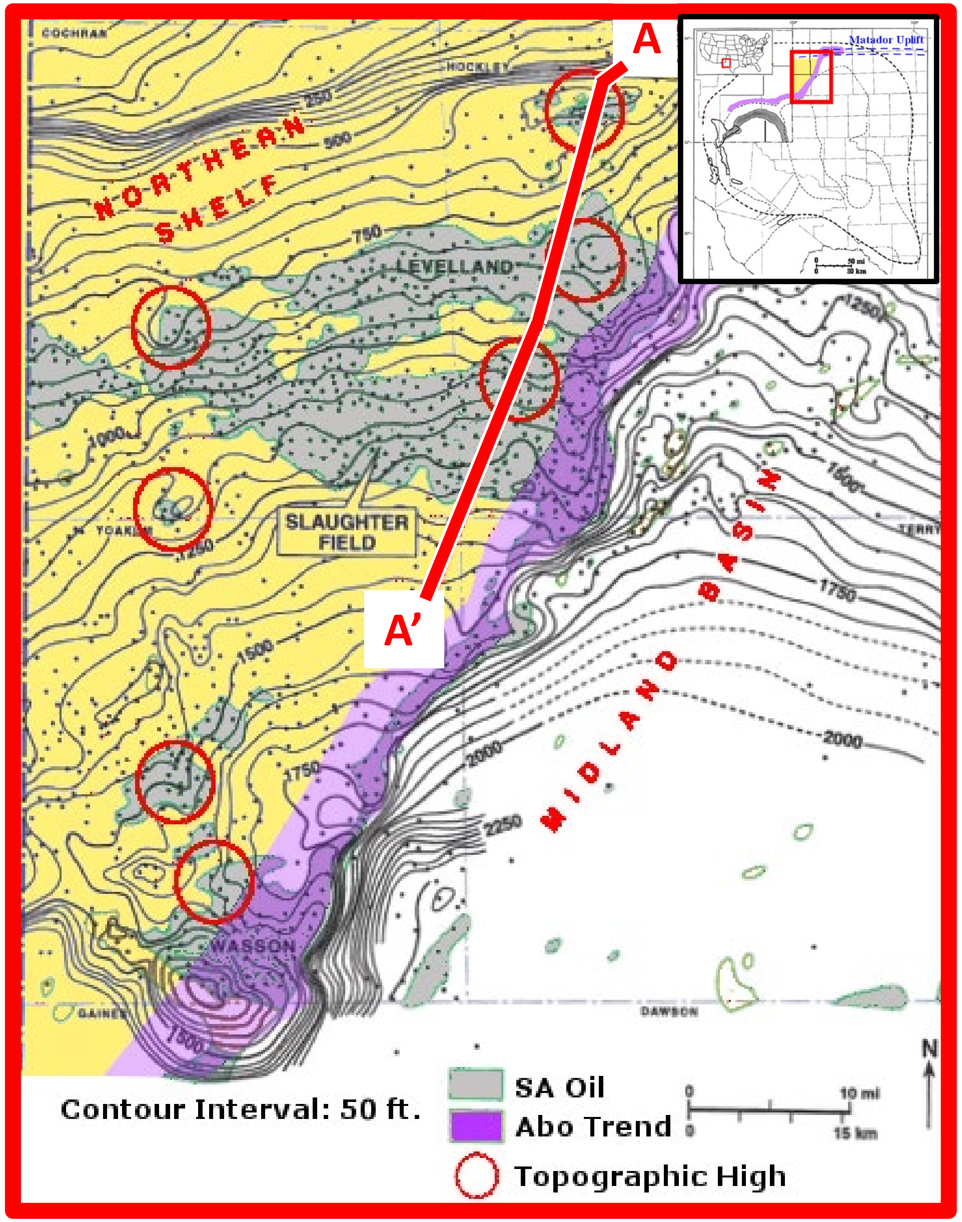

(Ramondetta, 1982a; Ramondetta, 1982b)

Inner-to-Outer Shelf Reservoir Architecture

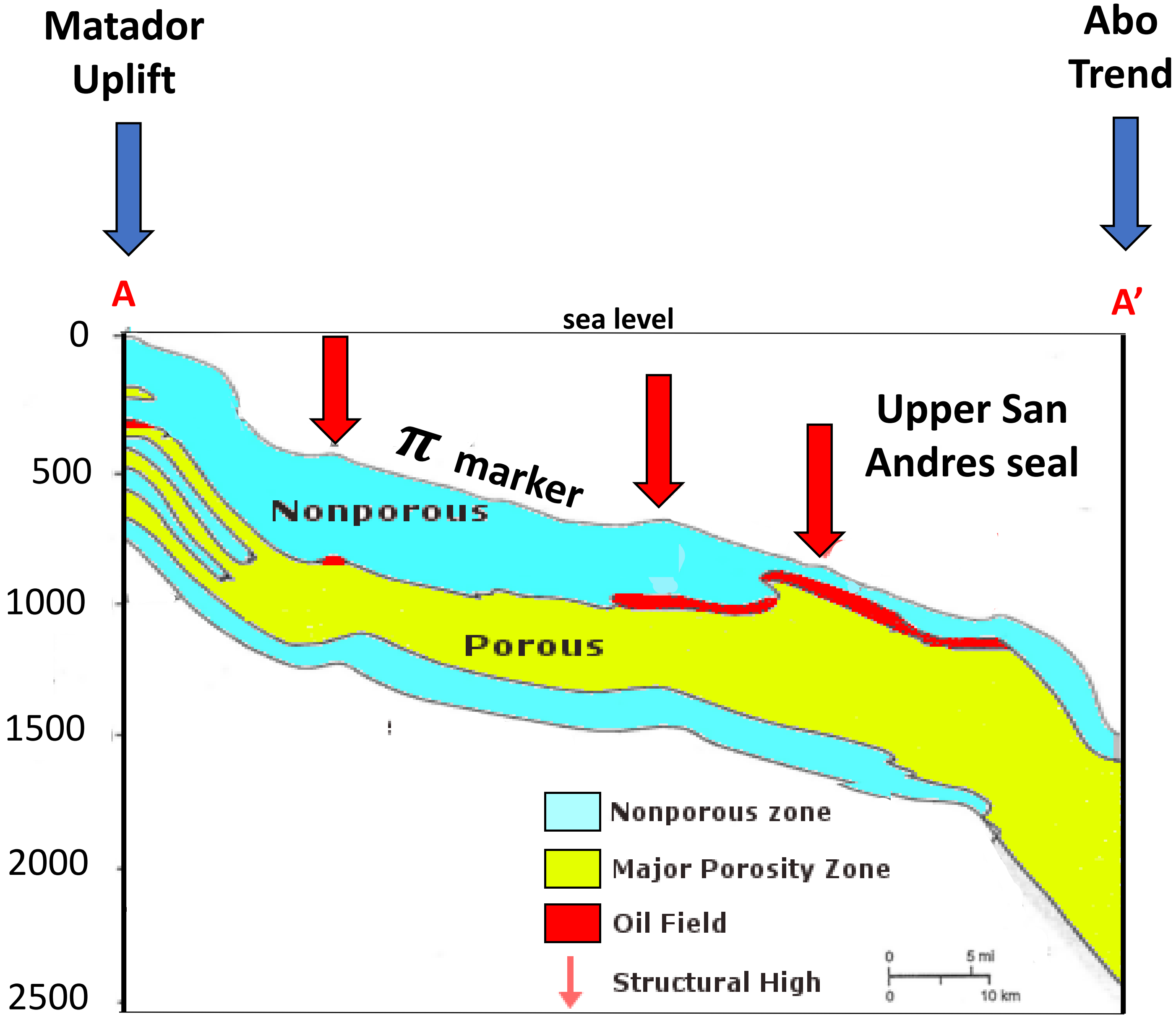

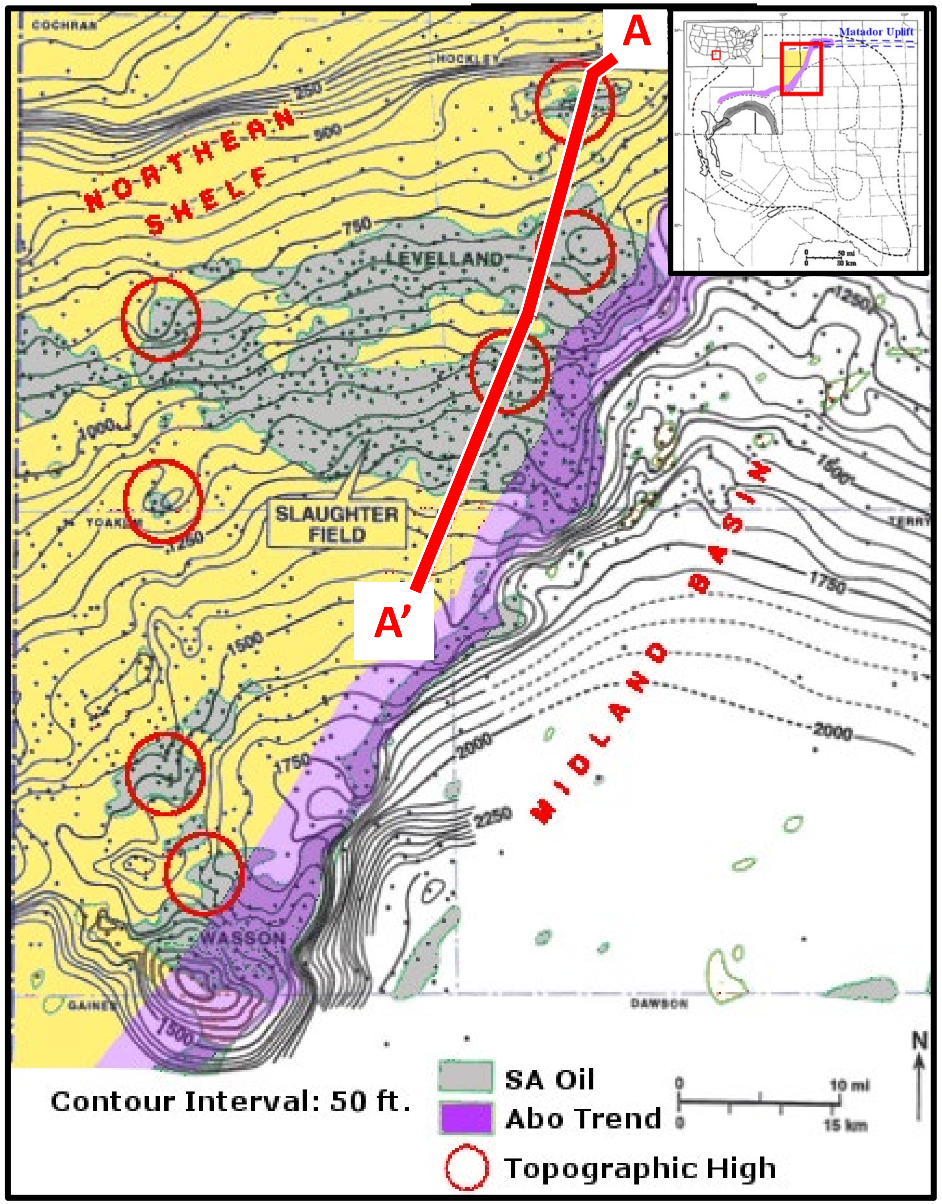

(Ebanks, 1990; Ramondetta, 1982a; Ramondetta, 1982b)

Migration and Successive Trapping in Updip Porosity Pinchouts

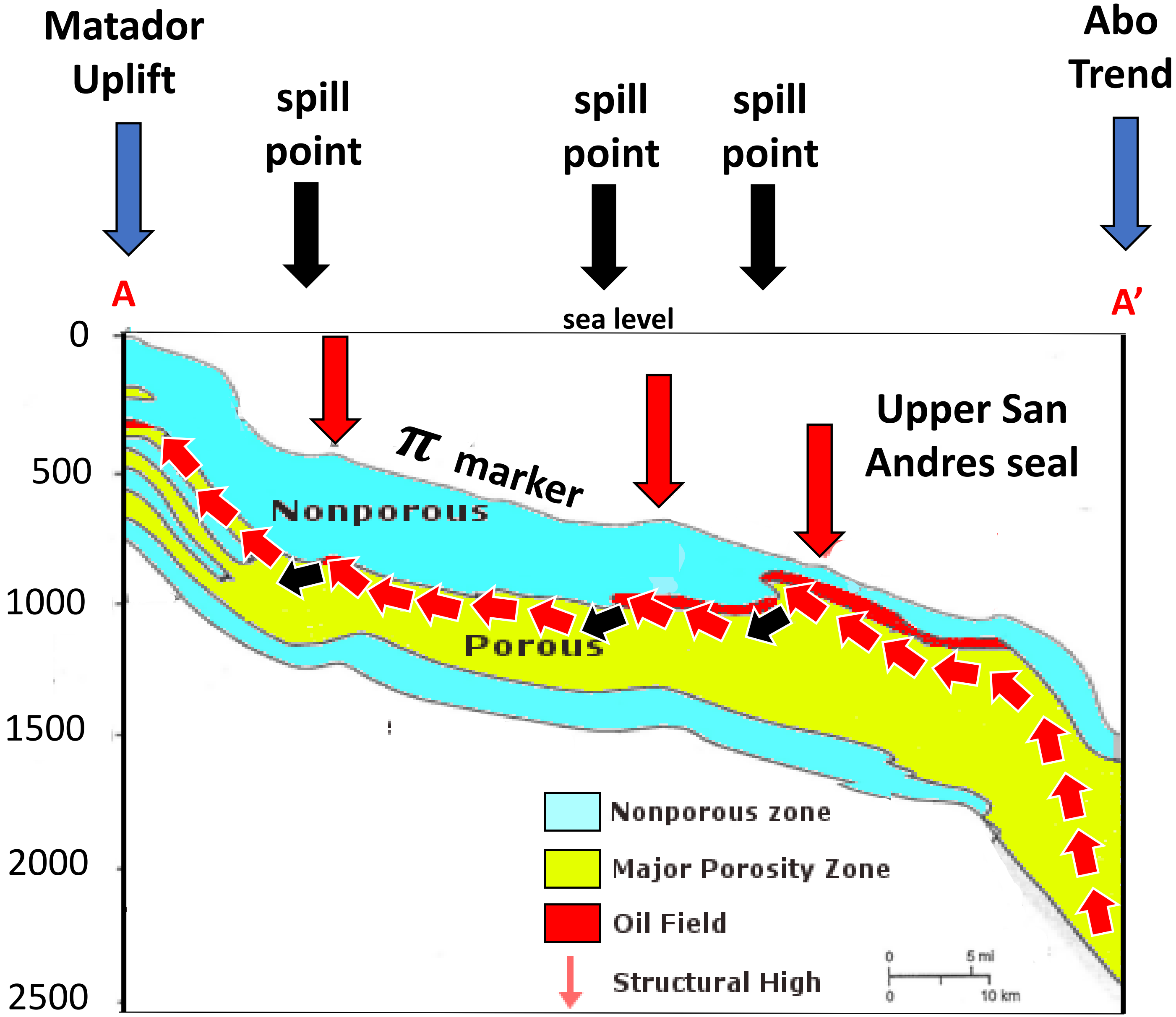

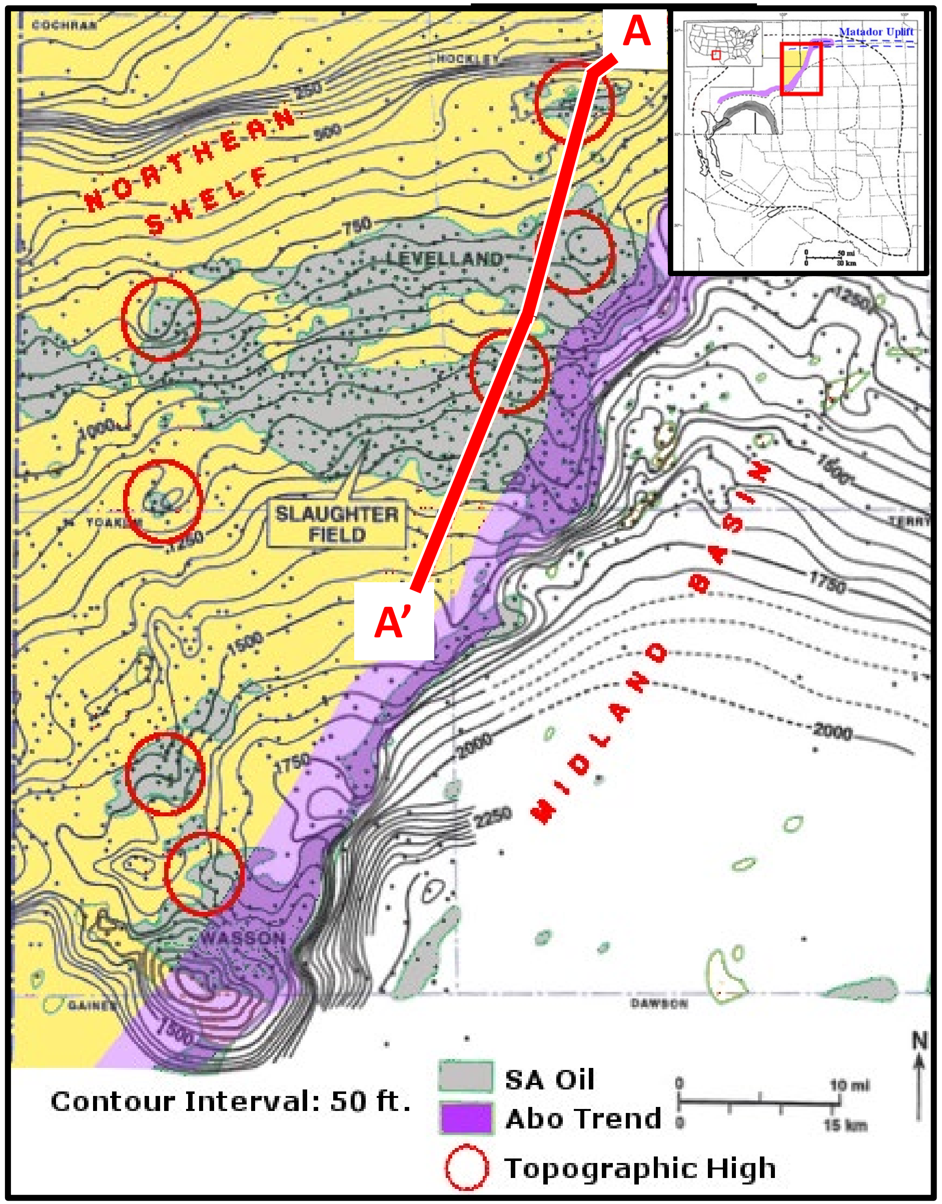

(Ebanks, 1990; Ramondetta, 1982a; Ramondetta, 1982b)

Oil Saturation Continues Below the Conventional Fields

Vertical Oil Saturation Profile

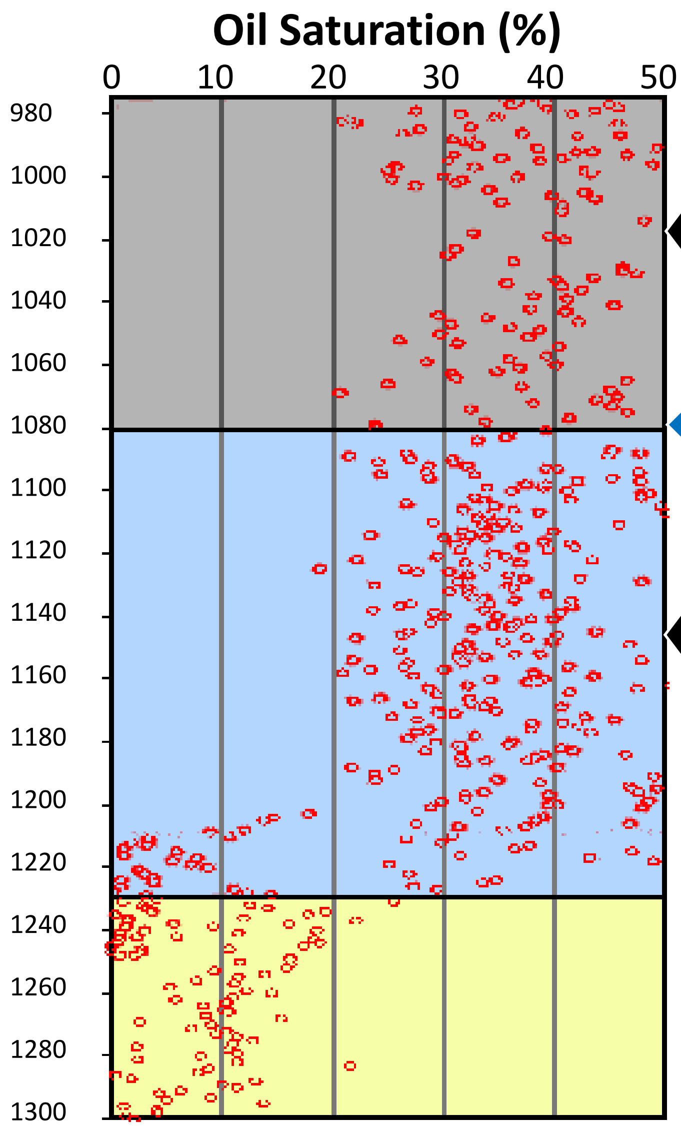

main pay zone:
vertical target – occurs on low-relief structures

Oil-water contact

transitional oil zone:
water-laden interval (decreasing oil saturation with depth & increasing water saturation)

Goldsmith Landreth San Andres Unit, Ector Co., TX

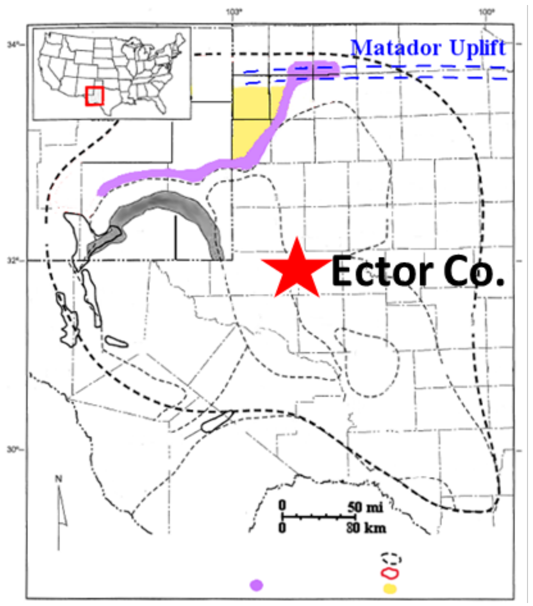

(Ruppel, 2019; Trentham and Melzer, 2019)

Oil Saturation Decreases With Depth; Water Saturation Increases

Vertical Oil Saturation Profile

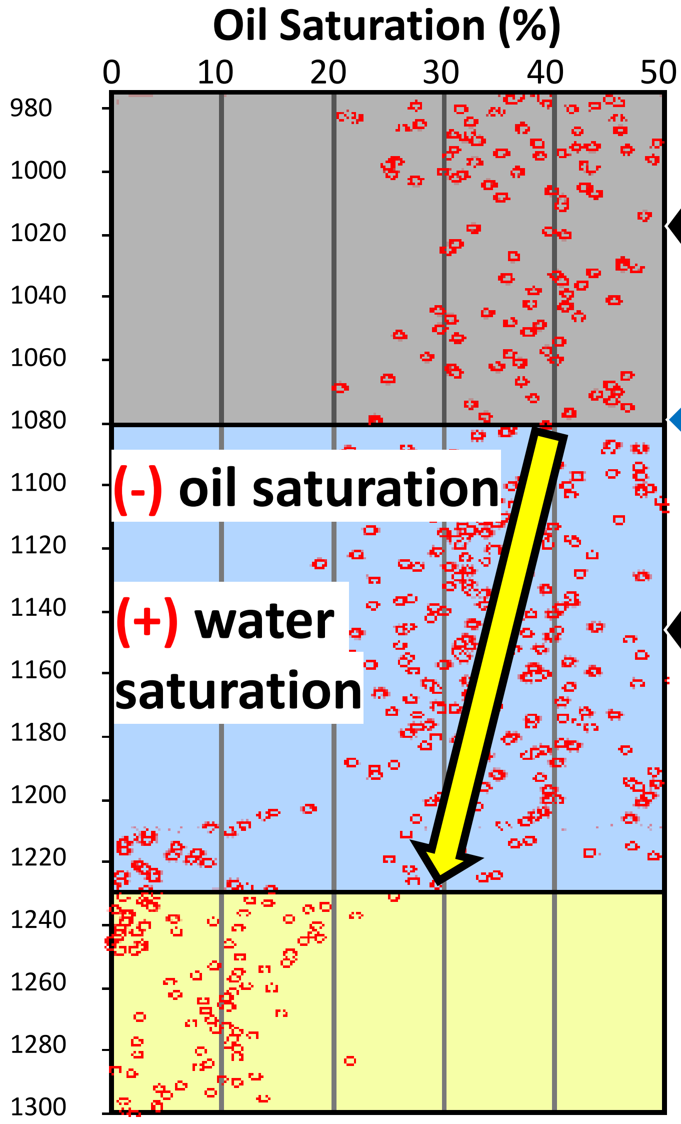

main pay zone:
vertical target – occurs on low-relief structures

Oil-water contact

transitional oil zone:
water-laden interval (decreasing oil saturation with depth & increasing water saturation)

Goldsmith Landreth San Andres Unit, Ector Co., TX

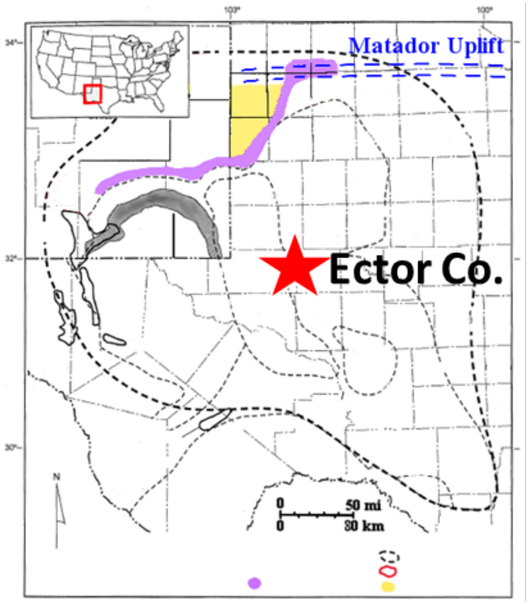

(Ruppel, 2019; Trentham and Melzer, 2019)

Indication of a Larger Paleo Oil Trap and Subsequent Flushing

Vertical Oil Saturation Profile

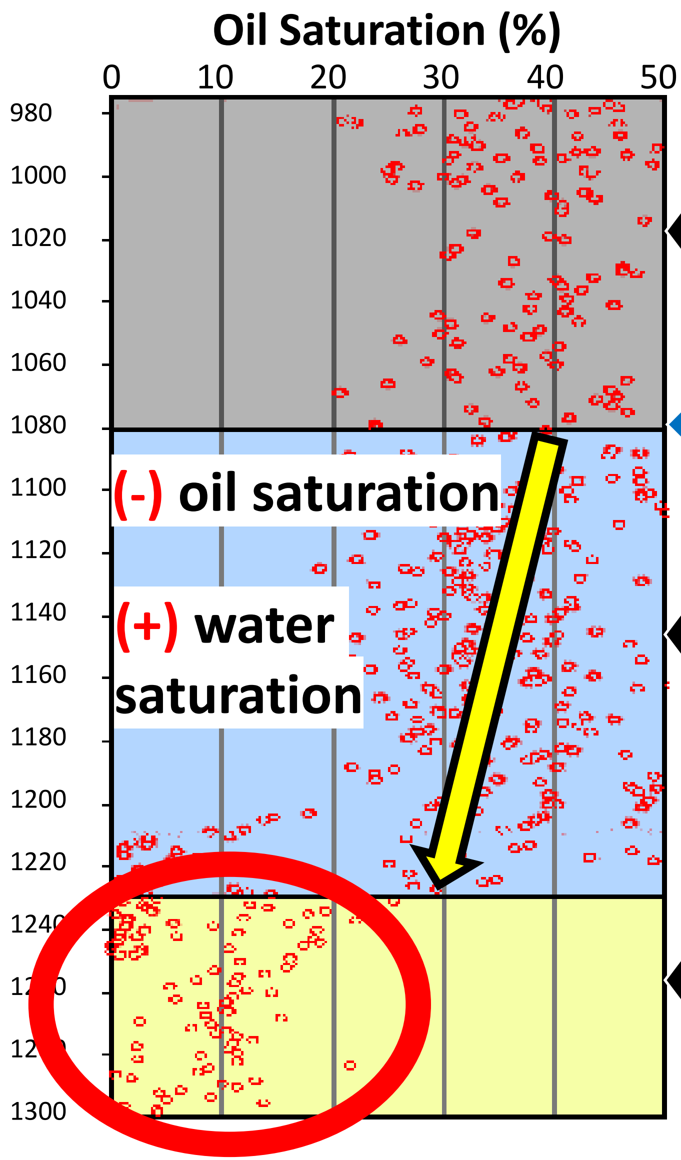

main pay zone:
vertical target – occurs on low-relief structures

Oil-water contact

transitional oil zone:
water-laden interval (decreasing oil saturation with depth & increasing water saturation)

San Andres basal limestone:
Minor oil saturation indicates previous saturation to the base of the reservoir

Goldsmith Landreth San Andres Unit, Ector Co., TX

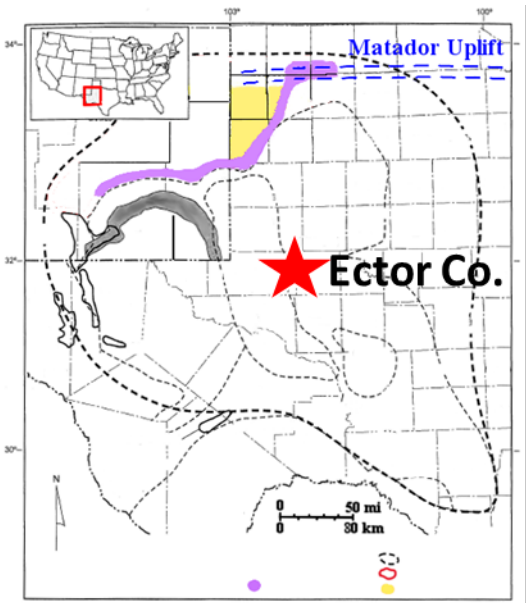

(Ruppel, 2019; Trentham and Melzer, 2019)

Uplift and Exposure of Guadalupian Strata in New Mexico

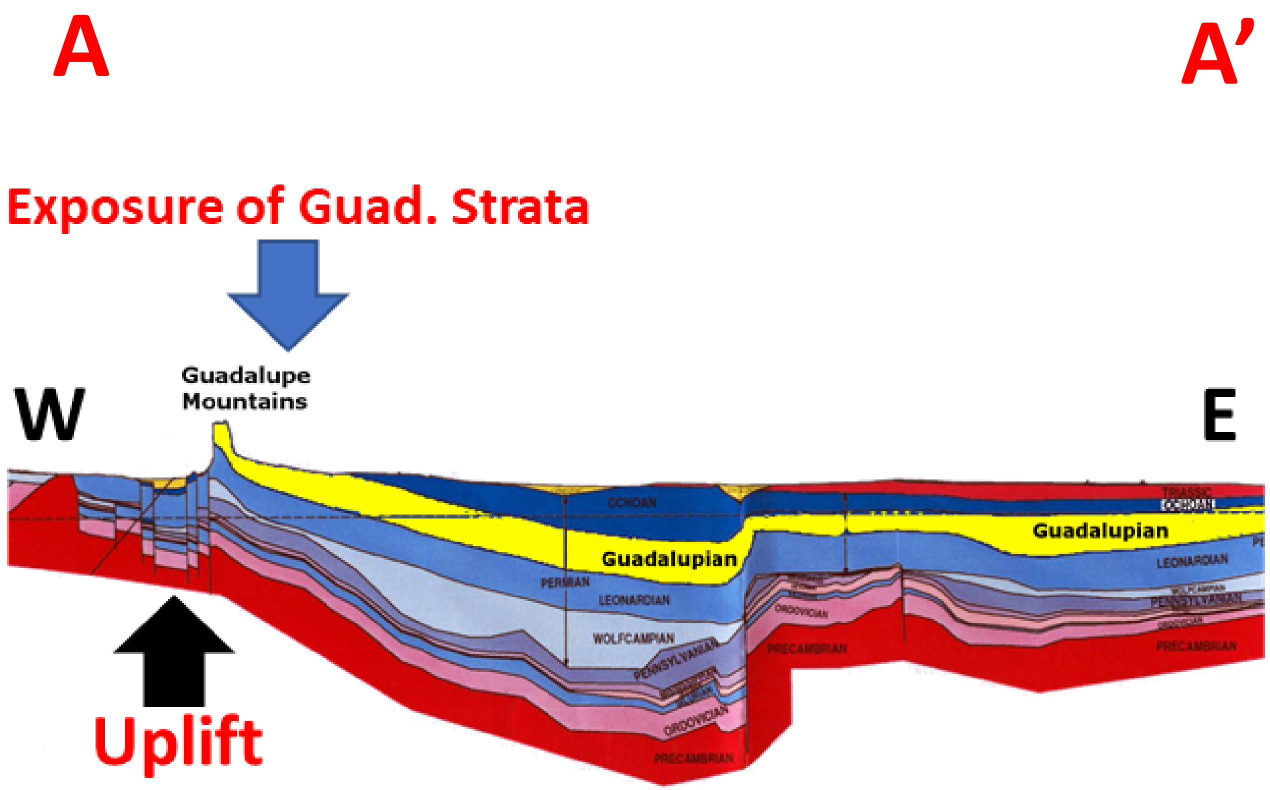

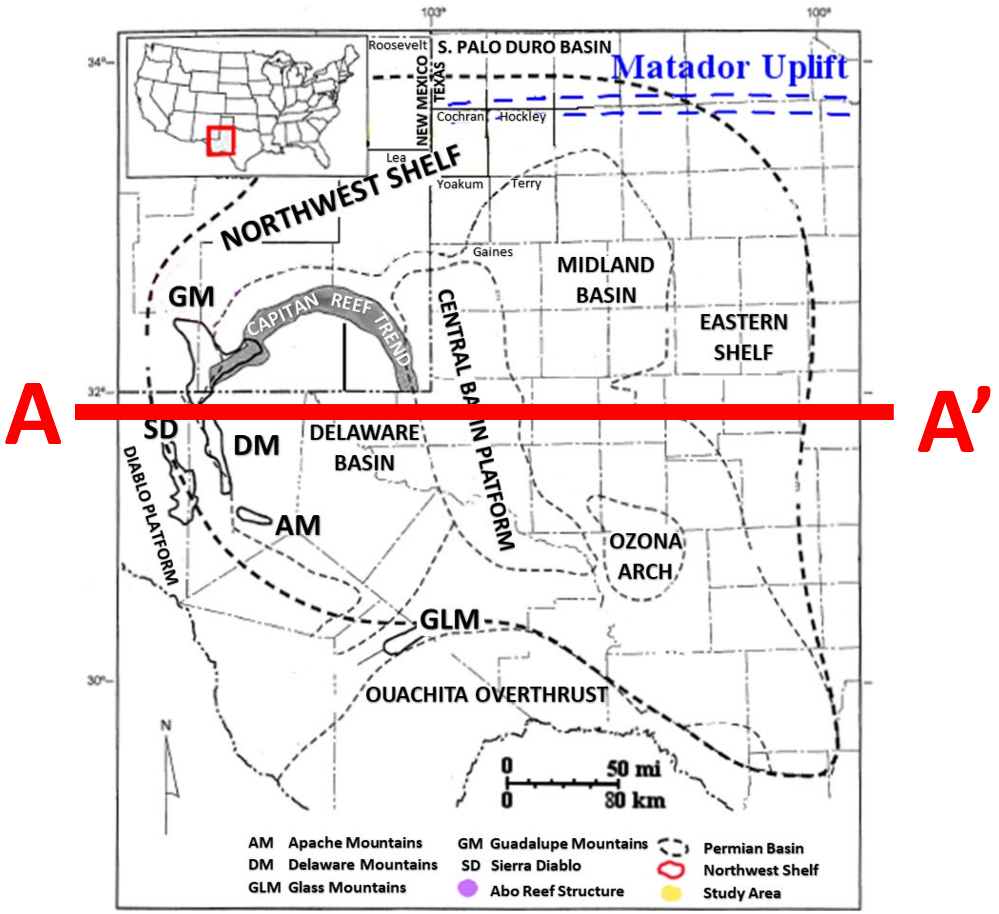

(Melzer, 2006; Ruppel, 2019)

Influx of Meteoric Water and Sweeping of the Lower Oil Column

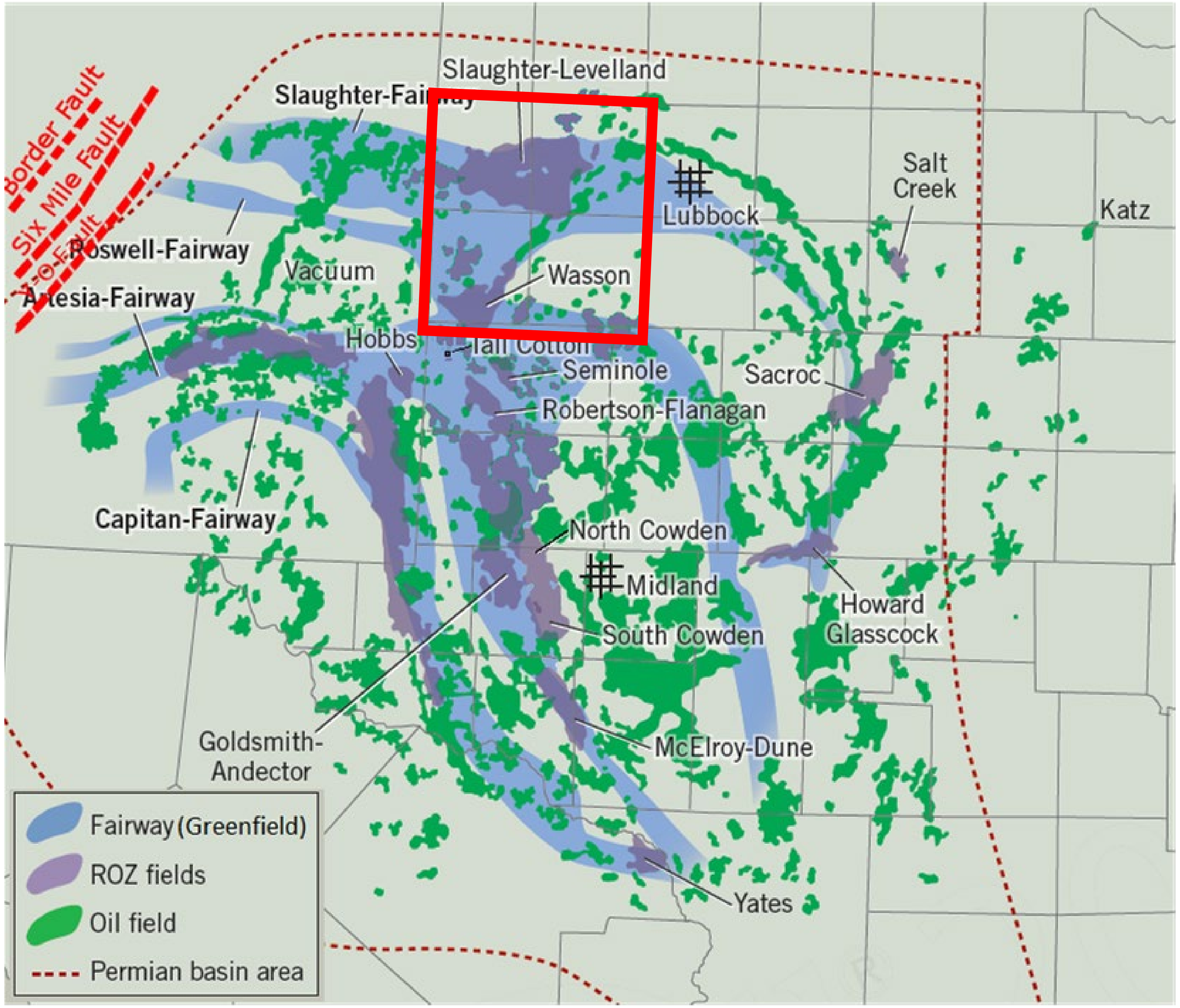

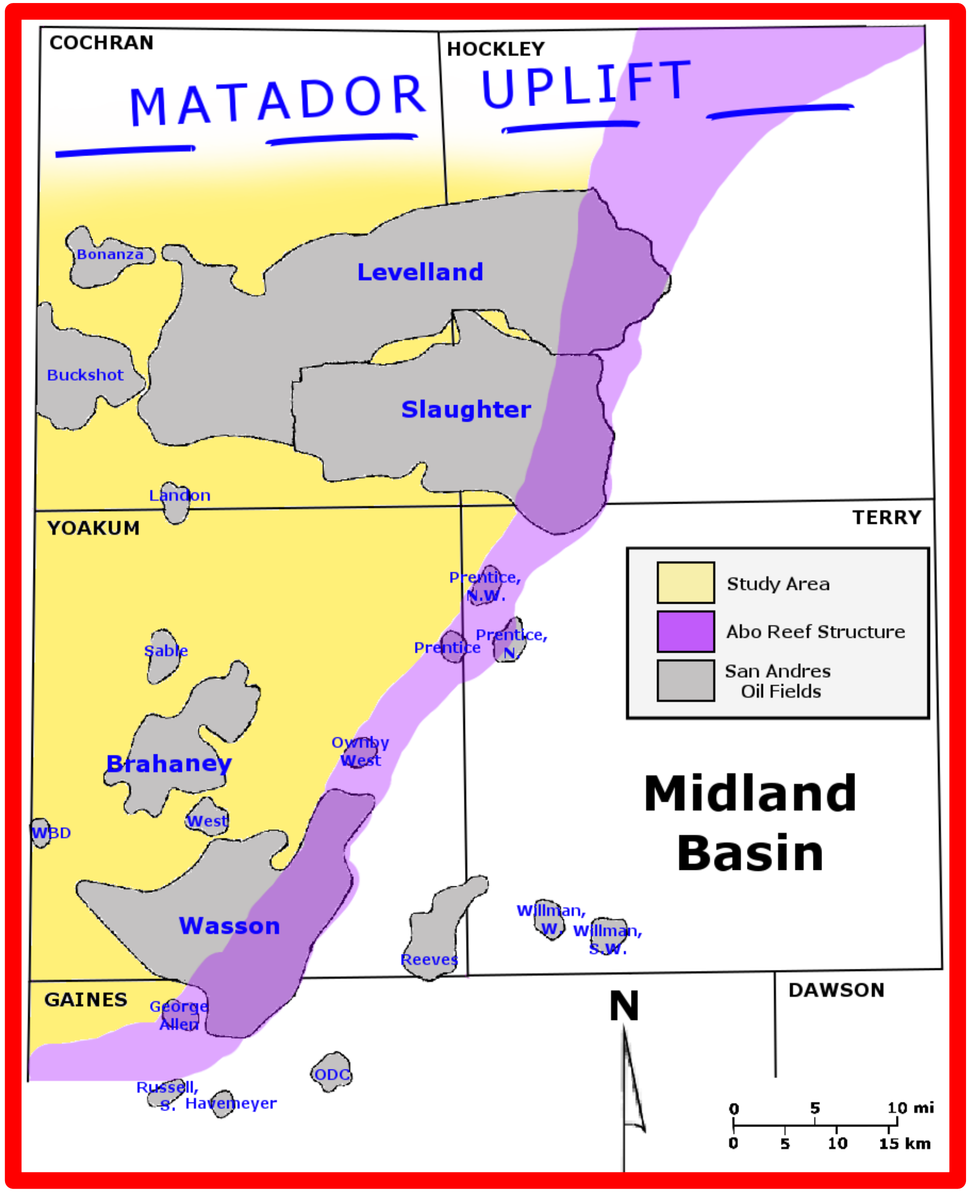

(Ruppel, 2019; Trentham et al., 2015)

Flushing of the Lower Oil Column

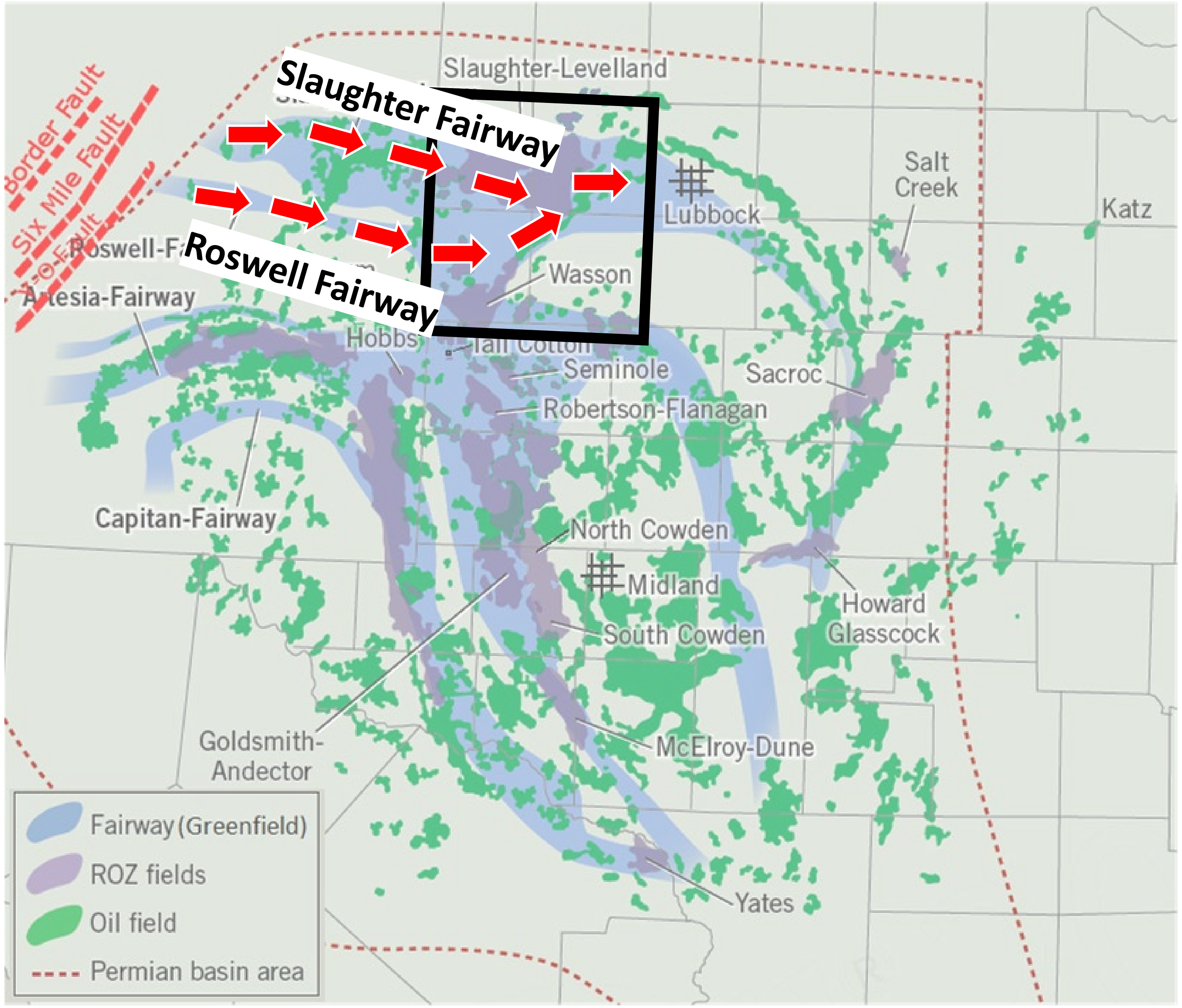

(Trentham et al., 2015)

Resurgent Play Extends Beyond the Flanks of Legacy Fields

main pay zone (MPZ)	vertical target – on structural highs
transitional oil zone (TZ)	150-300 ft. thick water-laden interval below oil-water contact
horizontal target	
residual oil zone (ROZ)	no primary oil recovery

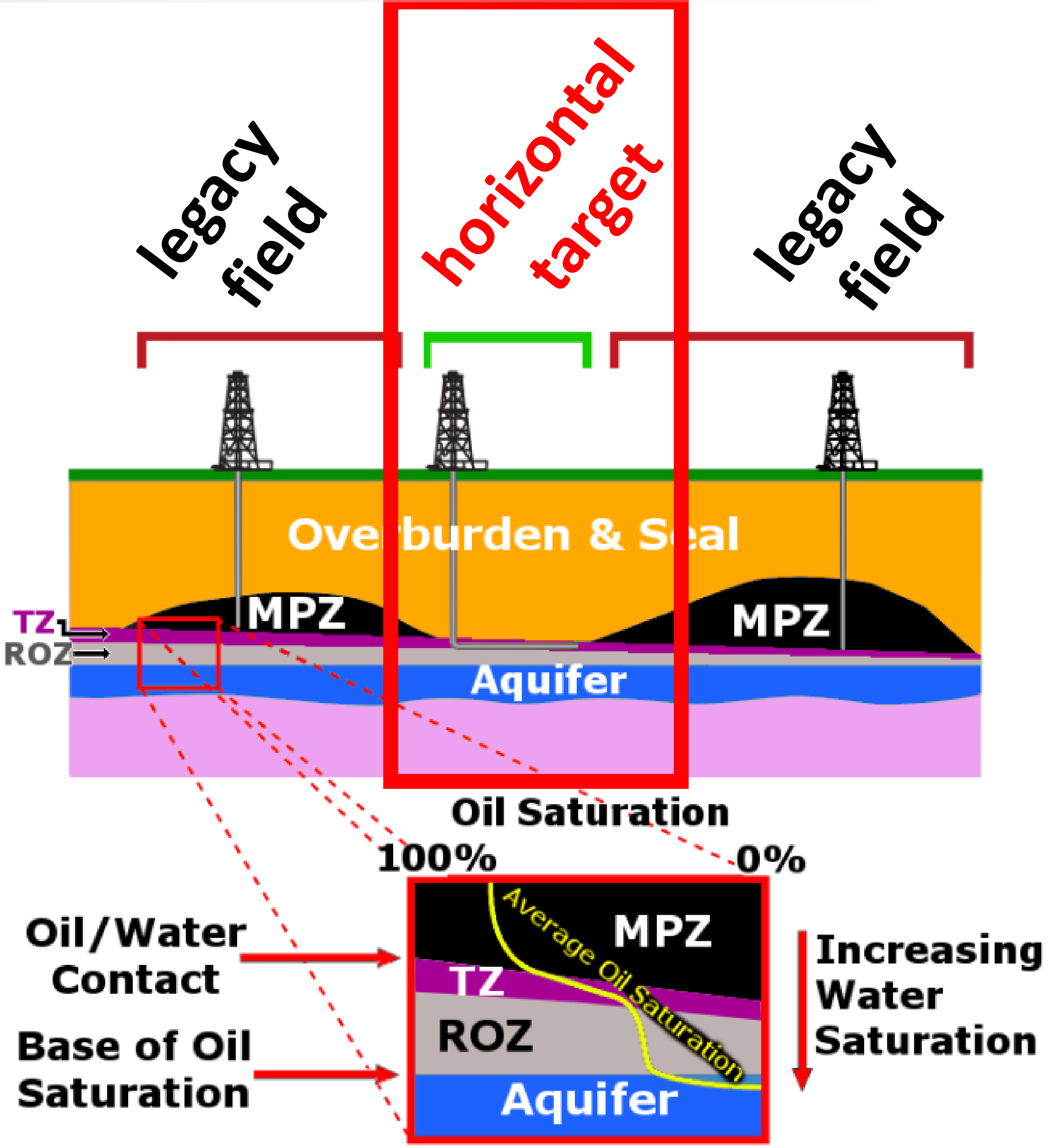

(Melzer, 2006)

Petrophysical Analysis Indicates Prograding-Aggrading Shelf

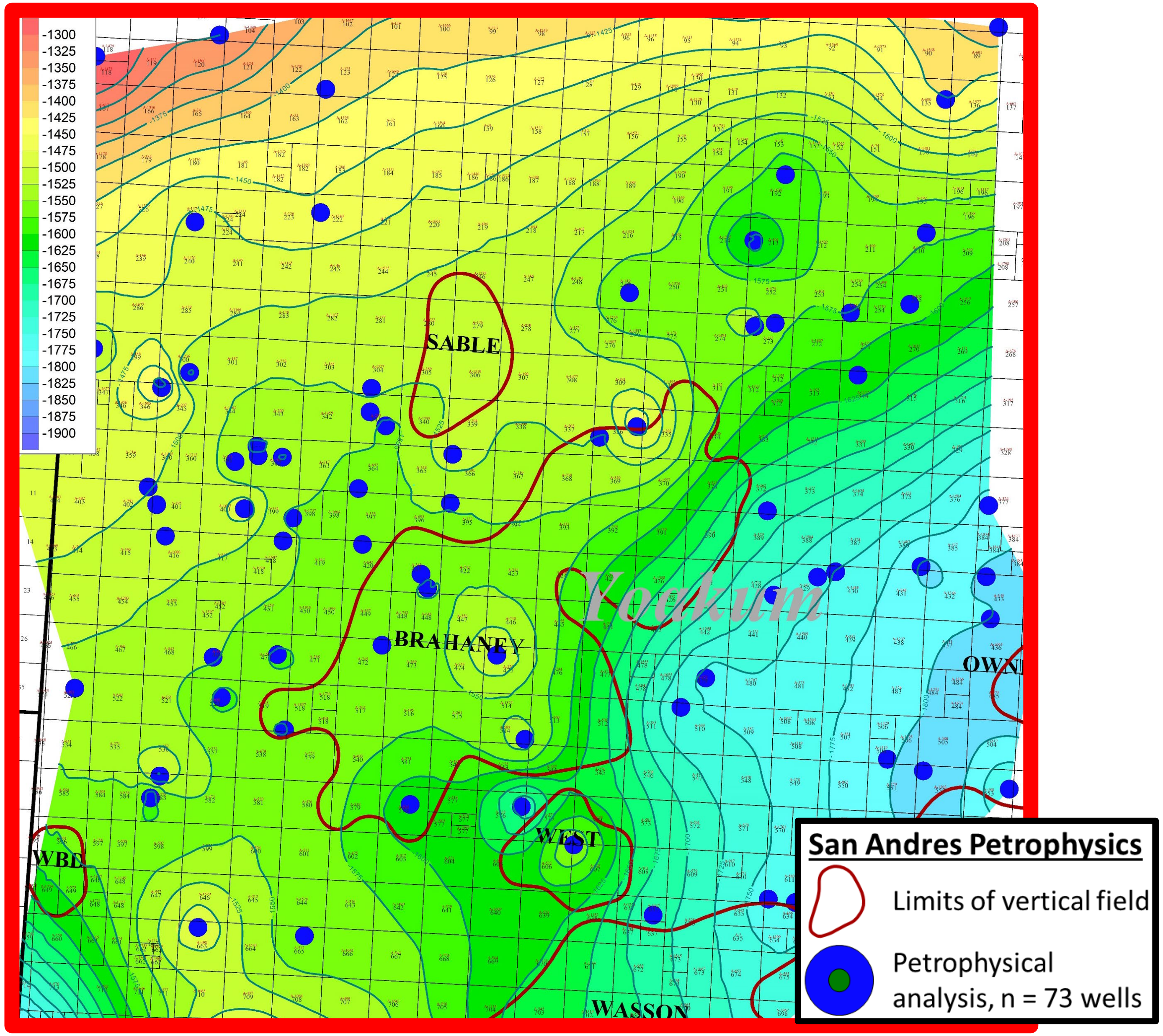

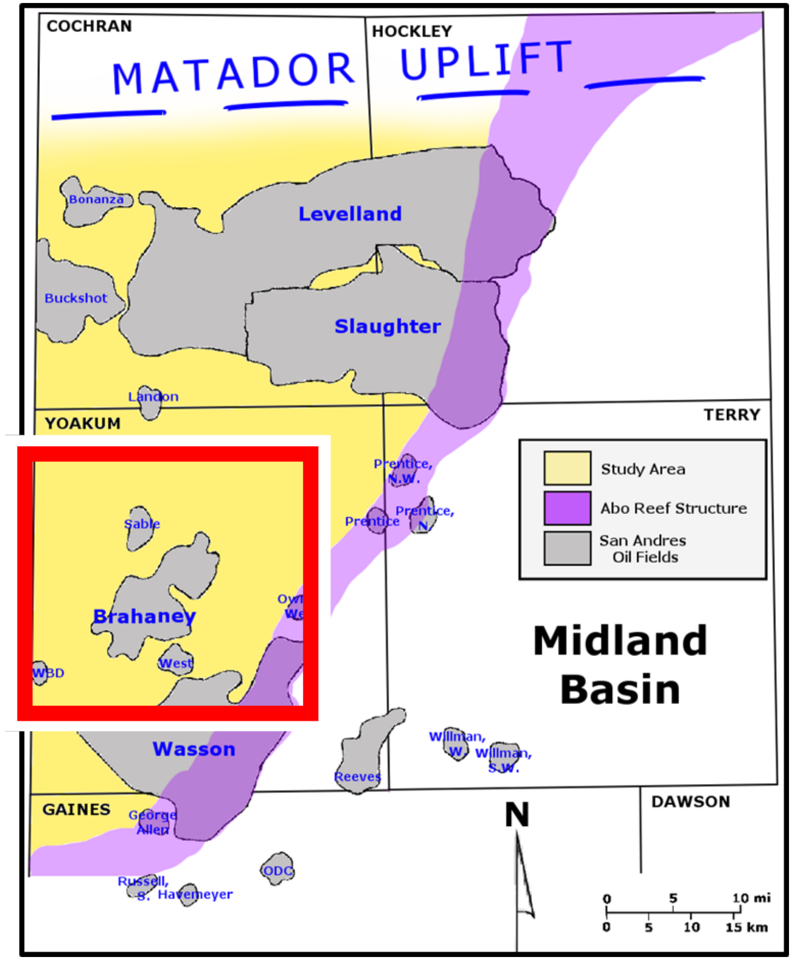

Petrophysical Analysis Indicates Prograding-Aggrading Shelf

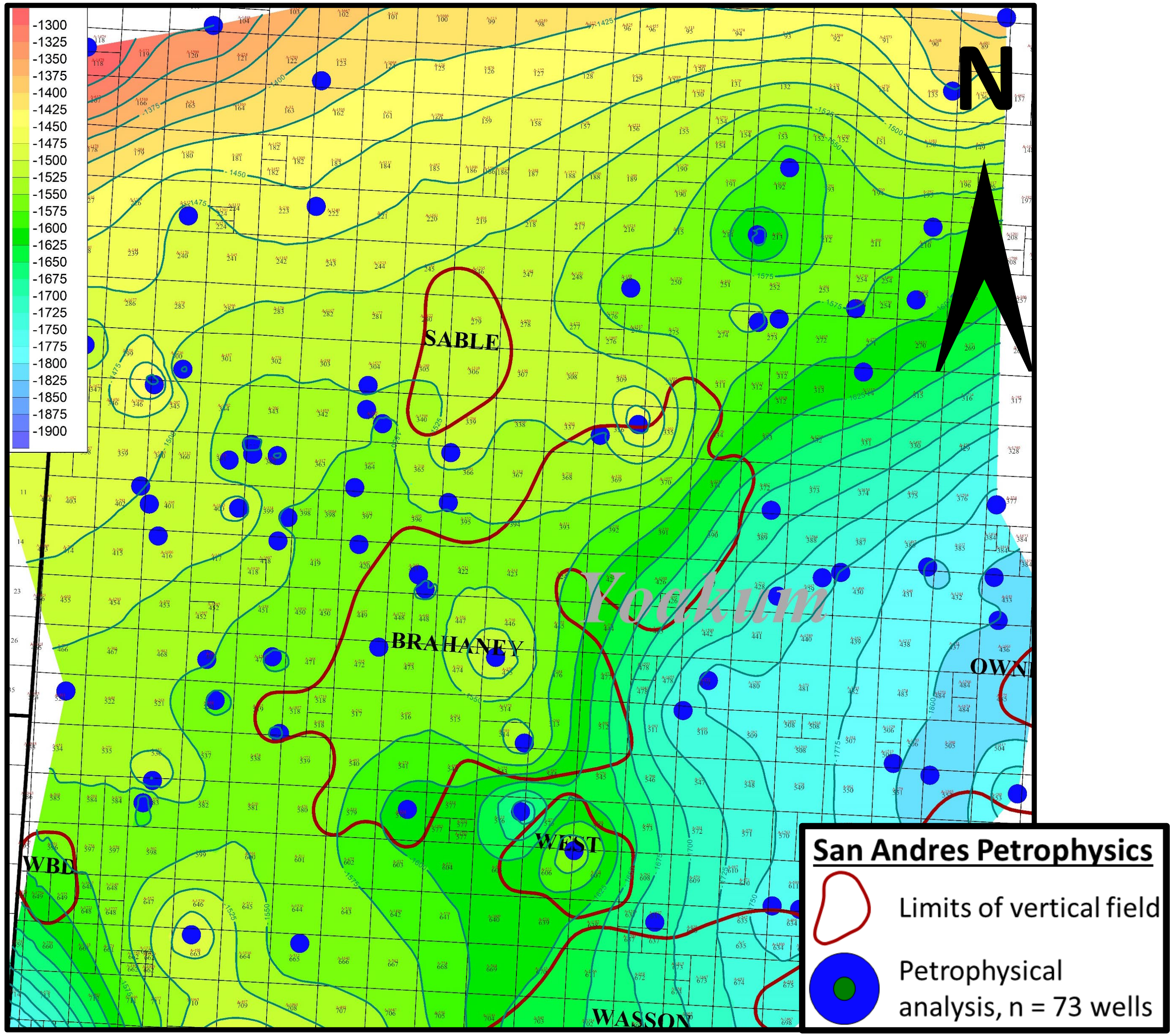

Methodology:

1. Calculate oil-in-place from petrophysical analyses
2. Indicate the depth of most saturated 100 ft. reservoir interval
3. Contour similar depths

Petrophysical Analysis Indicates Prograding-Aggrading Shelf

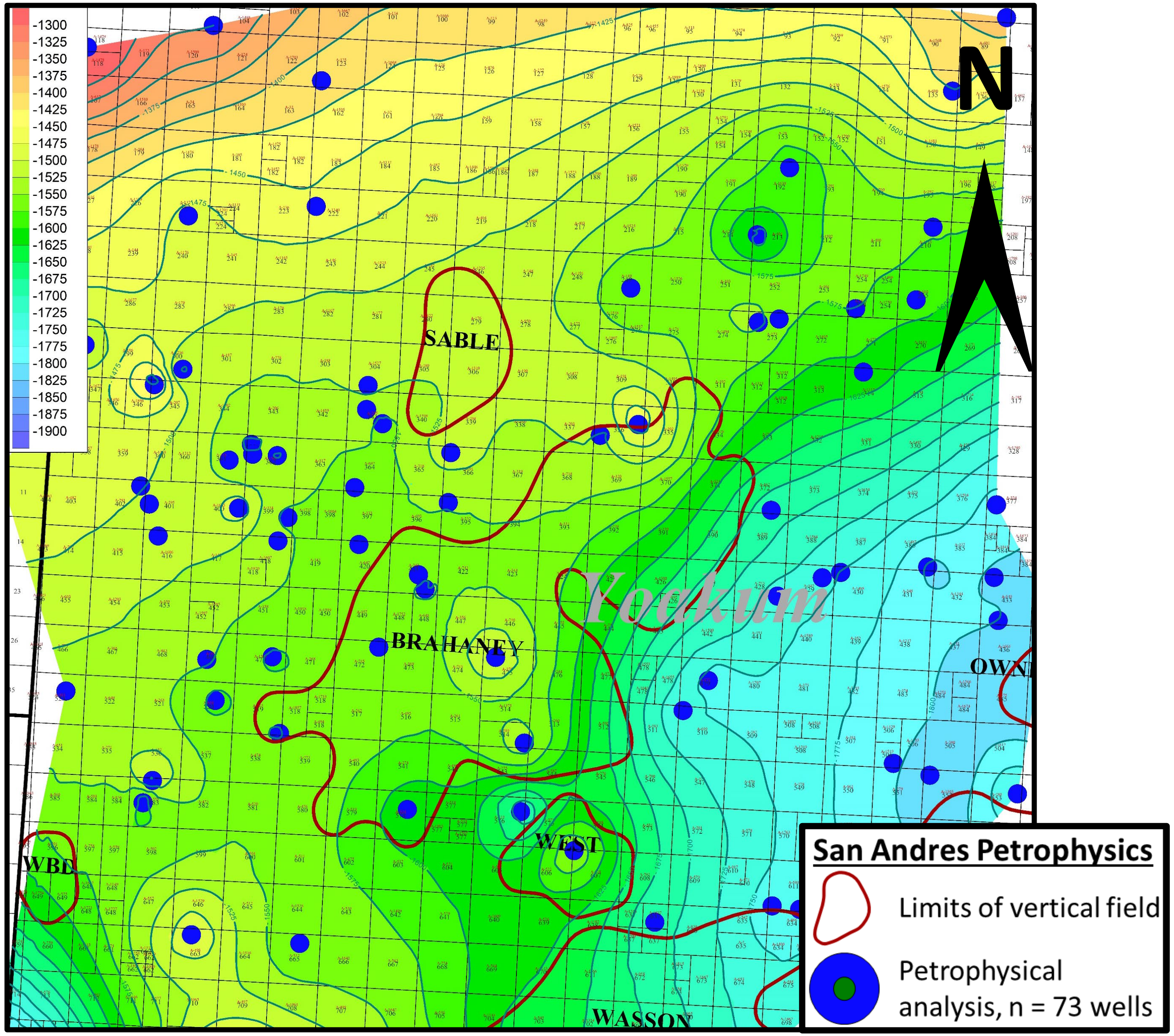

Results:

The depth of the “best 100 ft.” interval indicates the depth of the restricted shelf margin.

Moving basinward (southeast), the depth of the restricted shelf margin indicates progradational-aggradational shelf migration.

Petrophysical Analysis Indicates Prograding-Aggrading Shelf

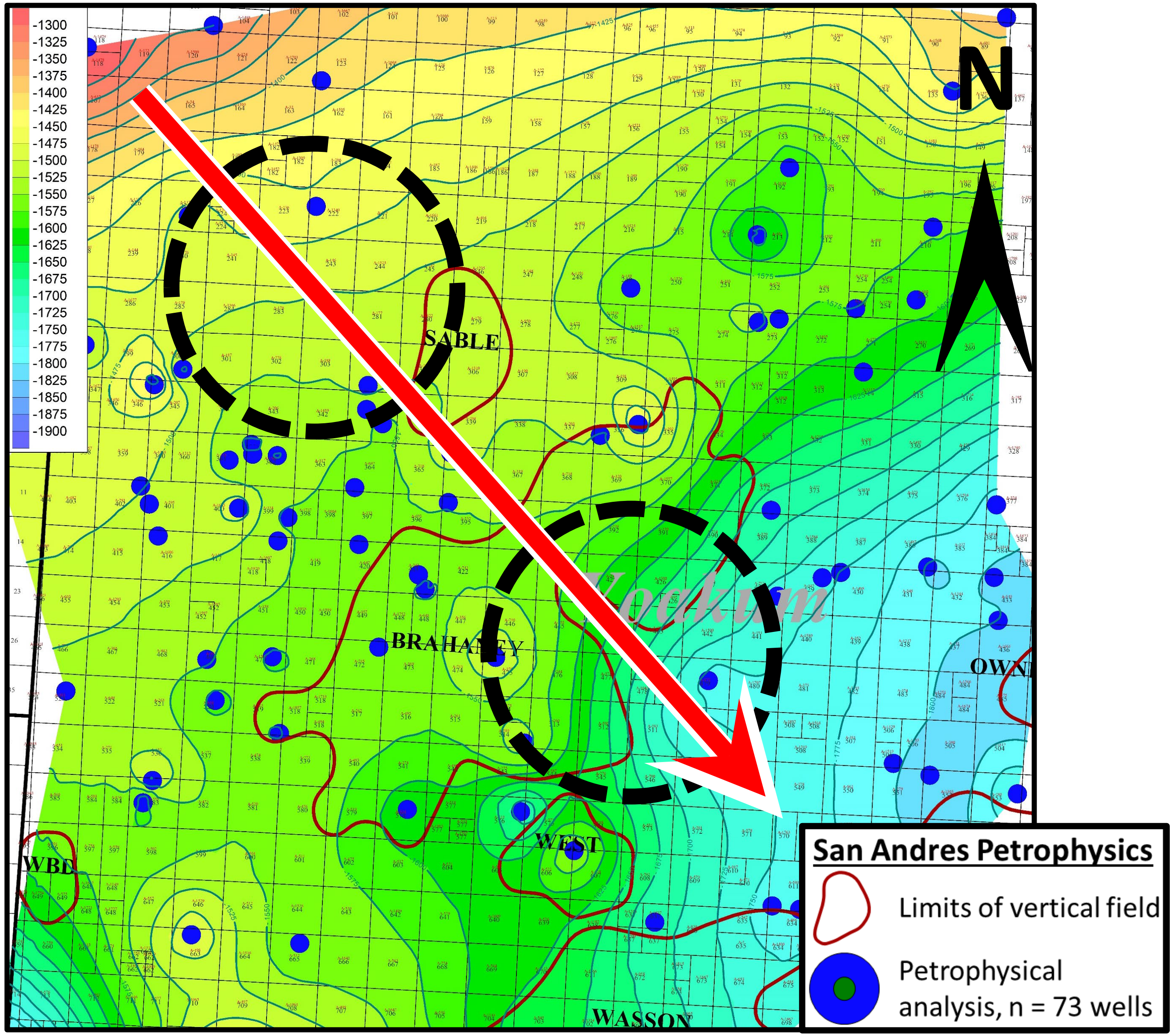

Results:

The depth of the "best 100 ft." interval indicates the depth of the restricted shelf margin.

Moving basinward (southeast), the depth of the restricted shelf margin indicates progradational-aggradational shelf migration.

Core Properties Within the "Best 100 Ft." of Reservoir

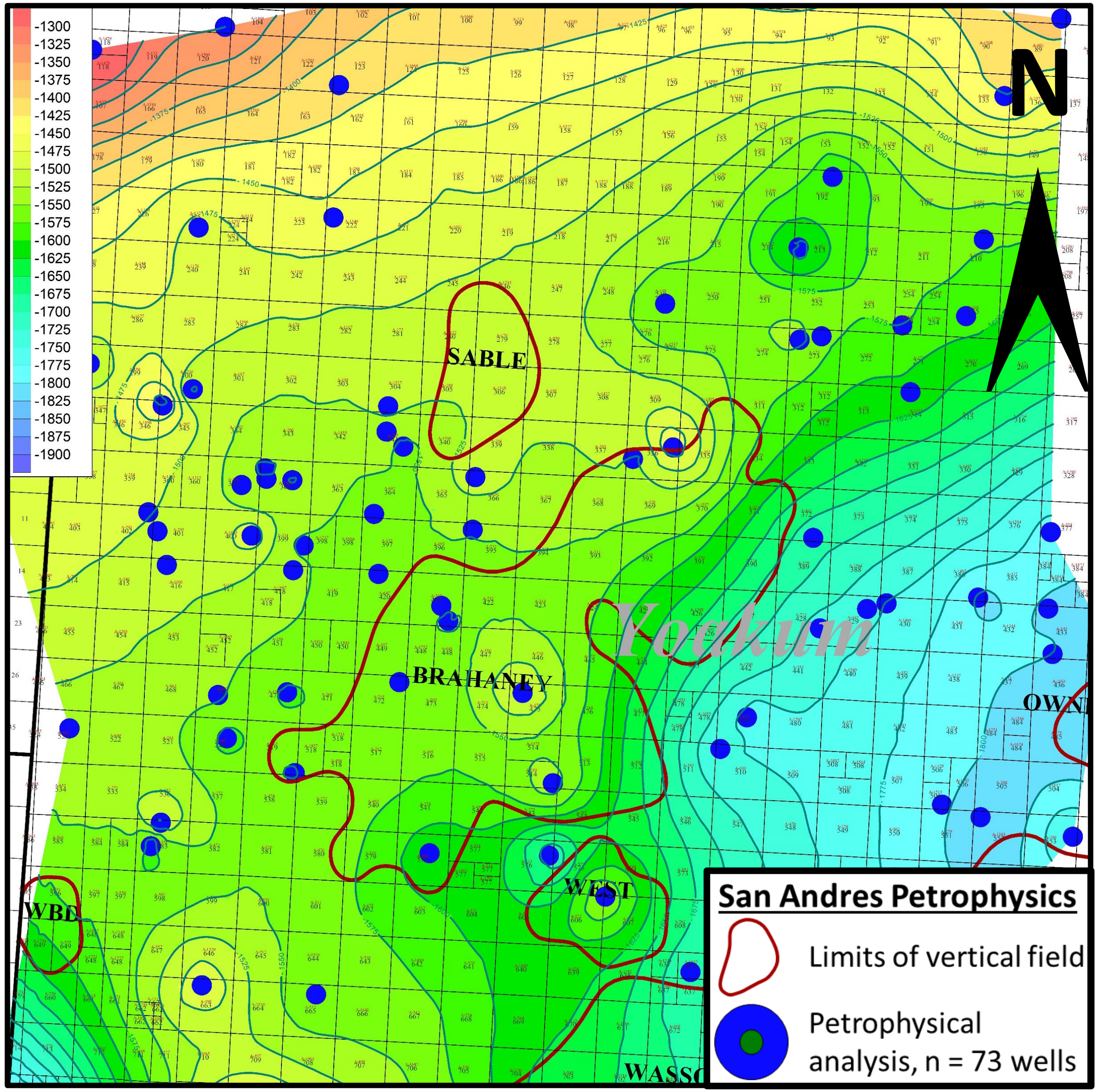

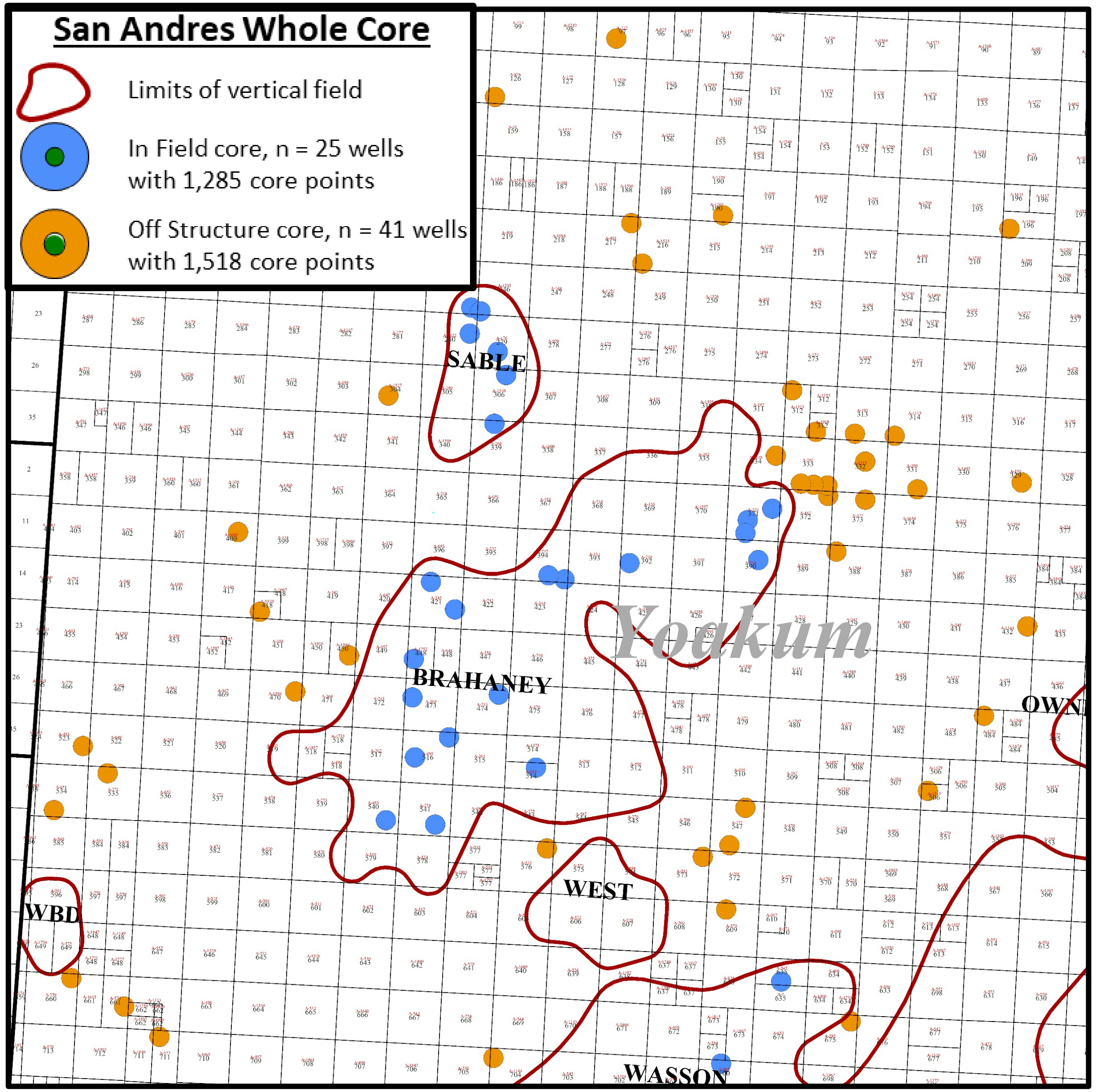

Core Properties Indicate Porosity Enhancement on Paleo-Structural Highs

Porosity of "In Field" & "Off Structure" Core Points

Porosity [%]			
Area	P90	P50	P10
In	3.3	8.3	13.3
Out	2.2	6.3	11.5

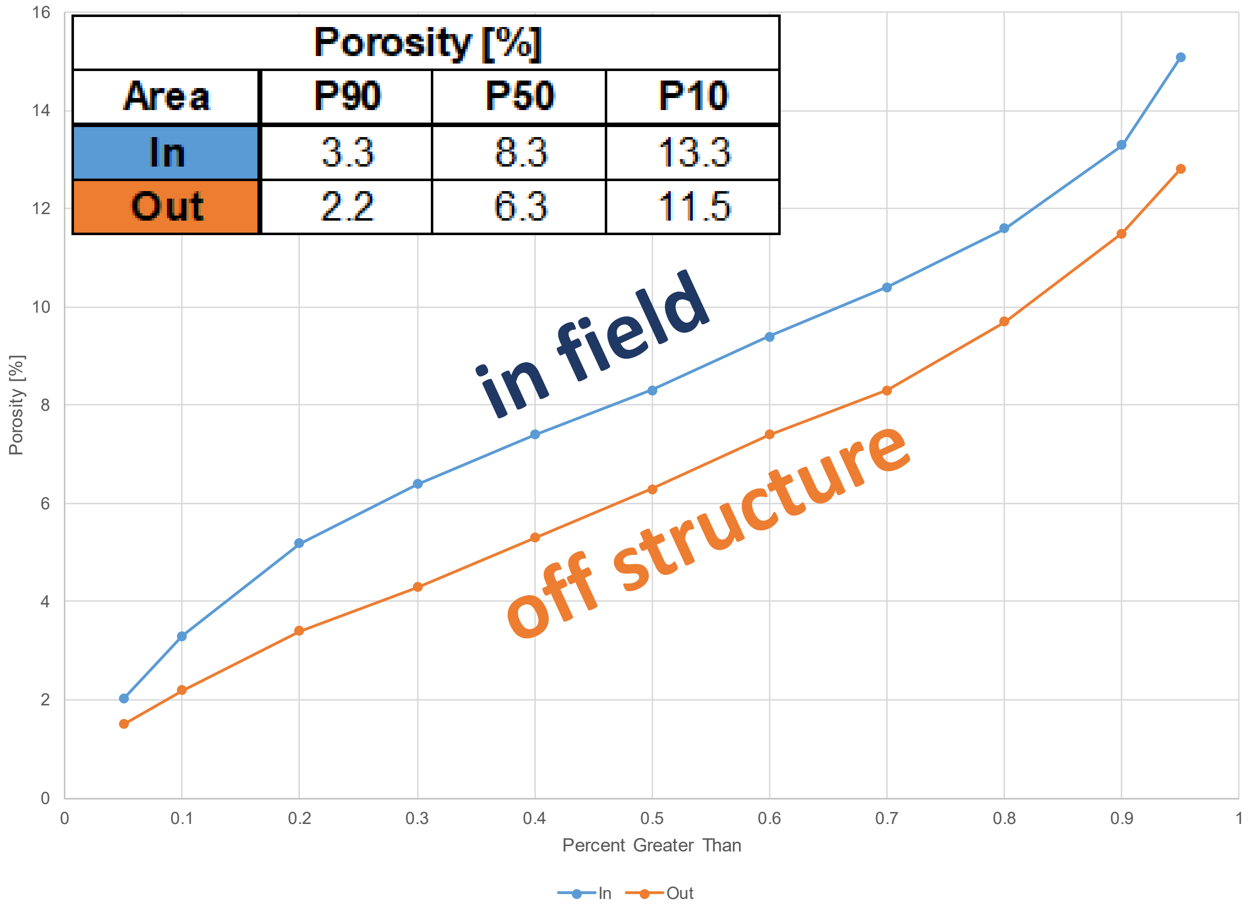

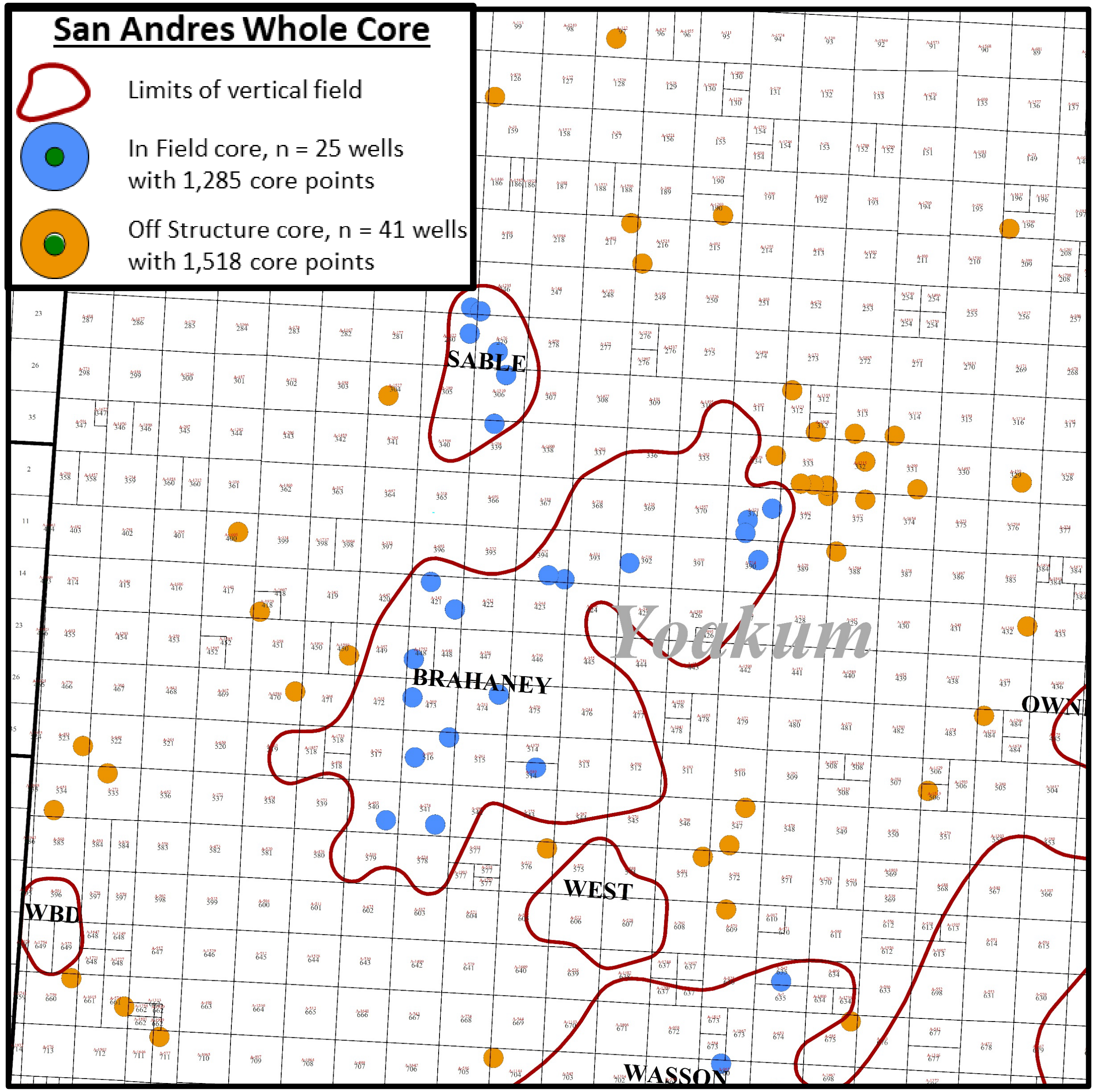

Core Properties Indicate Porosity Enhancement on Paleo-Structural Highs

Porosity of “In Field” & “Off Structure” Core Points

Porosity [%]			
Area	P90	P50	P10
In	3.3	8.3	13.3
Out	2.2	6.3	11.5

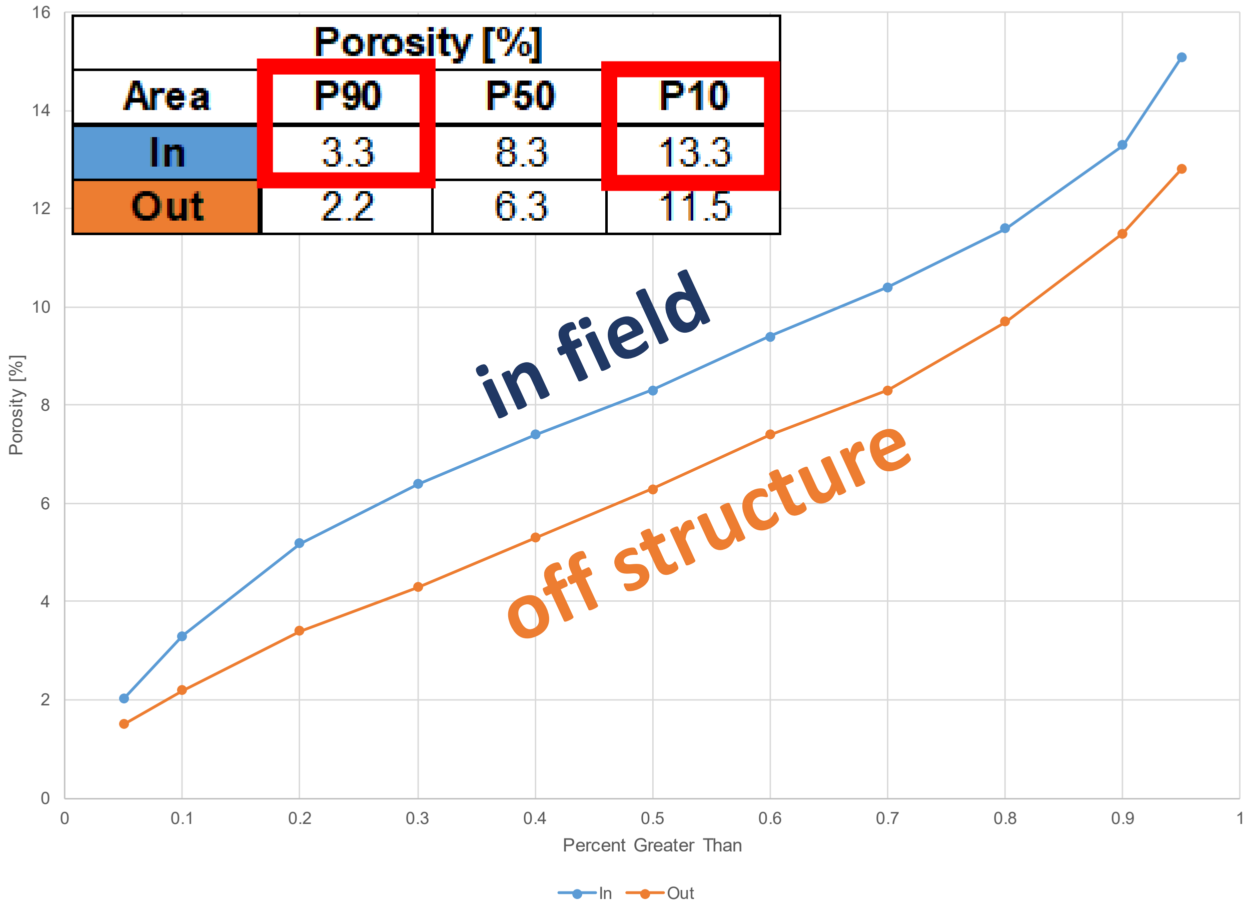

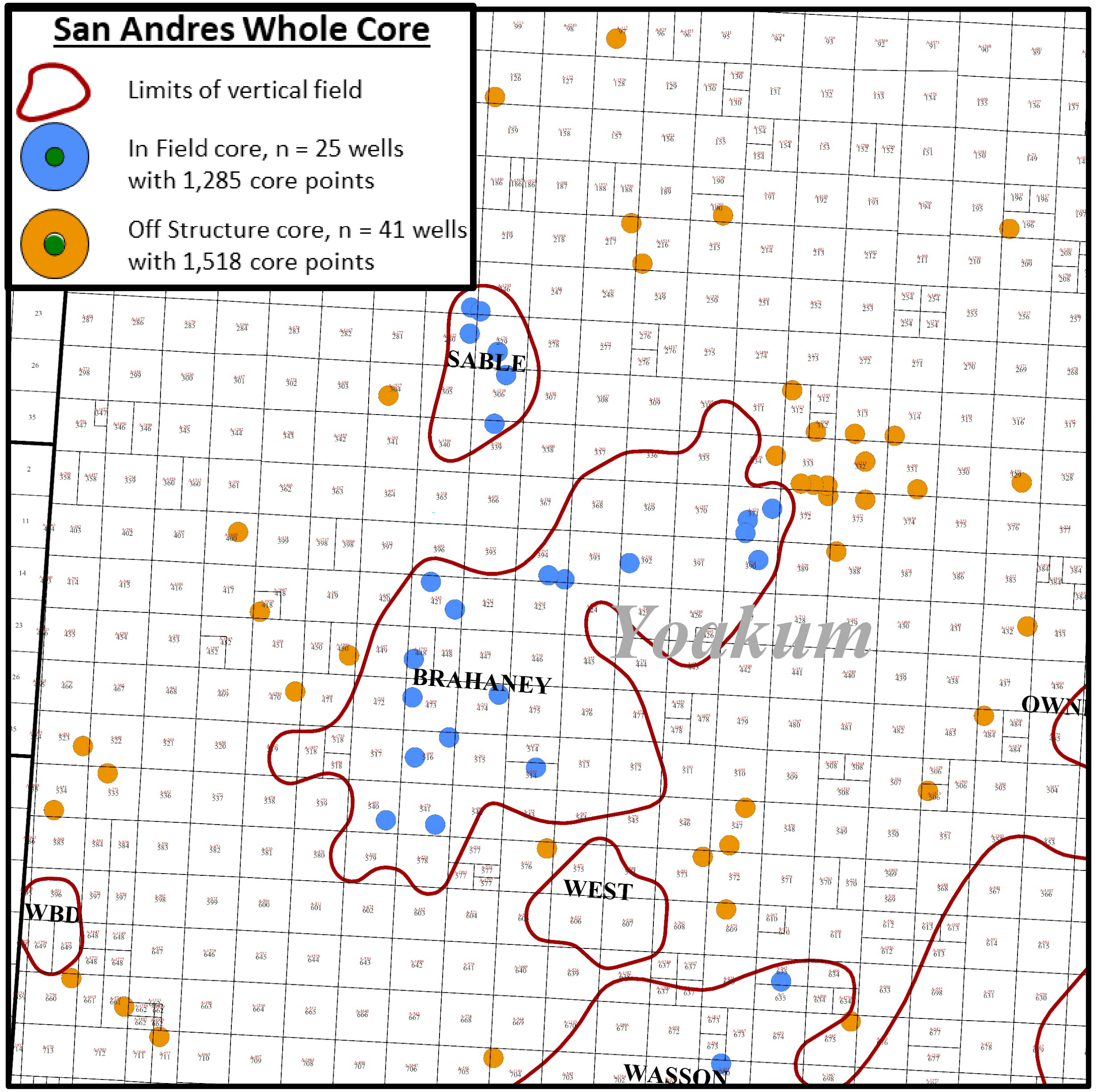

Core Properties Indicate Porosity Enhancement on Paleo-Structural Highs

Porosity of "In Field" & "Off Structure" Core Points

Porosity [%]			
Area	P90	P50	P10
In	3.3	8.3	13.3
Out	2.2	6.3	11.5

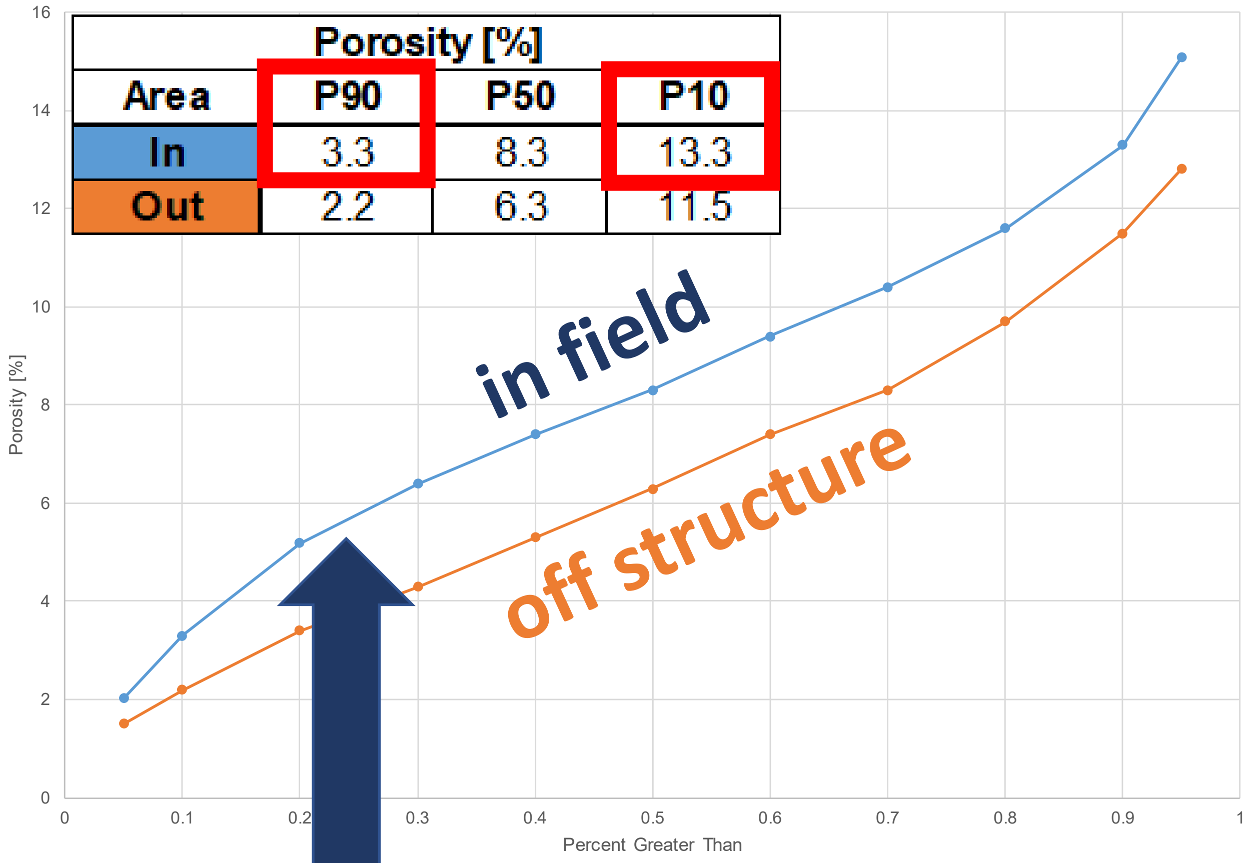

porosity enhancement of "in field" reservoir facies

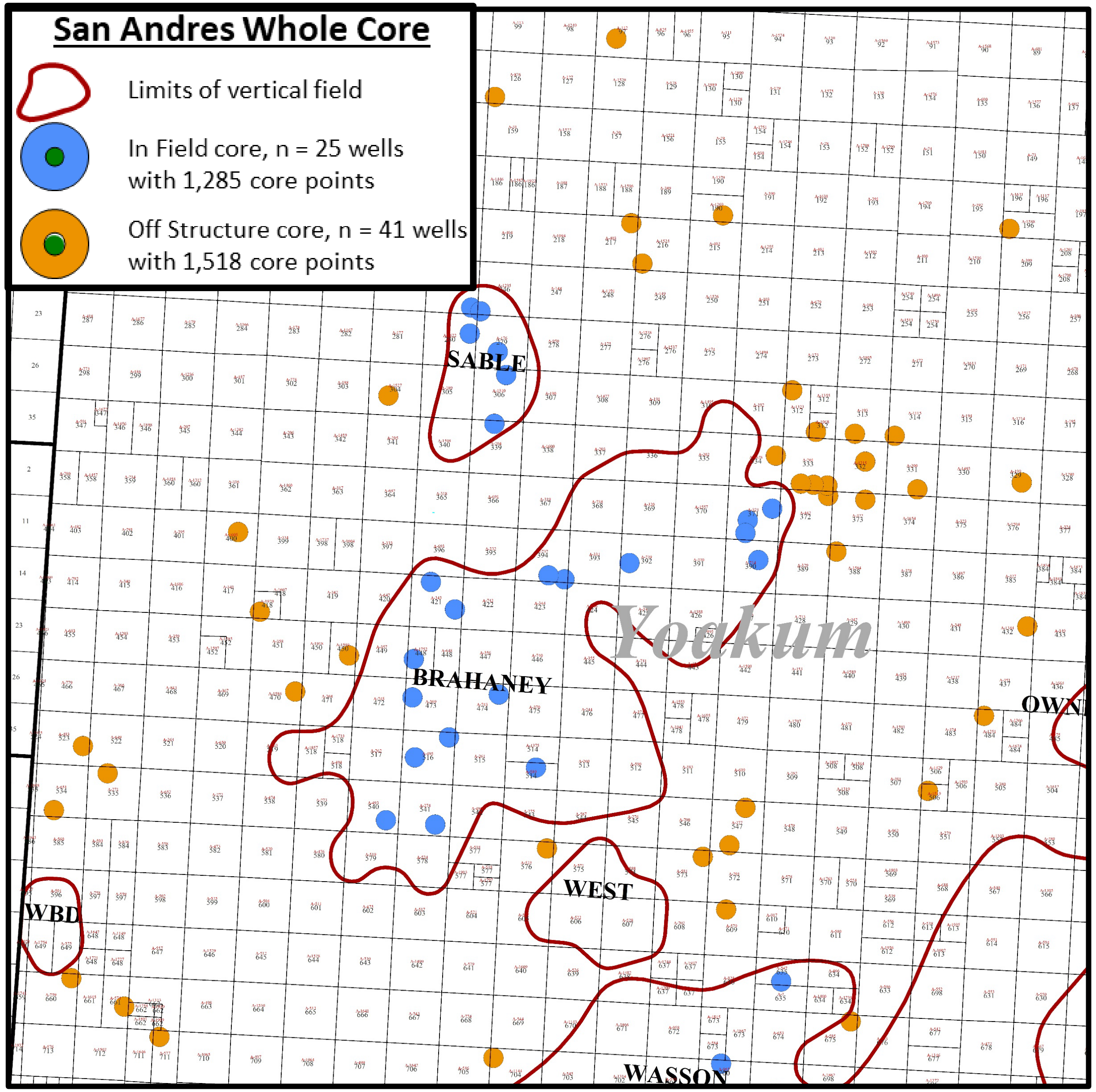

Core Properties Indicate Permeability Enhancement on Paleo-Structural Highs

Permeability of "In Field" & "Off Structure" Core Points

Permeability [mD]			
Area	P90	P50	P10
In	0.03	0.47	4.00
Out	0.03	0.30	3.00

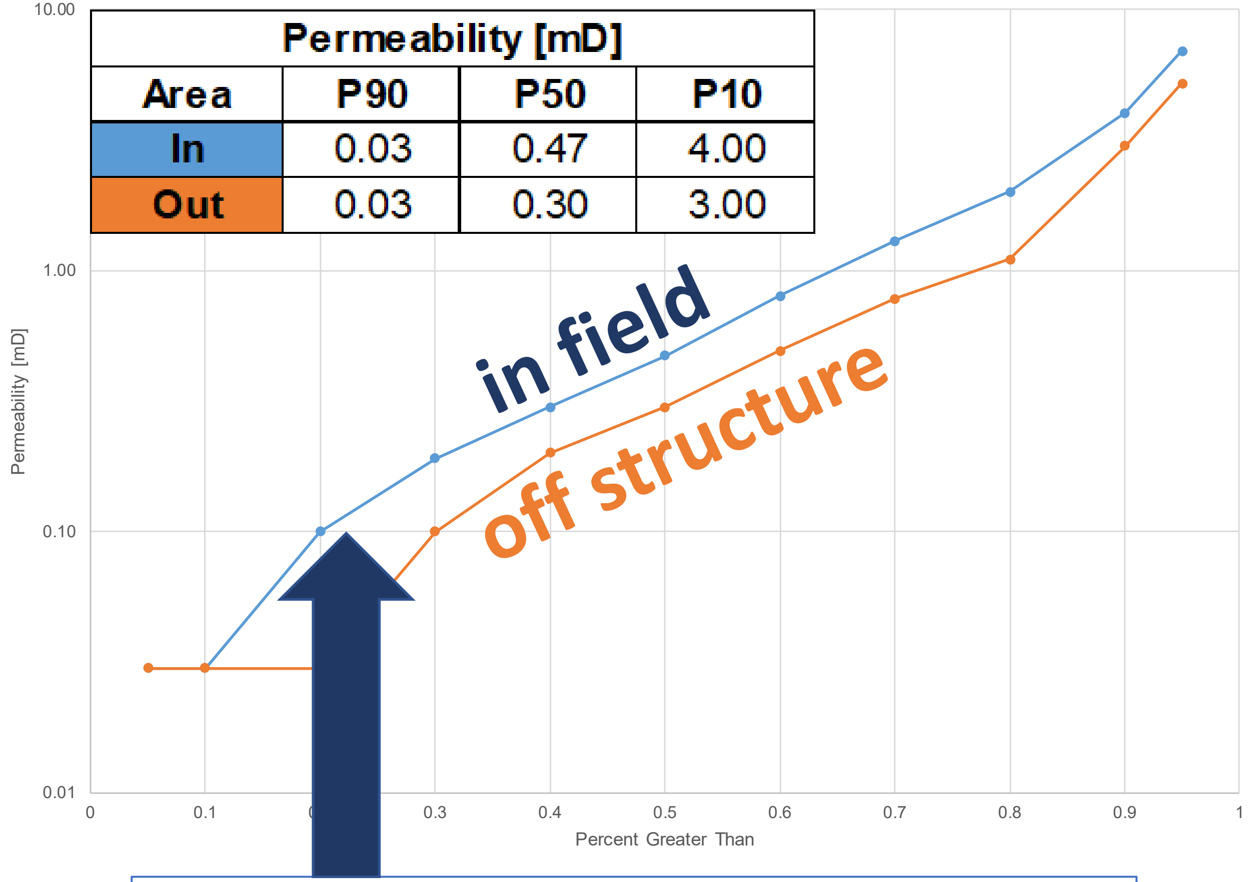

permeability enhancement of "in field" reservoir facies

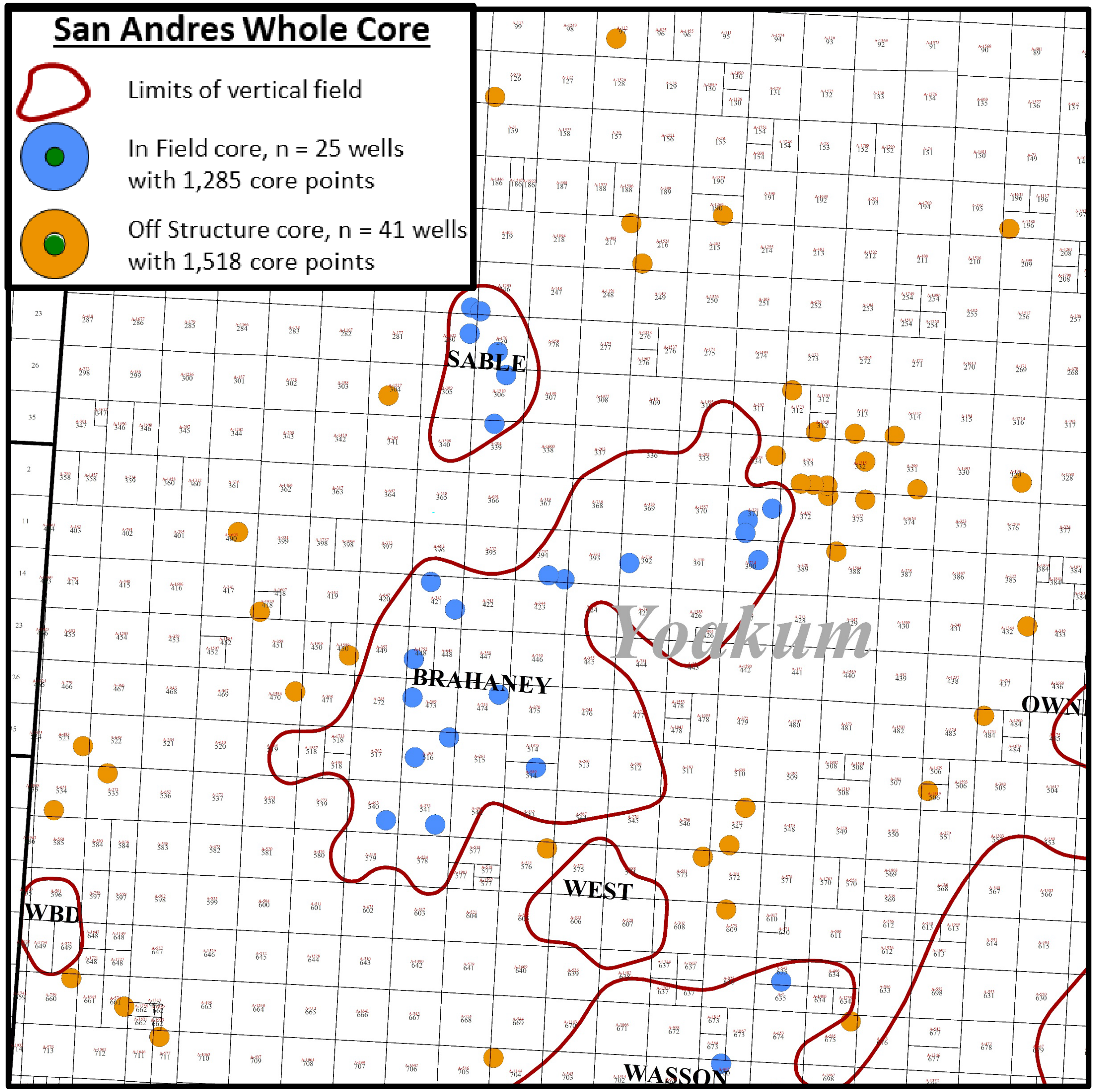

Core Properties Indicate Greater Water Saturation in "Off" Structure Reservoir

Water Saturation of "In Field" & "Off Structure" Core Points

Water Saturation [%]			
Area	P90	P50	P10
In	15.9	29.8	58.2
Out	20.4	36.4	63.4

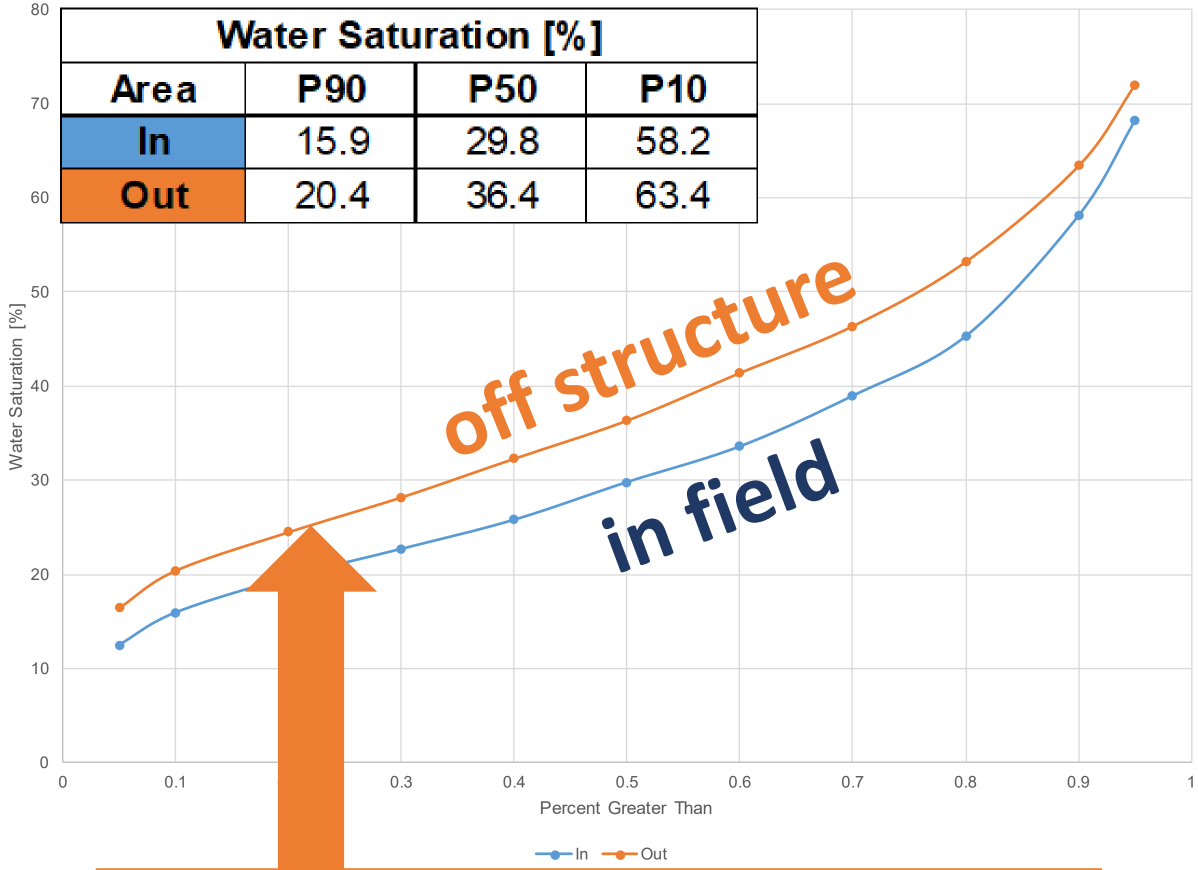

greater water saturation in "off" structure reservoir

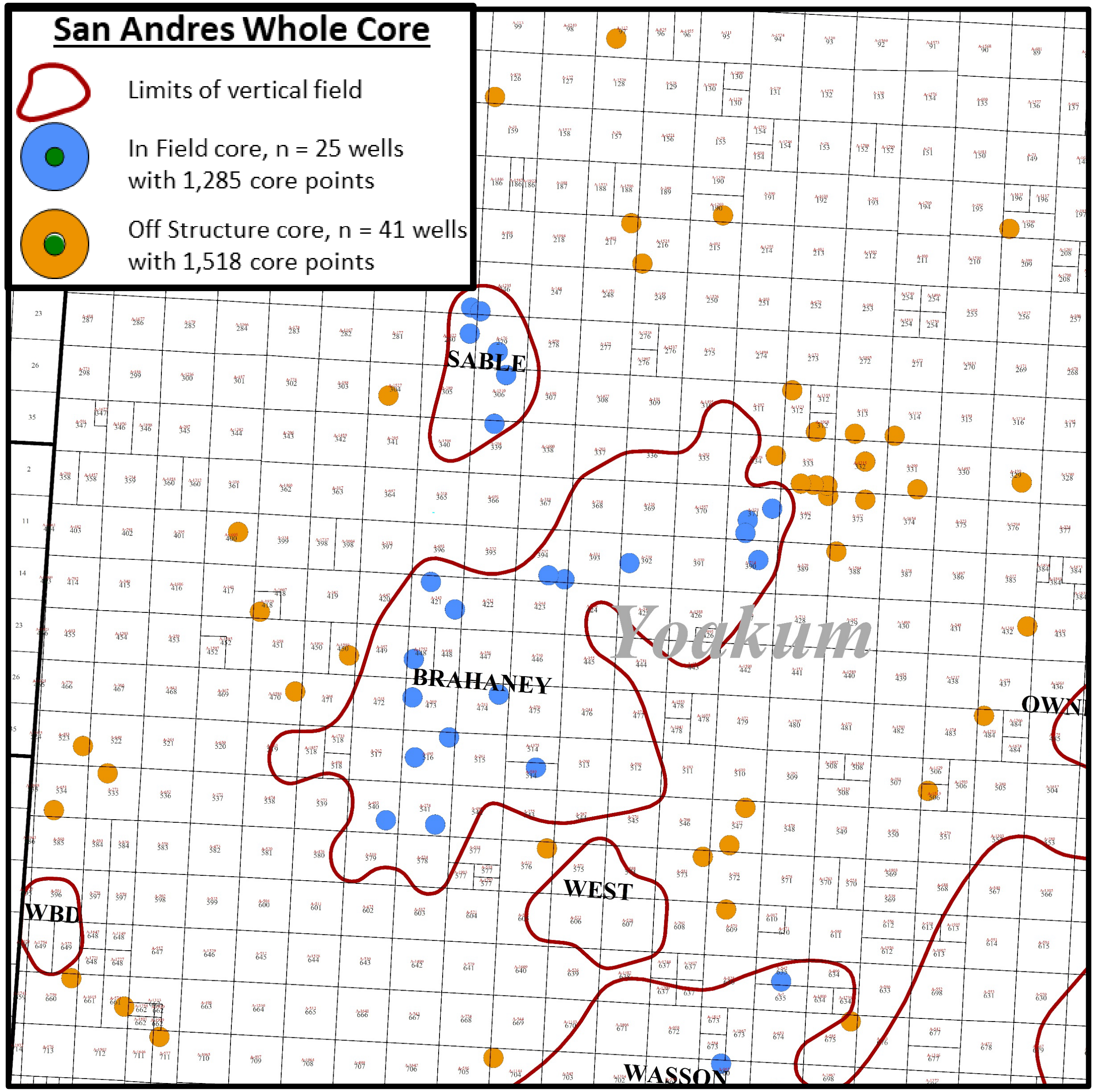

Reservoir Quality Diminishes Off the Flanks of Legacy Fields

Porosity

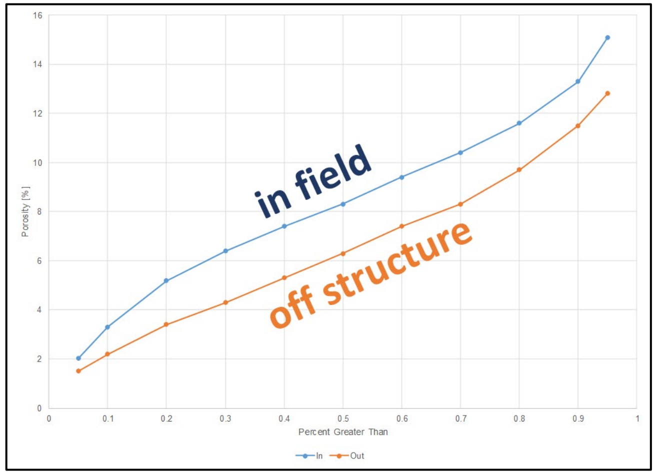

Permeability

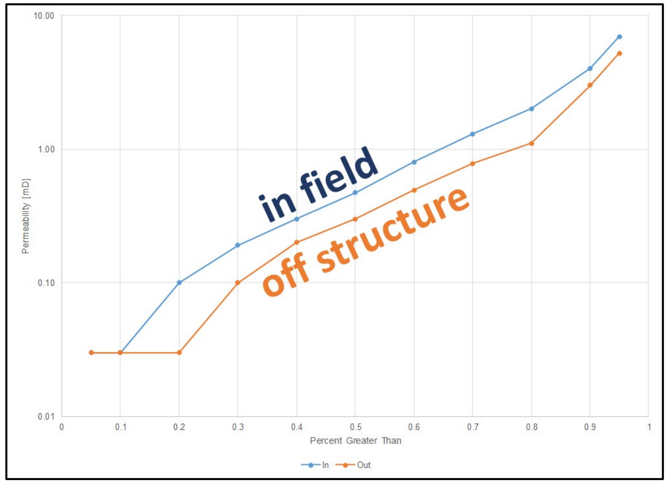

Water Saturation

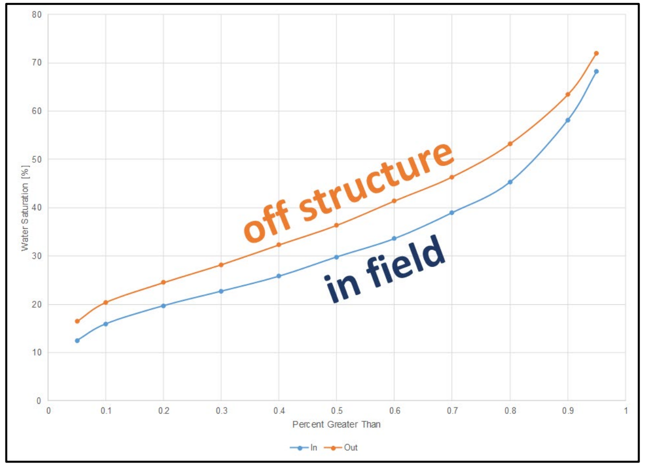

- **porosity enhancement by secondary dolomitization**
- **porosity occlusion in lagoonal or intertidal facies**

- **paleo-waterflood and sweeping of the lower oil column**

Takeaways

- The San Andres Fm. on the Northwest Shelf in W. Texas represents a "world-class" carbonate hydrocarbon reservoir – formed by the complex interactions of supratidal and subtidal environments during a hierarchy of sea-level fluctuations and increasingly arid climatic conditions

- A paleo-waterflood flushed the lower oil column of the reservoir, leaving a distribution of distinct targets for production that vary in oil-water saturation, distribution, and method of production

- Petrophysical and core analyses of these targets provide a quantitative method of analysis of the prograding-aggrading migration of shelf environments, and the diminishing reservoir quality, moving from the "in field" to "off" structure reservoir

References

Blakey, R., n.d., Greater Permian Basin: http://deeptimemaps.com/greater-permian-basin-map-list/ (accessed October 21, 2019).

Dutton, S.P., Kim, E.M., Broadhead, R.F., Raatz, W.D., Breton, C.L., Ruppel, S.C., and Kerans, C., 2005, Play analysis and leading-edge oil-reservoir development methods in the Permian Basin: Increased recovery through advanced technologies: AAPG Bulletin, v. 89, p. 553–576, doi: 10.1306/12070404093.

Ebanks, W. J., 1990, Geology of the San Andres Reservoir, Mallet Lease, Slaughter Field, Hockley County, Texas: Implications for Reservoir Engineering Projects: Geologic and Engineering Approaches in Evaluation of San Andres/Grayburg Hydrocarbon Reservoirs - Permian Basin, Bureau of Economic Geology, p. 75–85.

Kerans, C., 2014, San Andres Formation: Outcrop to Subsurface Stratigraphic Framework: SlideServe, https://www.slideserve.com/tekla/san-andres-formation-outcrop-to-subsurface-stratigraphic-framework (accessed March 2020).

Lopez-Gamundi, C., 2019, INTEGRATED GEOCHEMISTRY AND SEDIMENTOLOGY OF THE WOLFCAMP B3 AND B2 INTERVALS, MIDLAND BASIN, TX: University of Oklahoma: <https://www.researchgate.net/publication/333516360_INTEGRATED_GEOCHEMISTRY_AND_SEDIMENTOLOGY_OF_THE_WOLFCAMP_B3_AND_B2_INTERVALS_MIDLAND_BASIN_TX> (accessed October 21, 2019).

Melzer, S. L., 2006, Stranded Oil in the Residual Oil Zone: Advanced Resources International and U.S. Department of Energy: Office of Fossil Energy – Office of Oil and Natural Gas: http://residualoilzones.com/wp-content/uploads/2018/02/Melzer2006.pdf (accessed November 17, 2019).

References

Ramondetta, P.J., 1982a, Facies and Stratigraphy of the San Andres Formation, Northern and Northwestern Shelves of the Midland Basin, Texas and New Mexico: Bureau of Economic Geology, The University of Texas at Austin, doi: 10.23867/ri0128d.

Ramondetta, P.J., 1982b, Genesis and Emplacement of Oil in the San Andres Formation, Northern Shelf of the Midland Basin, Texas: Bureau of Economic Geology, The University of Texas at Austin, doi: 10.23867/ri0116d.

Ross, C.A., and Ross, J.R.P., 1987, Late Paleozoic Sea Levels and Depositional Sequences: Cushman Foundation for Foraminiferal Research, Special Publication No. 24.

Ruppel, S.C., 2019, Anatomy of a Paleozoic basin: the Permian Basin, USA: Austin, TX, The University of Texas at Austin, Bureau of Economic Geology, v. 1.

Saller, A.H., 2004, Palaeozoic dolomite reservoirs in the Permian Basin, SW USA: stratigraphic distribution, porosity, permeability and production: Geological Society, London, Special Publications, v. 235, p. 309–323, doi: 10.1144/gsl.sp.2004.235.01.13.

Trentham, B. L., and Melzer, S. L., 2019, A "Cookbook" Approach to Evaluating Residual Oil Zones Completed as Horizontal Depressurizing (DUROZ) Wells in the San Andres Formation: AAPG: Search and Discovery, no. 51570, doi:10.1306/51570Trentham2019.

Trentham, B.L., Melzer, S.L., Vance, D.B., Kuuskraa, V., and Petrusak, R., 2015, Identifying and Developing Technology f or Enabling Small Producers to Pursue the Residual Oil Zone (ROZ) Fairways of the Permian Basin, San Andres: Residual Oil Zones, http://residualoilzones.com/rpsea-ii/.

Ward, R.F., Kendall, C. G. ST., and Harris, P.M., 1986, Upper Permian (Guadalupian) Facies and Their Association with Hydrocarbons--Permian Basin, West Texas and New Mexico: AAPG Bulletin, v. 70, p. 239–262, doi: 10.1306/9488566f-1704-11d7-8645000102c1865d.